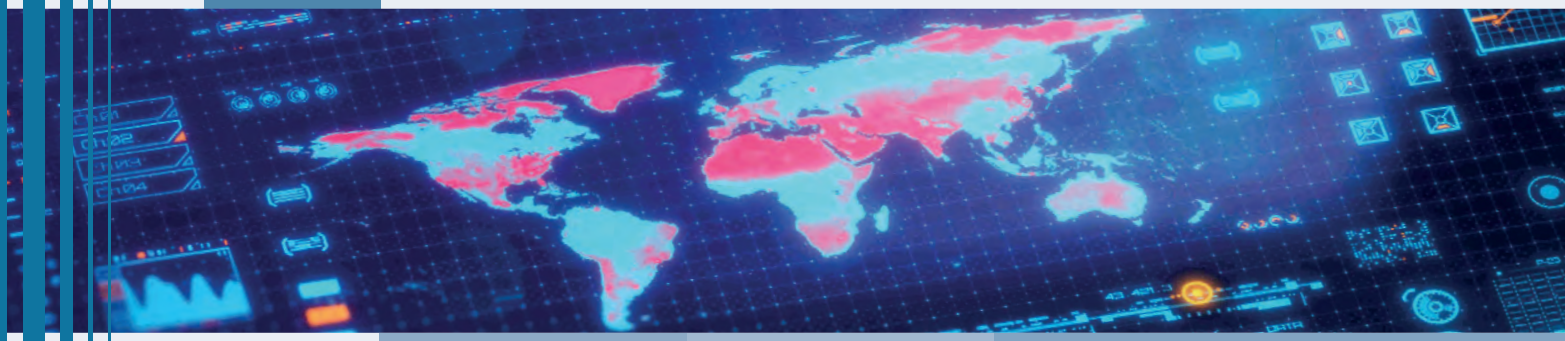

December 2025

An EDHEC Climate Institute Working Paper

The Global Geography of Long-Term Projected Macroeconomic Damages from Chronic Physical Climate Risk: Country vs. Intra-Country Distribution

EDHEC Climate Institute
London - Nice - Paris - Singapore

Table of Contents

Keywords: Climate Econometrics; Climate Damages; Physical Risks; Projections.
JEL N°: Q54, O44, C23.

Declaration of competing interest

The author declares that he has no competing interests and, specifically, that he has no financial and personal relationships with other people or organisations that could inappropriately influence (bias) his work, such as, but not limited to, employment, consultancies, stock ownership, honoraria, paid expert testimony, patent applications and registrations, grants or other funding.

Authors and acknowledgments

The author gratefully acknowledges support from the EDHEC Climate Institute (ECI), and particularly Riccardo Rebonato, Lionel Melin and Frederic Ducoulombier for their useful guidance and feedback.

Copyright

Disclaimer

About the Author

Nicolas Schneider, PhD is a Senior Research Engineer - Macroeconomist at EDHEC Climate Institute, working with the "Climate Scenarios" research team. His focus includes the development of physical climate risk assessment methodologies implemented over sectors, time and space to support the scientific needs of both the EDHEC Climate Institute and Scientific Climate Ratings, an EDHEC Venture. Before that, he worked under the management of Riccardo Rebonato on the Research Programme 'Impact of Climate Change on Asset Prices and Investment Management'. Nicolas holds a Ph.D. from Boston University, funded by the U.S. Department of Agriculture's National Institute of Food and Agriculture (NIFA), and MSc degrees from both the London School of Economics and Paris-Panthéon Sorbonne University. He has co-authored over a dozen peer-reviewed articles and has taught at Harvard University's Department of General Education and the Quantitative Methods Seminar at the Oxford Smith School. He has also consulted for the New York City Mayor's Office of Climate and served as a fellow in the Coupled Human and Earth Systems Program of the U.S. Department of Energy's MultiSector Dynamics Modeling Initiative.

Abstract

This paper elucidates the heterogeneity of countries' and subnational regions' economic responses to plausibly exogenous annual fluctuations in temperature and precipitation, using unbalanced panels over 1970–2018 (166 countries from Penn World Tables 10.01; 1,661 regions from MCC-PIK). We project climate change-driven damages to per capita GDP by combining econometrically-estimated responses with an ensemble of NEX-GDDP CMIP6 simulations from 30 global climate models (GCMs) extrapolated to 3,672 provinces responsible for 95% of global economic production. We find substantial agreement among GCMs of average end-of-century per capita GDP declines of up to 70% solely attributable to the central component of chronic physical climate risk (i.e., climate change-driven shift in average temperature) - with the largest effects in provinces bordering the equator and the tropics under a vigorous SSP5-8.5 scenario. First, our study provides a basis for producing spatially disaggregated projections of climate-induced economic damages that consistently encompass the majority of administrative regions. Second, we show that accounting for small-scale variations in localized climatic exposure and intra-country economic heterogeneity yields aggregatedlosses that fundamentally alter the conclusions of previous global GDP models.

1 Introduction

The global production systems, particularly food and energy, are expected to face critical pressure from increased demand and a changing climate over the next century (Foley et al, 2005; Bodirsky et al, 2015). Prior regression analyses quantified the environmental determinants of economic production components (i.e., crop yields) using high-frequency micro-data[1]; and have extensively focused on exposure to extreme heat (Blanc and Schlenker, 2017; Massetti and Mendelsohn, 2020; Sue Wing et al, 2021), change in soil moisture (Ortiz-Bobea et al, 2019), or a combination of the two (Haqiqi et al, 2021).

Meanwhile, macro-scaled econometric analyses provided strong correlation evidence between total economic output and temperature over temporal (Dell et al, 2012; Hsiang, 2010) and spatial (Nordhaus, 2006; Dell et al, 2009) vectors, but it is unknown whether these results are connected, and if so, how? Relatively absent from macro-level assessments (Dell et al, 2012), strong non-linear responses of output to temperature derived from micro data[2] are mainly based on developed countries data and remain hardly extendable to places exposed to humid tropical climates like the emerging world is, besides unveiling a major *aggregation* problem. If micro-level declines are captured within aggregated macro-level data, the integration of production across extensive spatial (e.g., national) and temporal (e.g., annual) scales introduces variability in exposure to momentary temperature fluctuations. Unit components of the economy—such as crops or labour—are subject to a wide distribution of localized thermal conditions. If acute output reductions occur predominantly under extreme temperature conditions, the aggregation process, which combines these moments with many cooler, highly productive

[1] A large body of cross-sectional studies suggested that farmland values and temperature have a hill-shaped relationship with a peak value near the mean growing season exposure (Seo et al, 2009; Mendelsohn and Massetti, 2017).

[2] Mainly due to data availability constraints, studies assessing the weather determinants of agriculture productivity have focused on the U.S. using state or county-level data. See Schlenker and Roberts (2009); Schlenker and Lobell (2010) and Burke and Emerick (2016). Similar conclusions can be drawn from the climate-energy nexus literature (Deschênes and Greenstone, 2011; Auffhammer and Aroonruengsawat, 2011; Auffhammer et al, 2017; Auffhammer, 2022). Temperature-energy demand responses have primarily been estimated via state-level monthly averages of residential electricity load (Deschênes and Greenstone, 2011), high-frequency data at the single-state or regional level (Franco and Sanstad, 2008; Miller et al, 2008; Allen et al, 2016; Coffey et al, 2015) residential (Auffhammer and Aroonruengsawat, 2011) and city-level billing data from electric utilities (Romitti and Sue Wing, 2022); and are mainly based on California and the American South data.

intervals, would yield an overall output that exhibits only modest declines in response to increases in the aggregate average temperature (Burke et al, 2015).

Historically, significant advancements have been achieved in integrating updated methodologies for discounting (Drupp et al, 2018; Newell et al, 2022) and climate dynamics (Millar et al, 2017) into the Integrated Assessment Models (IAMs) used for Social Cost of Carbon (SCC) estimations (Rennert et al, 2022). Earlier IAMs struggled to capture and monetize the full spectrum of sector-specific impacts and their interlinkages. This limitation tended to favour improved approaches able to identify plausibly causal damages on broad economic metrics, such as total economic output (Burke and Tanutama, 2019; Kalkuhl and Wenz, 2020; Callahan and Mankin, 2022). The emergence of pioneer econometric studies quantifying macroeconomic productivity responses to climate spurred major revisions to SCC estimates (Ricke et al, 2018), frequently yielding significantly higher values compared to studies focused on sector-specific damages (Anthoff and Tol, 2013) or aggregated damages derived from meta-analyses (Nordhaus, 2017).

Climate change is shifting the distribution of extreme heat events, making them more frequent and intense over time (Orlowsky and Seneviratne, 2012). Shared socioeconomic pathways (SSP) forecasts unanimously predict rising global average surface temperature circa-2050 (Meinshausen et al, 2020). Recent developments in both large-scale spatial econometric regressions and the elaboration of global climate databases have increased the level of spatial granularity, constrained the persistence, and widened the scope of potential climatic drivers of macroeconomic productivity, but their implications for regional economic outputs remain unexplored. The absence of mid-century projected changes in GDP accounting for small-scale variations in localized climatic exposure and intra-country economic heterogeneity in the literature leaves our geographic understanding of macroeconomic systems' adaptation potential incomplete. If aggregated, the magnitude of resulting damages on economic production can spatially vary greatly and fundamentally alter the conclusions of Burke et al (2015)'s global GDP response model. Our intuition is that macro-level predictions of climate economic damages, because structured via country-by-year smoothed average variations in output, may have significantly underestimated the true economic cost of climate shocks. In response, Kotz et al (2024) laid a first stone by providing pioneer econometric evidence

showing how temperature-attributed historical gross regional output responses may potentially imply larger and more spatially heterogeneous projected economic impacts. Our paper aims to illuminating previously unanticipated interactions between technical aspects of the production system and the spatial determinants of output sensitivity to climatic conditions, while offering more fine-grained decompositions of existing averaged estimates of projected damages (Burke et al, 2015; Kotz et al, 2024) that have masked localized disparities.

This leaves us with two main questions: (*i*) to what extent country-averaged temperature deviations from the means sort out critical weather variability central to causal inference in econometrics?; (*ii*) in projecting future climate change implications on gross regional economic production, can mid- and end-century global average damages from rising average temperature reveal larger magnitudes?

This paper contributes to the literature by quantifying weather components' responses of country- and administrative province-level annual per capita GDP for most regions responsible for 95% of global economic production using an unbalanced panel covering the 1970-2018 period from both Penn World Tables version 10.01 (PWT) and the MCC-PIK Database of Subnational Economic Output (DOSE). Using a panel specification similar to what is commonly used in the literature quantifying climate change impacts, we elucidate heterogenous output' responses to temperature and precipitation, which we attribute to both time-series and cross-sectional variations in plausibly exogenous year-to-year weather fluctuations (i.e., *the* major propagation channels of climate change, because unanticipated) and the identification of long climate normals causing actors' adaptation along the 'extensive margin' (i.e., which manifests itself over time in response to long stochastic warming processes following an upward trend). We follow McIntosh and Schlenker (2006) and structure our fixed-effects model with a non-linear polynomial temperature function enabling both within-country and cross-country sources of variation to re-enter our equation, thus implicitly allowing economic units in the dataset to adapt over time. We leverage spatial deviations by considering the exposure of administrative provinces to climate fields, weighted by a time-invariant measure of intra-country population density distributions derived from the 2015 Gridded Population of the World dataset (CIESIN, 2004). Meteorological covariates are compiled from historical 3-hourly global surface temperature and precipitation fields on

a 0.25 deg. grid from the Global Land Data Assimilation System (GLDAS) (Rodell et al, 2004) collapsed and merged with our country- and province-specific economic production data over matching years. We then compare our country-level GDP responses (i.e., *à la Burke et al (2015)*) to our two main propagation channels of climate change impacts (i.e., temperature and precipitation) with those inferred from province-level data (i.e., *à la Kotz et al (2024)*). Combining our non-linear GDP responses derived from the period 1970-2018 with an ensemble of NEX-GDDP CMIP6 simulations from 30 distinct global climate models (GCMs), we use the predictive structure of our equation to project climatically-driven changes in economic outputs under both moderate (SSP2-4.5) and vigorous (SSP5-8.5) warming scenarios. We then distribute our collection of simulated impacts across both spatial and temporal vectors (namely administrative provinces and future epochs spanning 2030-2099), GCMs, multi-model median subsets of 'hotter'-'cooler'/'likely'-'very likely' GCMs, and SSPs. The burgeoning availability of SSP-specific 30 GCMs simulated under the Coupled Model Intercomparison Project Phase 6 (CMIP6) exercise represents a golden opportunity to use the most achieved time- and spatially-downscaled global warming simulations as part of our macroeconomic projection modelling.

The rest of the paper is organized as follows. §2 presents the theoretical framework, data and empirical modeling. In §3, estimated climate-output response functions are presented along with projected damages distributed sub-nationally. In §4, our findings are discussed before concluding remarks are provided.

2 Methods

2.1 A simple theoretical framework

Where do we stand theoretically? Our starting place is that climate change is by nature a global public good problem that leaves no productive units or locations untreated (Schlenker and Walker, 2016). The absence of a formal *control group* has fundamental implications for the impact evaluation approach to climate change, whether historically-measured or future-projected.

A pioneering theoretical formalization of the aggregation of cross-climatic damage

to productive units was offered in Burke et al (2015) which we explicitly recall here. This serves as the foundation for our theoretical framework. It aims to model how highly non-linear changes in productivity in short time scales and across many micro-units do scale-up to explain the shape of macroeconomic responses over longer periods. Let partition a typical macroeconomy into industries indexed by i, assuming all individual units of production within each industry respond homogeneously to temperature shock[3]. Production in each industry occurs at various locations in space indexed by ℓ and countries, indexed by $\mathcal{L}$; which are large clusters of locations. The incremental moments (hours) in time analysed in micro studies are indexed by t and longer periods of time composed of many sequential moments (years) are indexed by τ.

Following Deryugina and Hsiang (2014), capital K_i and labour L_i in each industry show respective productivities A_i^K and A_i^L that are functions of instantaneous temperature $T_{\ell,t}$ experienced at a location ℓ and time t. The total quantity of capital and labour allocated to industry i is allowed to change with temperature. The price of a unit of output is p amd α is a constant in this stylized production function. For a sub-unit of the economy at a location ℓ at time t using technologies available in i, the total production function $Y_{i,\ell,t}$ is:

$$Y_{i,\ell,t}(T_{\ell,t}) = p_i(A_i^K(T_{\ell,t})K_{i,\ell,t}(T_{\ell,t}))^{\alpha}(A_i^L(T_{\ell,t})L_{i,\ell,t}(T_{\ell,t}))^{1-\alpha} \tag{1}$$

The model assumes that capital and labour reallocation across locations in response to temperature changes is slow. Changes in the total allocation of time individuals allocate to labour is known to vary with temperature, which can be captured by changes to labour productivity A_i^L since it has been empirically shown that labour is not mobile across different industries in response to temperature (Graff Zivin and Neidell, 2014). In a competitive equilibrium $\frac{K_{i,\ell,t}}{L_{i,\ell,t}} = \frac{\alpha}{1-\alpha}$, capital-to-labour ratios are fixed and output scaled linearly with the total quantity of capital and labour allocted to i (i.e., constant returns to scale). Define $U_{i,\ell,t} = p_i K_{i,\ell,t}^{\alpha} L_{i,\ell,t}^{1-\alpha}$ a scalar measure of resources applied to i at location ℓ at time t. U_i describe the number of modular units of production (firms)

[3]This is a constraining assumption. For instance, it has been shown that productive sectors' energy demand responses to temperature result from the intersection of: (*i*) the degree of individuals' energy demand sensitivity to weather (driven by people); (*ii*) the intensity of future climate shifts (driven by climate); and (*iii*) the properties of buildings and indoor adaptation technologies (driven by building characteristics) (Romitti and Sue Wing, 2022).

allocated to industry i. Eq. (1) can be simplified to:

$$Y_{i,\ell,t}(T_{\ell,t}) = \underbrace{(A_i^K(T_{\ell,t})^{\alpha} A_i^L(T_{\ell,t})^{1-\alpha})}_{f_i(T_{\ell,t}} p_i K_{i,\ell,t}^{\alpha} L_{i,\ell,t}^{1-\alpha} = f_i(T_{\ell,t} U_{i,\ell,t}) \tag{2}$$

Where $f_i(T_{\ell,t})$ is a function describing how overall productivity in industry i responds to instantaneous temperatures. The economic framework presumes additive separability across sectors and geographic regions, treating firms as atomistic entities operating independently. However, significant climatic changes likely induce emergent effects that extend beyond those experienced by individual firms responding to isolated alterations in their immediate climate conditions. These emergent impacts arise due to substantial inter-firm spillovers and the potential for novel price dynamics when climatic events exhibit temporal or spatial correlation. For instance, disruptions in a firm's supply chain caused by climate-driven events could magnify the economic consequences beyond the direct exposure of the firm itself. If such effects are significant and traverse international boundaries, the empirical methodology employed here—which analyzes country-specific impacts in isolation—may underestimate the broader economic ramifications of large-scale climatic shifts. A measure of aggregate output such as Gross Domestic Product (GDP) is formed by summing across all industries i and integrate production across all locations in a country and all moments in time within the period of observation. Total output in country $\mathcal{L}$ during year τ becomes:

$$Y_{\mathcal{L},\tau} = \sum_i Y_{i,\mathcal{L},\tau} = \sum \int_{t \in \tau} \int_{\ell \in \mathcal{L}} f_i(T_{\ell,t}) U_{i,\ell,t} d\ell dt \tag{3}$$

Where the spatial and temporal distribution of units $U_{i,\ell,t}$, as well as the spatial distribution of atmospheric temperatures, will determine what temperatures $T_{\ell,t}$ individual units are exposed to. Within country $\mathcal{L}$ and year τ, once can integrate the number of points in time when individual productive units are exposed to a momentary local temperature $T_{i,\ell,t}$ to construct a marginal distribution function summarizing temperature exposure within industry i. the shape of this marginal distribution function[4]

[4]Burke et al (2015) note that this marginal distribution is not a marginal probability distribution because the total number of units at each temperature are not normalized by the total number of units. i.e. this marginal distribution is more analogous to a histogram measuring frequencies rather than a histogram measuring probabilities.

is describes by $g_i(\cdot)$ which is mean zero and can be shifted by the location parameter $\overline{T}_{\mathcal{L},\tau}$ defined as the average temperature in country $\mathcal{L}$ during period τ. Hence, $g_i(T - \overline{T}_{\mathcal{L},\tau})$ takes the form of a histogram of the temperature that units U_i are exposed to within a large region and interval of time. Assuming $g_i(\cdot)$' shape is constant across countries or years[5], unlike the climate $\times$ location parameter $\overline{T}_{\mathcal{L},\tau}$, conferring $g_i(\cdot)$ two important properties. First, for a single industry, the total quantity or 'mass' of productive units M_i is the integral of $g_i(\cdot)$ over all possible temperatures (including those of the historical distribution):

$$M_i = \int_{-\infty}^{\infty} g_i(T - \overline{T}_{\mathcal{L},\tau})dT = \int_{t\in\tau}\int_{\ell\in\mathcal{L}} U_{i,\ell,t}d\ell dt \tag{4}$$

Second, the shape of $g_i(\cdot)$ reflects the distribution of productive units across space and time such that for $x \in (-\infty, \infty)$:

$$\int_{-\infty}^{x} g_i(T - \overline{T}_{\mathcal{L},\tau})dT = \int_{t\in\tau}\int_{\ell\in\mathcal{L}} U_{i,\ell,t}1[T_{\ell,t} < x]d\ell dt \tag{5}$$

Where we can now formalize the total production at the aggregate level in terms of average temperature $\overline{T}_{\mathcal{L},\tau}$ expressed at the aggregate level, and $g_i(\cdot)$:

$$Y(\overline{T}_{\mathcal{L},\tau}) = \sum_i Y_i(\overline{T}_{\mathcal{L},\tau}) = \sum_i \int_{t\in\tau}\int_{\ell\in\mathcal{L}} f_i(T_{\ell,t})U_{i,\ell,t}d\ell dt \tag{6}$$

$$= \sum_i \int_{t\in\tau}\int_{\ell\in\mathcal{L}} f_i(T)g_i(T - \overline{T}_{\mathcal{L},\tau})dT \tag{7}$$

Where available information on the spatial and temporal distribution of $U_{i,\ell,t}$ is no longer required. The reason is that if the shape of $g_i(\cdot)$ is relatively homogeneous across periods τ, then $\overline{T}_{\mathcal{L},\tau}$ is a sufficient statistic for temperature exposure at the aggregate level because changing annual average temperature $\overline{T}_{\mathcal{L},\tau}$ shifts the distribution of temperature exposure for individual micro-level units. Esstentially, Burke et al (2015) demonstrated that once can change variables by collapsing the joint spatial and temporal distribution of temperatures and micro-level productive units into the marginal distribution $g_i(\cdot)$ and a location parameter $\overline{T}_{\mathcal{L},\tau}$, which is a country's annual average temperature: our primary regressor of interest in the econometric framework

[5]In practice, the shape of $g_i(\cdot)$ may actually vary based on changes in the within-country and within-year distribution of temperatures that productive units are exposed to.

formalized below in §2.3.

In summary, if we let function $f_i(T)$ describe the productive contribution of an individual productive unit in industry i (e.g., a firm) relative to instantaneous (e.g., daily) temperature T. For a given country, period and industry, they denote the fraction of unit-hours spent below the critical temperature threshold as m_{i1} and the fraction above as m_{i2}; such that the distribution of unit-hours across all temperatures is $g_i(T - \overline{T})$ and centred at average temperature $\overline{T}$. Assuming $g_i(\cdot)$ is mean zero. If productivity loss within a single productive unit-hour has limited impact on other units as suggested by the economic literature, then aggregate production function Y equals the sum of output across industries, each integrated over all productive unit-hours in the country and period analysed:

$$Y(\overline{T}) = \sum_i Y_i(\overline{T}) = \sum_i \int_{-\infty}^{+\infty} f_i(T) \cdot g_i(T - \overline{T}) dT \tag{8}$$

As $\overline{T}$ rises a location warms on average, m_{i2} increases gradually for all productive units whose coordinate centroids fall inside the warming country. This growing number of hours beyond the temperature threshold imposes gradual but increasing losses on total output $Y(\overline{T})$. In this view, Eq. (8) predicts that $Y(\overline{T})$ is a smooth concave function with a derivative that is the average derivative of $f_i(T)$ weighted by the number of unit-hours in each industry at each daily temperature. It also predicts that $Y(\overline{T})$ peaks at a temperature lower than the threshold value in $f_i(T)$, only if the slope of $f_i(T)$ above the threshold is steeper than minus the slope below the threshold, as shown by micro-scale evidence (Schlenker and Roberts, 2009). Predictions challenge the assumption that macroeconomic responses should directly mirror highly non-linear micro-level responses (Hsiang, 2010; Heal and Park, 2013). More critically, while aggregate productivity losses are expected to align temporally with temperature fluctuations, such changes may also exert significant influence on the long-term trajectory of an economy's output (Dell et al, 2012; Hsiang and Jina, 2014). For instance, transient productivity shocks could disrupt the rate of investment in new productive assets, thereby inducing persistent effects on future macroeconomic production.

How can we empirically test these theoretical derivations? Our direction is to next use panel data on geo-economic production matched to historical measures of me-

teorological fields spanning the 1970-2018 period. We elaborate a version of Burke et al (2015) country-level econometric model which we regionally-downscaled to sub-national administrative areas, à la Kotz et al (2024). In an ideal experimental design, the optimal setup would consist of two identical economic regions, one exposed to an exogenous temperature increase and the other left unaffected—allowing for a direct comparison of economic outcomes. Since such a counterfactual is unobservable in reality, researchers approximate it by leveraging temporal variability within the same region, contrasting years with anomalously high temperatures against those with unusually low ones, driven by stochastic atmospheric fluctuations (Willmott and Matsuura, 2012). In this framework, cooler years serve as a 'control' and warmer years as the 'treatment' (Burke et al, 2015). This within-region, over-time comparison avoids the confounding influences inherent in conventional cross-country or -region analyses, which infer temperature effects from economic differences across nations (Nordhaus, 2006).

2.2 Data

Our analysis brings together four sets of data:

Historical country-level GDP records. Countries' annual real (inflation-adjusted) per capita GDP series are taken from the Penn World Tables version 10.01[6] (Feenstra et al, 2015), sub-setting 1970-2020 years for 166 economies, from which we compute the first differences of the natural logarithmic transformation. As a robustness, we alternatively process and collect World Development Indicators (WDI) data for identical macroeconomic variables, sample of countries and time periods.

Historical gross regional GDP records. Administrative areas' gross regional product per capita data are taken from the MCC-PIK Database of Subnational Economic Output (DOSE)[7] (Wenz et al, 2023). Its most recent version provides harmonized data on reported economic outputs from 1,661 subnational regions across 83 countries with varying temporal coverage from 1960 to 2019 from which we subset 1970-2018 years. Sub-national units constitute the first administrative division below national. Recent work has used interpolation and downscaling to yield estimates of sub-national eco-

[6]Available at: https://www.rug.nl/ggdc/productivity/pwt/?lang=en
[7]Available at: https://zenodo.org/records/7659600

nomic output at a global scale, but respective data sets based on official, reported values only are lacking. Wenz et al (2023) instead assembled values from numerous statistical agencies and yearbooks prior to apply harmonisation methods free of linear interpolations for both aggregate and sectoral output. Resulting records have been shown to be temporally- and spatially-consistent in regional boundaries, enabling coherent matches with geo-spatial climatic fields. Following the general literature (Gennaioli and La Porta, 2014; Kalkuhl and Wenz, 2020; Kotz et al, 2021, 2022) and most particularly Kotz et al (2024), we focus on real subnational output per capita and convert values from local currencies to US dollars to account for diverging national inflationary tendencies and then account for US inflation using a US deflator. Conversions between currencies are conducted using exchange rates from the FRED database of the Federal Reserve Bank of St. Louis[8] and the national deflators from the World Bank[9].

Historical weather exposures. Countries' and administrative regions' climate exposures are calculated based on 3h 0.25 degree gridded surface temperature and precipitation fields from NASA's Global Land Data Assimilation System[10] (GLDAS— Rodell et al, 2004). GLDAS is a new generation global high-resolution reanalysis data product developed jointly by the National Aeronautics and Space Administration (NASA), Goddard Space Flight Center (GSFC) and National Centers for Environmental Prediction (NCEP) (Ji et al, 2015). GLDAS incorporates satellite and ground-based observations, producing consistent quality-controlled long global gridded time series of optimal fields of land surface states and fluxes in near real time; while making available other meteorological variables that are not commonly available in other reanalysis data products either as consistent long time series, or at a high-spatial resolution[11]. GLDAS 0.25 degree fields are then collapsed into daily meteorological records over 1970-2018, and matched to the spatial and temporal resolution of our GDP realizations using a two-stage method.

First, we spatially aggregate the 0.25 degree grid-cell-level[12] (x) weather expo-

[8]Available at: https://fred.stlouisfed.org/series/AEXUSEU(2022)

[9]Available at: https://data.worldbank.org/indicator

[10]Available at: https://ldas.gsfc.nasa.gov/gldas

[11]Other reanalysis data products available have either (i) a coarser spatial resolution (e.g. ECMWF-ERA40 and JRA-55, both available from the mid-1950s but at 1.125 deg.) or (ii) a shorter time series (e.g. newly released ECMWF-ERA5 at 0.281 deg. from 1979–present day and NCEP-CFSv2 at 0.205 deg. from 2011–present day).

[12]Latitude (Y) and longitude (X) values are concatenated (Y_X) to generate a grid-cell string variable

sure estimates to the administrative level (i) of GRP records (i.e., level 1 provinces) and GDP records (i.e., level 0 countries) by day (d), using the population weighting method[13] presented below.

We use our network of NASA's GLDAS 0.25 deg coordinates to compute time-invariant weights (w) from highly-resolved population density estimates ($D_{x,w}$) taken from downscaled time-invariant 2015 information from the Gridded Population of the World raster dataset[14] (updated version) (CIESIN, 2004); linking each country or province (i) of the dataset with all NASA's GLDAS centroids (x) that fall within its boundaries. The population-density-weighted daily (d) average weather by country country/region i, say for the temperature component ($T_{i,d}$), is computed from grid-cell-level daily climate values ($T_{x,d}$) matched with locationally-specific population density information (D_x):

$$T_{i,d} = \frac{\sum_{x \in i} D_x \, T_{x,d}}{\sum_{x \in i} D_x} \tag{9}$$

Second, resulting daily (d) weather records matching each country/region-day are collapsed to the yearly frequency of our GDP observations t. We thus compute annual measures of heat and moisture exposures –i.e., average temperature values ($\overline{T}_{i,t}$ in deg. C) and cumulative precipitation (in mm/year); are matched to each country/region-year output observation. Our raw estimation dataset contains 166 countries $\times$ year (∼9,000 obs.) and 1,661 administrative region $\times$ year (∼82,000 obs.) spanning 1970-2018.

Simulations of climate change driven shifts in average temperature exposure. We conduct a large-scale processing of high-resolution time- and spatially downscaled climate forecasts from NASA's Earth Exchange Global Daily Downscaled Projections (NEX-GDDP CMIP6). NEX-GDDP CMIP6 is an ensemble of 30 distinct global climate models (GCMs) simulated under the Coupled Model Intercomparison, Phase VI (CMIP6— Eyring et al, 2016) exercise, whose outputs are biased-corrected and down-

uniquely identifying each 0.25 deg. resolved location of weather records; denoted x hereafter.

[13] We alternatively test the unweighted approach to straightforwardly aggregate NASA's GLDAS grid-cell-level information to the spatial resolution of our GDP records. Estimated responses, available upon request, exhibit slightly weaker statistical power and are less reliable as they do not account for the heterogeneously distributed populations within countries.

[14] Available at: https://sedac.ciesin.columbia.edu/data/collection/gpw-v4

scaled to a 0.25 deg. grid[15]. Temperature projections are truncated to the historical geographic extents of the GDP realizations, and used to calculate variables, as in the estimation dataset, for years in the historical (1985-2004) and future epochs (2021-2040, 2031-2050, ..., 2099) under vigorous and moderate warming scenarios (SSP5-8.5 and SSP2-4.5, respectively). To account for uncertainty in the temporal realisation of temperature forecasts, resulting time-series of GCM-specific simulated temperature values are averaged over 20 year windows containing our mid-points of interest (e.g., 2041-2060 averaged measures are thought more likely to accurately represent expected 2050 values than the GCM-simulated year 2050 alone) in each epoch before taking the inter-epoch difference between current and future means, giving us the 'Delta' values that we force into our global GDP model as part of our projection exercise; which we have prior calibrated via historical responses econometrically estimated in §2.3.

Burke et al (2015) pointed out that estimates of the economic effects of climate change are GCM-sensitive, and hence, multi-median impacts should be simulated from a wide set of GCMs. Other sources of uncertainty propagation are attributable to downscaling and bias-correction which can potentially alter local climate projections in CMIP6 (Lafferty et al, 2023). A final concern is that a subset of CMIP6 GCMs may be "too hot", with representations of cloud feedbacks in some models associated with higher-than-consensus global surface temperature response to doubled atmospheric CO_2 concentrations—equilibrium climate sensitivity (ECS) and global warming after 70 years of a 1% per annum increase in CO_2—transient climate response (TCR) (Sherwood et al, 2020; Tokarska et al, 2020; Zelinka et al, 2020; Hausfather et al, 2022). To mitigate the threat of bias potentially introduced by this phenomenon, we follow Hausfather et al's (2022) recommended procedure of excluding models with TCR and ECS outside "likely" ranges (1.4-2.2°C, 66% likelihood, and 2.5-4°C, 90% likelihood, respectively). That leaves us with 15 "likely" GCMs[16] that form the basis of our impact projections.

A regional summary statistics of the primary macroeconomic and climatic variables is provided in Table A.1. Maps of 2000-2015 linear trends in temperature and precipi-

[15]The raw NetCDF4 files weigh approximately 14TB. Processing and computation stages are performed using a High Performance Computing (HPC) cloud system.

[16]The exhaustive list of 15 "likely" models that we subset from the full *ensemble* of 30 GCMs is provided in Table A.2.

tation (i.e., expressed as the ratio of the total trend for the 16-year period [°C per 16 years] normalized by the historical standard deviation σ of year-to-year fluctuations for the period 1985-2015) in each of the 249,000 unique 0.25 $\times$ 0.25 grid-cells from NASA's Global Land Data Assimilation System (GLDAS) and covering all land surfaces globally are provided in Fig. 1. Looking forward, Figs A.6-to-A.12 show spatially distributed SSP-specific average temperature 'Deltas' between multi-GCM median 20-year average future epoch (2021-2040 [2030 mid-point], 2031-2050 [2040 mid-point],..., 2099) simulations and the global 1985-2004 historical baseline in each 0.25 $\times$ 0.25 NEX-GDDP CMIP6 cell. This leaves an *ensemble* of absolute Deltas (Δ) showing the spatial distribution of future climatically-driven shifts in temperature simulated under both SSP2-4.5 moderate (bottom panel) and SSP5-8.5 vigorous (top panel) warming scenarios, and with respect to the global temperature baseline ($\overline{T}$) recorded historically.

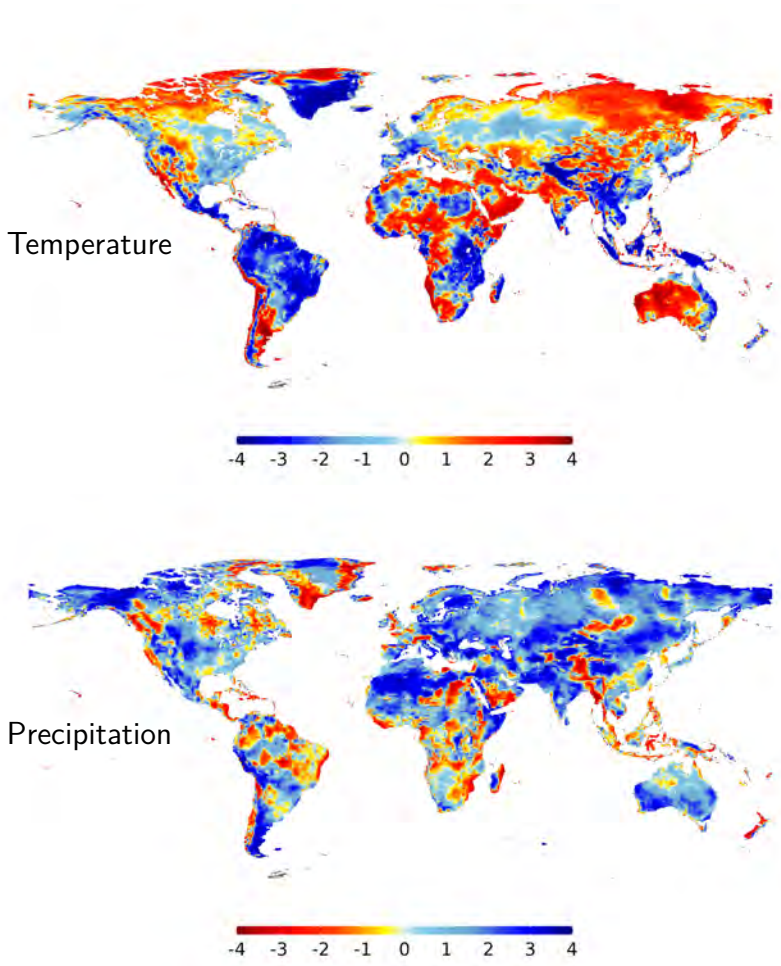

Figure 1: Maps of the 2000-2015 linear trend in average temperature (top-panel) and precipitation (bottom-panel) in each of the 249,000 unique 0.25 × 0.25 grid-cells from NASA's Global Land Data Assimilation System (GLDAS) and covering all land surfaces globally.
For each cell, trends are computed as the ratio of the trend effect estimated via linear model (lm) over the 16-year period (i.e., °C per 16 years) normalized by the historical standard deviation (σ) of year-to-year average weather component fluctuations over the period 1985-2015. For instance, a T trend of 1.0 means that temperatures at the end of the period were 1.0σ higher than at the beginning of the period.

2.3 Econometric Modeling of Climate-GDP/GRP Responses

We first empirically model the responses of per capita GDP to weather (temperature, precipitation) using a 49-year longitudinal sample of 166 countries covering the most recent period. We use a panel fixed effects (FEs) OLS model, similar to specifications commonly used in the climate economics literature (Schlenker and Roberts, 2009; Burke et al, 2015; Kotz et al, 2024).

We use the indices i, and t to represent countries and years. Historical data provides annual observations of first-differenced natural logarithm of per capita GDP (ΔY–per-period growth rates in income). We deconvolve the factors that might affect these changes via a polynomial function of temperature; and a quadratic function cumulative precipitations (P). We estimate the benchmark empirical model:

$$\Delta y_{i,t} = \Delta lnY_{i,t} = \mu_i + \nu_t + f[t;\Theta_{z(i)}] + f_T(T_{i,t}) + \lambda_1 P_{i,t} + \lambda_2 P_{i,t}^2 + \epsilon_{i,t} \tag{10}$$

Where i are country-specific constant terms (fixed effects) that capture unobserved idiosyncratic spatially-varying time-invariant influences (e.g., history, culture or topography). Given the long time span of our dataset, attributing year-to-year plausibly exogenous variations in per capita income to weather typically allows the use of low frequency controls such as year fixed effects ν_t because they account for abrupt global events (such as shocks to energy markets or global recessions) without over-capturing cyclical temperature fluctuations. In addition to year dummies, gradual changes to individual countries' growth rates that may be driven by slowly changing factors within a country (e.g, demographic shifts, trade liberalization, and evolving political institutions) are gradually accounted for by flexible time trends (Dell et al, 2012), formalized as $f[t;\Theta_{z(i)}]$: a zone-specific[17] function of time trend in years of sample that capture unobserved country- or regionally- time-varying dynamics influencing per capita income and correlated with climate. To do so, we use the Database of Global Administrative Areas (GADM)[18] and spatially intersected grid-cell coordinates with the different subnational administrative region identifiers in which they fall. Output is GID(0), GID(1)

[17] Starting at unity ($z(i) = 1$ for country), zones' size may extend to economic, trade or geographic clusters of countries likely to share that of a common trend.

[18] Available at: https://gadm.org/data.html

and GID(2) for countries, provinces, and counties/district, respectively. Finally, ϵ is a random disturbance term that captures variations in per capita GDP orthogonal to time and spatially-varying local climate conditions.

Note that our approach that simultaneously controls for both time-invariant and time-varying influences is more reliable than only controlling for fixed observed variables (e.g. performing regressions on explicit covariates, such as demographic or political variables) because it is robust to mismeasurement of controls, and it allows these controls to differentially influence each country's GDP level. For instance, our equation does not need to explicitly model the effect of demographic trends since our model accounts for the fact that non-linear demographic trends may be different in different countries, with measurement errors that differ between countries, and the effect of demographic trends on income may also differ across them. Furthermore, many traditionally adopted "control" regressors are themselves likely confounded by climatic events, with possible bias if included as is (Hsiang et al, 2013). This issue named *'bad control'* is discussed in detail in Angrist and Pischke (2009).

Estimated parameters of interest are the per capita GDP growth impacts of the potentially non-linear effects of heat (captured by the function $f_T(T_{i,t})$) together with precipitation (λ); because idiosyncratic changes in local annual temperatures have been shown to correlate with variations in precipitation (Auffhammer et al, 2013). We start by estimating $f_T(T_{i,t})$ as a simple quadratic ($f_T(T_{i,t}) = \beta_1 T_{i,t} + \beta_2 T_{i,t}^2$); prior to explore more flexible functional forms (see §2.4).

We then transpose our econometric framework into a spatially-downscaled structure following the same variable parametrization as for Eq. (10). Let indices r, and t represent elements of 1,661 sub-national administrative regions level I (i.e., GID(1)) and years. Our panel FEs specification becomes:

$$\Delta y_{r,t} = \Delta ln Y_{r,t} = \mu_r + \nu_t + f[t; \Theta_{z(i)}] + f_T(T_{r,t}) + \lambda_1 P_{r,t} + \lambda_2 P_{r,t}^2 + \epsilon_{r,t} \qquad (11)$$

Where the remaining structure of this augmented model is identical to its baseline versions in Eq. (10). Although the motivating micro evidence focus on the output level effect of temperature, we explicitly model the effect of temperature on output

growth (Δ) because measures of GDP within a country exhibit such high levels of serial correlation ($\rho = 0.999$) that they are hardly indistinguishable from a random walk (i.e., their time-series present a unit root); likely to cause spurious estimates and test statistics fail (Granger and Newbold, 1974; Angrist and Pischke, 2009; Hsiang et al, 2013). Using first difference-transformed income values, besides accounting for year fixed effects as well as country-specific quadratic trends in growth, leave a much less problematic serial correlation in outcome ($\rho = 0.125$). Because some serial correlation persists in the outcome, even after first differencing, we parametrically adjust our standard errors by clustering them at the country-level to account for spatial correlation and non-independence following (Cameron et al, 2011); thus controlling for arbitrary patterns of autocorrelation between residuals within each location. In this framework, and as for countries in Eq. (10), each administrative area is finally allowed its own level and non-linear trend in growth, and the impact of temperature on growth is identified from within-region deviations from this trend. It has been shown that controlling for trends and convergence in incomes (Barro, 2003) using location-specific trends outperforms auto-regressive models (Hsiang and Jina, 2014).

Temporary versus lasting productivity shocks. Short-term temperature fluctuations are expected to influence productivity as changes in the current growth rate, similar to Eq. (10). However, in economies exhibiting persistent growth dynamics (unit-root-like behavior), temperature variations could have enduring consequences on income trajectories. This could occur for two main reasons: (*i*) a one-period deviation can modify future output by altering the growth rate of the capital stock, an effect that could be intensified if resources must be reallocated toward costly adaptation investments (Pindyck, 2013); (*ii*) temperature shifts might directly influence the pace of technological progress—the primary driver of growth in standard models—such as through negative impacts of higher temperatures on cognitive performance essential for innovation (Graff Zivin et al, 2018; Dell et al, 2014).

If such temperature shocks permanently influence growth, the long-term economic consequences of climate change become considerably larger, since even small annual growth changes can compound to substantial differences in total GDP. Thus, correctly characterizing whether temperature affects income through levels or growth is critical for designing optimal policies (Moore and Diaz, 2015). Following Dell et al (2012),

we incorporate lagged temperature terms (lag $k \in [1:5]$) into Eq. (10) to explicitly examine these dynamics[19]. Qualitatively, our central climate projections remain robust under these alternative specifications, largely because our estimates align with a growth effect that has lasting impacts on income.

A common misconception is that the empirical specification in Eq. (10) assumes that economies are unable to adapt. In a fixed-effects setup with a simple linear temperature term, identification relies exclusively on within-country variation (i.e., deviations from a country's mean temperature), which are difficult for agents to anticipate. Yet, when using a higher-order polynomial for temperature, McIntosh and Schlenker (2006) demonstrate that both within- and between-country variation contribute to identification. This allows countries with higher mean temperatures to exhibit different sensitivities to within-country deviations. By leveraging both types of variation, the model implicitly accounts for historical adaptation to long-term climate, while short-run temperature fluctuations still capture unanticipated shocks. Importantly, for our projections, as a country's average temperature increases, additional warming effects are modeled in line with observed responses of other countries at similar temperatures. For completeness, we summarize McIntosh and Schlenker (2006)'s formal demonstration in § A.2; see also McIntosh and Schlenker (2006) for a detailed discussion.

Global function $f_T(\cdot)$. A critical assumption of this approach is that there exists a global function $f_T(\cdot)$ on which all units (countries and administrative regions) lie. We test this assumption by examining subsamples of the data and find no evidence that $f_T(\cdot)$ is dramatically different across various subsamples. Another related approach to understanding whether the non-linear response observed in Fig. 2 is globally generalizable, or whether it is just a composite effect of a negative and linear response in poor, hot countries and no response in rich, cooler countries, is to allow temperature to enter linearly in the regression and then to interact it with both country average temperature as well as country average income. $f_T(\cdot)$ becomes:

$$f_T(T_{i,t}) = \beta_1 T_{i,t} + \beta_2 (T_{i,t} \cdot \overline{T}_i) + \beta_3 (T_{i,t} \cdot \overline{Y}_i) \tag{12}$$

[19]For simplicity, in the remainder of this subsection we treat countries i as time-invariant indices and omit provinces r. A simple model with five lags and no controls would be: $Y_{i,t} = \beta_1 T_{i,t} + \beta_2 T_{i,t}^2 + \beta_3 T_{i,t-1} + \beta_4 T_{i,t-1}^2 + \cdots + \beta_{2k-1} T_{i,t-5} + \beta_{2k} T_{i,t-5}^2$, and the marginal effect on growth at temperature T^* is given by the derivative of $Y_{i,t}$ evaluated at T^*.

where $\overline{T}_i$ and $\overline{Y}_i$ denote the average temperature and (log) average GDP per capita in country i, respectively. In the absence of the third term (i.e., $\beta_3(T_{i,t} \cdot \overline{Y}_i)$), a non-linear and concave temperature response similar to Fig. 2 would be indicated by $\beta_1 > 0$ and $\beta_2 < 0$. However, if this differential response was actually being driven by income – and in particular by the fact that poor countries respond differently to temperature and that hot countries tend to be poor - then the inclusion of $\beta_3(T_{i,t} \cdot \overline{Y}_i)$ should mean that $\beta_2 = 0$; with $\beta_1 < 0$ and $\beta_3 > 0$ (i.e, negative effects of temperature at low income levels that attenuate as incomes rise).

Differential responsiveness. To test for differential responsiveness across income groups and across different sectors of the economy in our data; we interact the temperature and precipitation variables in Eq. (10) with an indicator for whether a country's purchasing-power-parity-adjusted (PPP)[20] per capita income was below the 1990 global median. Say $D_i = 1$ for a country with below-median PPP per capita income in 1990 ($D_i = 0$ otherwise); then the function $f_T(T_{i,t})$ in Eq. (10) becomes:

$$f_T(T_{i,t}) = \beta_1 T_{i,t} + \beta_2(T_{i,t}^2) + \beta_3(T_{i,t} \cdot D_i) + \beta_4(T_{i,t}^2 \cdot D_i) \tag{13}$$

Where β_1 and β_2 describe the response function for rich countries, and β_3 and β_4 describing adjustments to these parameters that are only applicable to countries with below-median PPP per capita income in 1990 ($D_i = 1$). If the response of rich and poor countries are different in structure, than the adjustments β_3 and/or β_4 will be significantly different from zero and the null hypothesis is to be rejected.

2.4 Empirical uncertainty

We account for empirical uncertainty by varying the functional form (FF) of the (i) temperature component and (ii) and the specification fixed effects.

FF of the temperature component. Given the considerable uncertainty surrounding the shape of the temperature-GDP response function, we test a number of ways of specifying its potential impact on output.

(1) Both historical and future economic impacts are likely to be the largest at the temperate extremes. We account for this convexity by estimating non-linear quadratic

[20]PPP incomes adjust for price differences across countries.

temperature components $f_T(T_{i,t}) = \Phi_1 T_{i,t} + \Phi_2 T_{i,t}^2$, where $T_{i,t}$ are daily temperature averaged by country-year; allowing for marginal effects of a given amount of warming to vary locationally. We also explore more flexible functional forms of temperature effect. Note that if linear fixed effects models allow to estimate consistent marginal parameters under unobserved heterogeneity, the identification is solely driven by deviations from the group mean (i.e., equivalent to a joint demeaning of the dependent and all independent variables). When introducing a quadratic term, it modifies the identification which then results from within-unit variation over time but also from between-unit variation in means (McIntosh and Schlenker, 2006). As it is not clear whether a standard quadratic fixed effects model uses a source of variation which is not strictly 'within', estimating weather impacts on output requires testing distinct functions of its components. Our alternative quantification approaches include: (*i*) testing higher polynomial orders in a parametric FE-OLS framework as presented in §2.3; (*ii*) regressing restricted cubic splines with varying semi-parametric knots (2-7) capturing N-shaped relations; (*iii*) estimating non-parametric smoothed splines estimated via Generalized Additive Model (GAM) (Wood, 2004) with location and time fixed effects whose system of equations below presents both country-level (top, extends Eq. (10)) and administrative region-level (bottom, extends Eq. (11)):

$$\begin{cases} \mathbb{E}\left[\ln Y_{i,t(i)}\right] = \Psi^T\left[\mathcal{T}_{i,t(i)}; \boldsymbol{\theta}^T\right] + \mu_i + \nu_t + f[t; \Theta_{z(i)}] \\ \mathbb{E}\left[\ln Y_{r,t(r)}\right] = \Psi^T\left[\mathcal{T}_{r,t(r)}; \boldsymbol{\theta}^T\right] + \mu_r + \nu_t + f[t; \Theta_{z(r)}] \end{cases} \tag{5}$$

Where $\widehat{\Psi} = \Psi\left[\cdot; \widehat{\boldsymbol{\theta}}\right]$ are the fitted temperature splines we combine with average temperature, historically observed and future shifted over epoch-specific simulations of climate change.

(2) We complement our empirical approach with a panel version of Eq. (10) linking per capita income to a wider range of intervals capturing exposure to the full distribution of temperature. Instead of cumulative degree day (base 0°C) aggregated by year, we define a vector of dummies as the number of days by country-year in which the daily mean temperature falls within the j_T^{th} of the 12 bins of 3°C intervals (0-3,3-6°C, ect): $\sum_{j_T} \Phi^T[T_{i,t}^{j_T}]$. While it reduces the number of parametric assumptions structuring the estimated relationship, the primary low functional form restriction implied by

this quantile bin model is that the impact of the daily mean temperature on yearly GDP realizations is constant within 3°C intervals. The choice of 12 temperature bins results from a preference to allow the data, rather than parametric assumptions, to determine the shape of the temperature-per capita income relationship, while offering precisely estimated responses that remain empirically valid.

(3) We also test a more parsimonious model that focuses entirely on the upper and lower tails of the daily temperature distribution (j_T^0, j_T^{12}). The remaining structure of this augmented model is identical to its baseline versions in Eqs. (10) and (11).

FF of the FEs. Other omitted variables influencing both trends in temperature and economic output may play out. Starting from a simple FEs structure of country-specific linear time trends (i.e., $f[t;\Theta_{z(r)}] = \Theta_{i,1}t$), we test how log[per capita GDP] responses vary with: (1) increasing Chebychev polynomial orders from quadratic to octic (8^{th}) ($f[t;\Theta_{z(i)}] = \sum_{j=2}^{8} \Theta_{z(i),j}t^j$); (2) variation in the spatial clustering of the flexible trend function ($z(i)$–from administrative areas level I to countries, and extending towards multi-country economic or geographic clusters likely to share that of a common trend). For instance Burke et al (2015)'s preferred specification – quadratic country-specific time trends ($\Theta_{i,1}t + \Theta_{i,2}t^2$), is again of interest because it allows growth rates to evolve non-linearly over time; and since the dependent variable is the derivative of income, each country is allowed its own level and non-linear trend in growth, and the impact of exogenous changes in temperature and precipitation on growth is identified from within-country deviations from this trend (McIntosh and Schlenker, 2006).

2.5 A Simple Damage Projection Framework: the *Delta* Method

Our fitted regional GDP model in Eq. (10) facilitates projection of long-run GRP per capita changes associated with climate change-driven shifts in the temperature factor. We provide below a simplified formalization of our projection framework: the Delta-method.

Use $\boldsymbol{x} = \{\boldsymbol{T}\}$ to denote the main weather covariate: temperature. Recall that in Section §2.2, we have computed and concatenated GCM-simulated values of this factor's exposure for an ensemble of future 20-year averaged values corresponding to

the climate epochs' midpoints being analyzed (2021-2040, 2031-2050, ..., 2099); and, following the same temporal parametrization as for an historical baseline period (1995-2014); we have calculated the inter-epoch differences to construct local region-specific shifters ($\Delta \boldsymbol{x}$) and added these offsets to the 1995-2014 historical mean of these same sub-national predictors ($\overline{\boldsymbol{x}}$) to construct projected future climate values: $\widetilde{\boldsymbol{x}} = \overline{\boldsymbol{x}} + \Delta \boldsymbol{x}$. The latter are combined with our fitted econometric model estimated in Section §2.2 to project GRP per capita changes induced by these region- and epoch-specific climate shifters.

For communication purpose, we reduce the temperature functional form $f_T(T_{r,t})$ to one simple semi-elasticity ($\widehat{\beta^T}$) of a linear temperature variable – instead of the actual polynomial characterising $f_T(T_{r,t})$. A simple projection framework for region r in future epoch t^* can be formulated as:

$$\widetilde{y}_{r,t^*} = \widehat{\mu}_{i,r} + \widehat{\nu}_{t^*} + f[t^*; \widehat{\theta}_{z(r)}] + \widehat{\boldsymbol{\beta}^T} \widetilde{\boldsymbol{T}}_{r,t^*} \tag{14}$$

and for our historical benchmark period t^0:

$$y^0_{r,t^0} = \widehat{\mu}_{i,r} + \widehat{\nu}_{t^0} + f[t^0; \widehat{\theta}_{z(r)}] + \widehat{\boldsymbol{\beta}^T} \overline{\boldsymbol{T}}_{r,t^0} \tag{15}$$

Facilitating computation of our primary impact metric: the projected fractional change (%) in GRP per capita as the inter-epoch difference ($\widetilde{y}_{r,t^*} - y^0_{r,t^0}$) in outputs; such that the sub-national region × weather factor × epoch combination of climate shift-induced % change in regional GRP per capita can be computed as:

$$\boldsymbol{\Psi}_{r,t^*} = \widehat{\beta^T}[\widetilde{T}_{r,t^*} - \overline{T}_{r,t^0}] \tag{16}$$

Where $\widetilde{T}_{r,t^*} = \overline{T}_{r,t^0} + \Delta T_{r,t^*}$. This leaves us with an ensemble of region-specific simulations $\boldsymbol{\Psi}_{r,t^*}$ that we distribute across the following vectors: (*i*) 15 'likely' Global Climate Models (GCMs); (*ii*) moderate (2-4.5) or vigorous (5-8.5) SSP warming scenarios; (*iii*) future epochs (2030, 2040, ..., 2100). The burgeoning availability of SSP-specific GCM simulations from the Coupled Model Intercomparison Project Phase 6 (CMIP6) presents a unique opportunity to incorporate the most advanced time- and spatially-downscaled warming projections into our macroeconomic modelling.

Within a given country, we assume regions to be heterogeneously exposed to climate deltas, leading to equally heterogeneous economic impacts. §2.2 describes the spatial coverage of administrative province-level gross regional product time-series data in the raw DOSE product. It is to be noted that spatial gaps in sub-national output for some African and Middle-Eastern countries remain, leaving an incomplete geographic coverage globally[21]. This is an obstacle that Kotz et al (2024) faced. To project climate-driven economic damages in administrative regions lacking DOSE data, we apply a two-step approach. First, by spatially intersecting the missing administrative regions with their respective ensembles of GCM simulated localized *Deltas* derived from outputs of the NEX-GDDP CMIP6 processing in Section §2.2. Second, by combining these with our globally estimated non-linear semi-elasticities deemed theoretically suitable to capture the sign and shape of the general temperature-output relationship from all countries. We thus obtain a synthetic 'enhanced' vectorized projection matrix linking predicted per capita GDP impacts to each administrative provinces. This approach has the advantage of offering consistent coverage across *all* 3,672 sub-national regions globally, while providing empirically valid damage estimates.

3 Results

3.1 Empirical results

The panel model results showing the log[GDP per capita] responses to country-annual average temperature exposure per year [deg.°C] are presented in Fig. 2.

Parametric FE-OLS findings in panel **a** Fig. 2 suggest that country-level economic production is smooth, non-linear, and concave in temperature, with a maximum at 13 °C, well below the threshold values recovered in micro-level analyses (Schlenker and Roberts, 2009) and consistent with predictions from equation (8). Cold-country

[21] Among its limitations, the global DOSE dataset of reported sub-national economic output exhibits both temporal and spatial inconsistencies, with coverage restricted to 83 countries. A key characteristic of DOSE is its strict reliance on officially reported macroeconomic data from diverse national statistical offices and yearbooks, as Wenz et al (2023) deliberately excluded interpolation methods to address data gaps. While this approach ensures fidelity to observed values, it also results in discontinuous time series, particularly in under-reported provinces. Moreover, challenges related to administrative boundary consistency persist due to historical changes, which can lead to spatial mismatches when integrating with geospatial climate data. This issue is discussed further in §2.2.

productivity increases as annual temperature increases, until the optimum. Productivity declines gradually with further warming, and this decline accelerates as average temperature rises. Note that our results almost perfectly match Burke et al (2015)'s response function (shown in *blue*) despite differences in the source of macroeconomic data, as well as the spatial and temporal resolution of climate fields prior aggregation. This study calculates countries' climatic exposures based on 3h 0.25 degree gridded surface temperature and precipitation fields from NASA's Global Land Data Assimilation System (GLDAS— Rodell et al, 2004) collapsed into daily climatic records over 1970-2018, and matched to the period of our macro-output realizations (see §*Methods*). Burke et al (2015) used reconstruction data from the University of Delaware containing 0.5 degree gridded monthly average metrological fields over 1960-2010. Both studies account for heterogenous intra-country population allocation and spatially aggregate grid-cell-level weather exposure by country via a weighted collapsing method incorporating time-invariant sub-national population density statistics from the Gridded Population of the World dataset (2015 Version) (CIESIN, 2004).

This non-linear temperature-GDP pattern is globally representative but not driven by outliers. Besides, it is robust to estimation procedures that allow heterogenous response functions across income groups; as well as more flexible functional forms than parametric FE-OLS. We have adopted Burke et al (2015)'s preferred specification of the FEs – country-by-year constant terms plus quadratic country-specific time trends in years of sample ($\mu_i + \nu_t + \Theta_{i,1}t + \Theta_{i,2}t^2$), is again of interest because it allows growth rates to evolve non-linearly over time; and since the dependent variable is the derivative of income, each country is allowed its own level and non-linear trend in growth, and the impact of exogenous changes in temperature and precipitation on growth is identified from within-country deviations from this trend (McIntosh and Schlenker, 2006). Panel **b** Fig. 2 showing non-parametric unrestricted spline of average temperature estimated globally from a Generalized Additive Model (GAM) (Wood, 2004) empirically validates the inverted-U shape of the response function. This method has the advantage of reducing the number of parametric assumptions constraining the shape of complex predictor's responses via unrestricted smooth functions. Panel **c** Fig. 2 complements our robustness approach with a semi-parametric restricted cubic spline with up to 3-8 Knots estimated globally. Knots are locations along a predictor variable's range

where pieces of the smooth function join; and thus where the shape of the smooth function can change. Splines fit the data in sections divided by these Knots, with each section's shape adjusted to minimize error. Finally, Panel **d** Fig. 2 extends the quadratic transformation of average temperature in panel **a** with $3^r d$ to 7^{th} polynomial orders; while holding the parametric setting constant. All macro-econometric models (including the more flexible functional forms) yield similar non-linear global per capita GDP-temperature response functions to our main estimates in panel **a**. Finally, panel **e** Fig. 2 shows that global non-linearity is driven by differences in countries' average temperature, not GDP. Orange dots and lines show the point estimate and 95% CI for the marginal effects of temperature on GDP per capita growth evaluated at different temperature baselines estimated from a model that interacts each country's year-to-year temperature fluctuation with its own average calculated across the sample period (i.e., $\delta y/\delta T_{i,t} = \hat{\beta}a + \hat{\beta}_b \cdot \overline{T}_i$). Orange dots and lines show equivalent estimates from a model that includes an interaction between annual temperature and average GDP per capita (i.e., $\delta y/\delta T_{i,t} = \hat{\beta}a + \hat{\beta}_b \cdot \overline{T}_i + \hat{\beta}_c \cdot \overline{y}_i$). Point estimates are similar across the two models, suggesting that the non-linear response is not due to hot countries being poorer on average. Panel **f** Fig. 2 shows a slightly varying cumulative marginal effect of temperature on per capita GDP as additional lag-transformed temperature variables ($h(T_{i,t-p})$ with $p = [1, 3]$) are included (note that standard errors are estimated from 1000 block-Bootstrap resampling iterations); suggesting that lagged effects and longer-term persistence may play out in the overall macroeconomic damages. This motivates us to differentiate between short- (contemporaneous regressors) and long-term (contemporaneous regressors plus lagged effects up to five lags) models to form the basis of our projections. Another area of investigation relates to the spatial structure of the estimation model. Regional heterogeneity in the temperature-GDP relationship gives additional weight to local climatic variability (because less smoothed by country-level averaging methods) which matter in our understanding of the heterogenous spatial distribution of climate shocks (Mahlstein et al, 2013).

This is now what we turn to. The panel model results showing the log[GDP per capita] responses to administrative province-annual average temperature exposure per year [deg.°C] are presented in Fig. 3.

Parametric FE-OLS findings in panel **a** Fig. 3 suggest that sub-national adminis-

trative province-level economic production is smooth, non-linear, and concave in temperature, with a maximum at 13 °C, again below the threshold values recovered in micro-level analyses Schlenker and Roberts (2009) and consistent with predictions from equation (8). Cold-province productivity increases as annual temperature increases, until the optimum. Productivity declines gradually with further warming, and this decline accelerates as average temperature rises. It is important to highlight that our estimated response-function almost perfectly matches Burke et al (2015)'s response function (shown in *blue*) despite differences in both the source and spatial resolution of macroeconomic data (Burke et al (2015): countries by year; this study: administrative provinces by year) and the implied differences in the spatial and temporal resolution of climate fields prior aggregation.

Here, we have adapted Burke et al (2015)'s preferred specification of the FEs to the spatial structure of our econometric model – province-by-year constant terms plus quadratic province-specific time trends in years of sample ($\mu_r + \nu_t + \Theta_{r,1}t + \Theta_{r,2}t^2$), serving the same purpose as in Eq. (10) (since the dependent variable is the derivative of income, each province is allowed its own level and non-linear trend in growth). The non-linear pattern of the responses found in **a** Fig. 3, while not driven by outliers, show an additional turning point (N-shaped) once more flexible functional forms are tested. In Panel **b** Fig. 3, the non-parametric unrestricted spline of average temperature estimated globally from a Generalized Additive Model (GAM) (Wood, 2004) exhibits a N-shaped response function. However, in Panel **c** Fig. 3, a semi-parametric restricted cubic spline show differential responses whether the number of knots is 3-4 (U-shaped), or 5-8 (N-shaped). This finding is confirmed by Panel **d** Fig. 3, whether the polynomial order of average temperature in the FE-OLS parametric equation is 2-3 (U-shaped) or 4-6 (N-shaped). We conclude that all province-level climate econometric models (including the more flexible functional forms) yield non-linear global per capita GDP-temperature response functions.

We consistently confirmed this pattern regionally by estimating locally-stratified response functions over typical climate zones (i.e., Asia [temperate continental]; Brazil [tropical savanna]; India [tropical monsoon]; Sweden [temperate to subarctic]) presented in Fig. A.5. Finally, estimated responses are highly robust to variation in the

specifications of the constant terms[22] and left-hand side variables (i.e., first-differenced log, natural log) as shown in Tables A.3-A.14 and Fig. A.2 (for parametric FE-OLS models), Fig. A.3 (for non-parametric GAM models), and Fig. A.4 (for semi-parametric restricted cubic splines).

[22]Separately for PWT, WDI and DOSE estimation datasets and across the full set of parametric FE-OLS, non-parametric and semi-parametric frameworks, we test our results' consistency against the following specifications of the fixed-effects (FEs): province-by-year fixed effects and province-specific quadratic time trends; province fixed effects and province-specific quadratic time trends; province-by-year fixed effects and province-specific linear time trends; province-by-year fixed effects excluding province-level time trends.

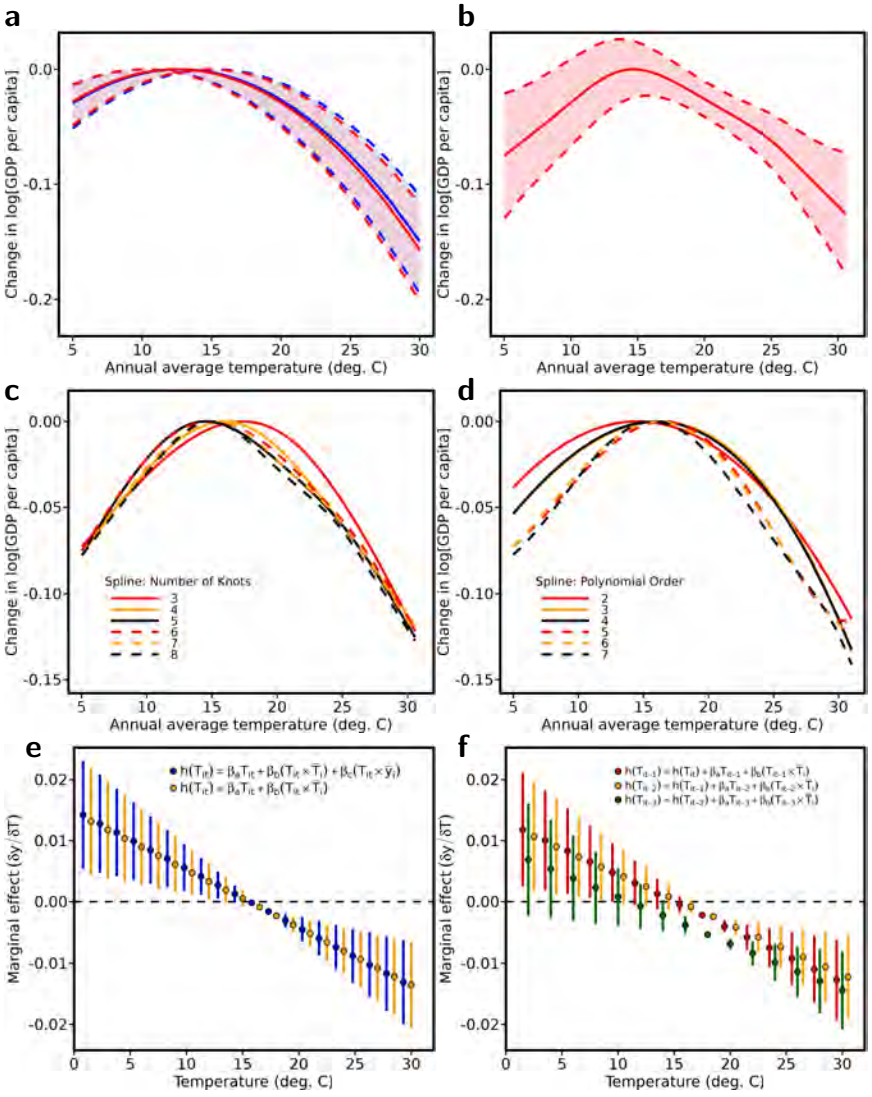

Figure 2: Global non-linear log[GDP per capita] responses to country-annual average temperature exposure per year [deg.°C].

a Parametric FE-OLS results from this study (N=6,697) versus Burke et al (2015) (N=6,584) are shown in solid red and blue lines (respectively) and normalised to the optimums. 95% confidence intervals shown in shaded red (this study) and blue (Burke et al, 2015) are derived from standard errors clustered at the country-level to account for spatial correlation and dependence across units. Regarding climate variables, this study calculates countries' climatic exposures based on 3h 0.25 degree gridded surface temperature and precipitation fields from NASA's Global Land Data Assimilation System (GLDAS— Rodell et al, 2004) collapsed into daily climatic records over 1970-2018, and matched to the period of our macro-output realizations (see §*Methods*). Burke et al (2015) used reconstruction data from the University of Delaware containing 0.5 degree gridded monthly average metrological fields over 1960-2010. Both studies account for heterogenous intra-country population allocation and spatially aggregate grid-cell-level weather exposure by country via a weighted collapsing method incorporating time-invariant sub-national population density statistics from the Gridded Population of the World dataset (2015 Version) (CIESIN, 2004).

b-c More flexible functional forms validate the non-linear shape of the global GDP-temperature relationship estimated from parametric FE-OLS in **a**. **b** Non-parametric unrestricted spline of average temperature estimated globally from a Generalized Additive Model (GAM). This has the advantage of reducing the number of parametric assumptions constraining the shape of complex predictor's responses via unrestricted smooth functions. **c** Semi-parametric restricted cubic splines with up to 3-8 Knots estimated globally. Knots are locations along a predictor variable's range where pieces of the smooth function join; and thus where the shape of the smooth function can change. Splines fit the data in sections divided by these Knots, with each section's shape adjusted to minimize error. **d** Parametric FE-OLS splines with up to 2-7 polynomial order in the calibration of the average temperature functional form. All regressions in **a-b-c-d**, whether parametric (**a, d**), non-parametric (**b**) or semi-parametric (**c**); include country-specific quadratic time trends in years of sample, country-by-year fixed effects and precipitation controls. All macro-econometric models (including the more flexible functional forms) yield similar non-linear global per capita GDP-temperature response functions to our main estimates. This suggests that the inverted-U shaped response function in our main specification is not an artifact of the parsimonious 2nd order polynomial.

e Global non-linearity is driven by differences in countries' average temperature, not GDP. Orange dots and lines show the point estimate and 95% CI for the marginal effects of temperature on GDP per capita growth evaluated at different temperature baselines estimated from a model that interacts each country's year-to-year temperature fluctuation with its own average calculated across the sample period (i.e., $\delta y/\delta T_{i,t} = \hat{\beta}a + \hat{\beta}_b \cdot \overline{T}_i$). Orange dots and lines show equivalent estimates from a model that includes an interaction between annual temperature and average GDP per capita (i.e., $\delta y/\delta T_{i,t} = \hat{\beta}a + \hat{\beta}_b \cdot \overline{T}_i + \hat{\beta}_c \cdot \overline{y}_i$). Point estimates are similar across the two models, indicating that the non-linear response is not due to hot countries being poorer on average. **f** Cumulative marginal effect of temperature on per capita GDP as additional lag-transformed temperature variables ($h(T_{i,t-p})$ with $p = [1, 3]$) are included. Solid points and lines indicate the sum of the contemporaneous and lagged marginal effects and its 95% CI at each temperature baseline. For all marginal effect models, standard errors are estimated from 1000 block-Bootstrap resampling iterations.

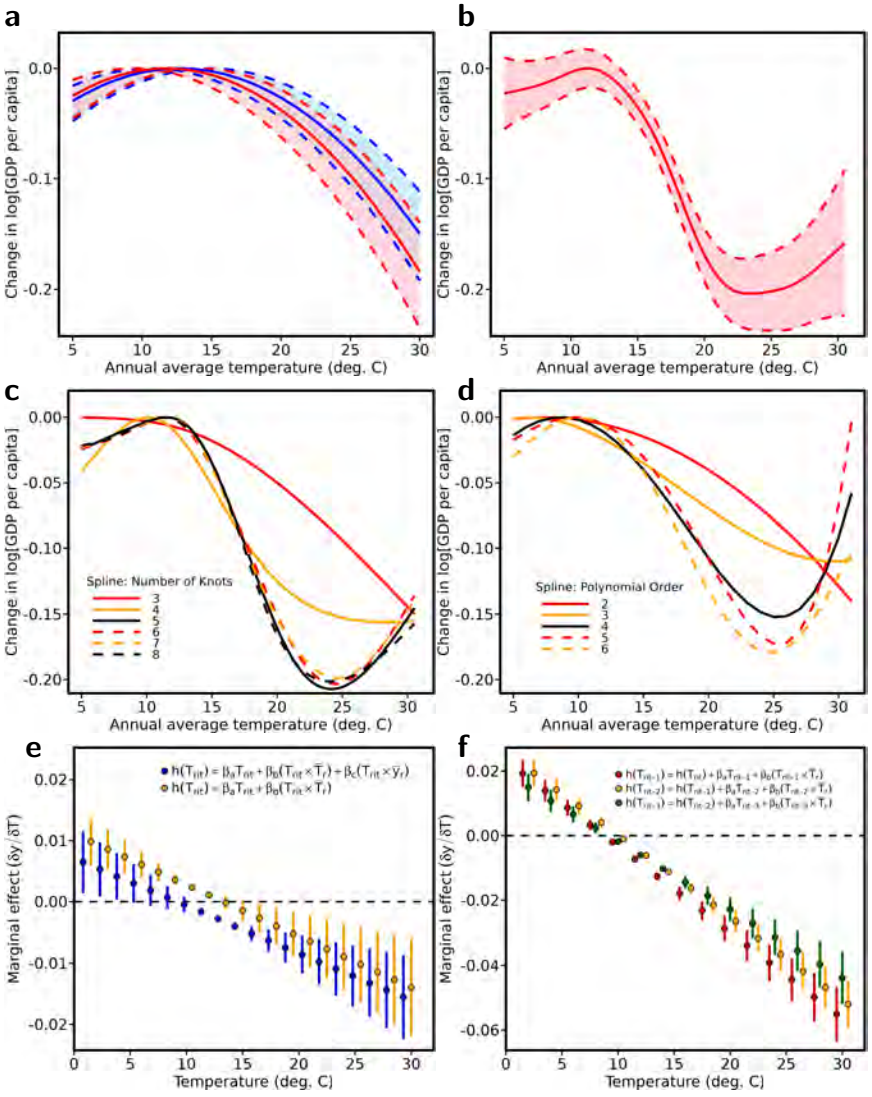

Figure 3: Global non-linear log[GDP per capita] responses to administrative province-annual average temperature exposure per year [deg.°C].

a Parametric FE-OLS results from this analysis on sub-national gross regional product per capita (N=36,583) versus Burke et al (2015)' study performed at the country-level (N=6,584) are shown in solid red and blue lines (respectively) and normalised to the optimums. 95% confidence intervals shown in shaded red (this study) and blue (Burke et al, 2015) are derived from standard errors clustered at the levels of sub-national regions (i.e., administrative provinces) and countries (respectively) to account for spatial correlation and dependence across units. Regarding climate variables, this study calculates sub-national provinces' climatic exposures based on 3h 0.25 degree gridded surface temperature and precipitation fields from NASA's Global Land Data Assimilation System (GLDAS— Rodell et al, 2004) collapsed into daily climatic records over 1970-2018, and matched to the period of our gross regional output realizations (see §*Methods*). Burke et al (2015) used reconstruction data from the University of Delaware containing 0.5 degree gridded monthly average metrological fields over 1960-2010. Both studies account for heterogenous intra-country population allocation and spatially aggregate grid-cell-level weather exposure by province/country via a weighted collapsing method incorporating time-invariant sub-national population density statistics from the Gridded Population of the World dataset (2015 Version) (CIESIN, 2004).

b-c More flexible functional forms validate the non-linear shape of the global GDP-temperature relationship estimated from parametric FE-OLS in **a**. **b** Non-parametric unrestricted spline of average temperature estimated globally from a Generalized Additive Model (GAM). This has the advantage of reducing the number of parametric assumptions constraining the shape of complex predictor's responses via unrestricted smooth functions. **c** Semi-parametric restricted cubic splines with up to 3-8 Knots estimated globally. Knots are locations along a predictor variable's range where pieces of the smooth function join; and thus where the shape of the smooth function can change. Splines fit the data in sections divided by these Knots, with each section's shape adjusted to minimize error. **d** Parametric FE-OLS splines with up to 2-7 polynomial order in the calibration of the average temperature functional form. All regressions in **a-b-c-d**, whether parametric (**a, d**), non-parametric (**b**) or semi-parametric (**c**); include province-specific quadratic time trends in years of sample, province-by-year fixed effects and precipitation controls. All macro-econometric models (including the more flexible functional forms) yield similar non-linear global per capita GDP-temperature response functions to our main estimates. This suggests that the inverted-U shaped response function in our main specification is not an artifact of the parsimonious 2nd order polynomial.

e Global non-linearity is driven by differences in sub-national provinces' average temperature, not GDP. Orange dots and lines show the point estimate and 95% CI for the marginal effects of temperature on GDP per capita growth evaluated at different temperature baselines estimated from a model that interacts each province's year-to-year temperature fluctuation with its own average calculated across the sample period (i.e., $\delta y/\delta T_{r,i,t} = \hat{\beta}a + \hat{\beta}_b \cdot \overline{T}_r$). Orange dots and lines show equivalent estimates from a model that includes an interaction between annual temperature and average GDP per capita (i.e., $\delta y/\delta T_{r,i,t} = \hat{\beta}a + \hat{\beta}_b \cdot \overline{T}_r + \hat{\beta}_c \cdot \overline{y}_r$). Point estimates are similar across the two models, indicating that the non-linear response is not due to hot provinces being poorer on average. **f** Cumulative marginal effect of temperature on per capita GDP as additional lag-transformed temperature variables ($h(T_{r,i,t-p})$ with $p = [1, 3]$) are included. Solid points and lines indicate the sum of the contemporaneous and lagged marginal effects and its 95% CI at each temperature baseline. For all marginal effect models, standard errors are estimated from 1000 block-Bootstrap resampling iterations.

3.2 Projected macroeconomic damages

This section presents and decomposes the projection results on economic production.

Using Eq. (14), future epoch temperature values are combined with with our estimated parameters from Eqs. (10) and (11) to calibrate our projected economic impacts of the shifts in temperature exposure in both high- and moderate-warming scenarios (SSP5-8.5 and SSP2-4.5, respectively) distributed at both country and administrative province levels. While they differ in terms of economic trajectories and climate stringency forecasts, both set of climate models predict vigorous warming to cause substantially more extreme high temperature circa-2050. Explained in §2.2, a subset of 15 "likely" GCMs is selected for the main analysis to account for the 'hot model' problem (Hausfather et al, 2022). An exhaustive model classification of the full *ensemble* of 30 GCMs is provided in Table A.2.

Fig. 4 shows projected damages derived from SSP5-8.5 vigorous warming GCM simulation scenario. Note that in Panels **a-b**, estimates are econometrically structured from country-level climatic data matched with year-to-year per capita GDP realisations (*à la Burke et al (2015)*). Panel **a** Fig. 4 shows the spatial distribution of the multi-model median impacts from our ensemble of 15 "likely" SSP5-8.5 realizations globally. From changes in temperature alone, end-century median per capita GDP declines are recorded for the most countries with striking heterogenous magnitudes identified in the 5%-55% range, interspersed with isolated regions of negligible losses (0-5%), whereas the largest damages are concentrated in areas overlapping the tropics or near the equator (particularly central Africa, America and Asia). For most countries, strong agreement on net negative climate-shift effect on per capita GDP increasing as the absolute latitude of the country's centroids declines. This geographic pattern empirically confirms previous findings on the heterogenous distribution of climate change effects on crop yields across agro-climatic zones (Sue Wing et al, 2021). Some countries experience slightly net positive per capita GDP increases, which we link to the minimal average temperature baseline at which they are exposed to (i.e., the left-side of the inverted U-shape curve in panel **a** Fig. 2), and the comparatively lower temperature 'delta' (Δ) predicted by CMIP6 in these northern areas. Note that this conclusions holds even under the most vigorous (SSP5-8.5) warming scenario realization.

Panel **b** Fig. 4 graphically summarizes model response × temporal effect combinations of aggregate percentage per capita GDP impacts. With considerable magnitude, results reveal wide macroeconomic damages ranging at 17%, 25%, 50%, 70% by end-century, depending on the choice of differentiated/short-run, pooled/short-run, differentiated/long-run, pooled/long-run (respectively). Pooled versus differentiated implies that each income group is then allowed its own temperature-GDP response function. We empirically confirm that additionally accounting (long-run model) for lagged temperature regressors up to 5 years leaves larger cumulative per capita GDP changes. This indicates that long-persisting dynamic effects in the initial calibration of the temperature-output response function, in agreement with Kotz et al (2024)'s most recent conclusion. This is the section of this analysis that we now turn to.

The 2^{nd}-to-3^{rd} array of Fig. 4 looks more holistically at the spatial, temporal, climate model distribution of per capita GDP projected damages. Panels **c-g** show estimates econometrically structured from sub-national administrative region-level climatic data matched with year-to-year gross regional per capita product realisations (*à la Kotz et al (2024)*).

Panel **c** Fig. 4 shows the spatial distribution of the multi-model median impacts from our ensemble of 15 "likely" SSP5-8.5 realizations globally. From changes in temperature alone, province-level end-century median per capita GDP declines show further heterogeneity (compared to country-level in panel **a**) ranging from 5%-to-85%. We empirical confirm the regional patterns identified in the first array of Fig. 4, although per capita GDP losses are larger once we account for intra-country local climatic variability exposing some administrative provinces at higher risks than others in the future (Mahlstein et al, 2013). Some general pattern of particularly high zonal impacts include southern Europe, south western United States (US), western Mali, north Nigeria and tropical Asia.

Panel **d** Fig. 4 shows projected per capita GDP damages (%) globally averaged across provinces leaving point-level estimates from each of the 30 CMIP6 GCMs at epoch 2099. We find that SSP5-8.5 (red) vigorous GCMs exhibit structural differences in temperature simulations, thus enabling us to empirically confirm Hausfather et al (2022)'s observation of the 'hot model problem' from their most recent analysis of CMIP6 exercise outputs (see §2.2. SSP2-4.5 (orange) moderate GCMs exhibit similar

but more concentrated patterns of model-specific heterogeneity in the prediction of output damages.

Panel **e** Fig. 4 displays province-level mean trajectories of multi-model median projected damages (%) from 15 'likely' GCMs distributed across epochs' mid-points. Most sub-national administrative are strongly concentrated around the global mean (captured by the solid black line), prior to diverge with time (i.e., which correlates with increases in both temperature anomalies - level, and their distribution - space), as shown by the relatively wide inter-region × decade range of impacts in the latter epochs. Panel **f** Fig. 4 looks more holistically at the global region-averaged multi-model median projected changes in per capita GDP from 15 'likely' GCMs. Despite heterogenous province-level trajectories of damages shown earlier (Panel **a**, which we link to the persisting weight of local temperature shifts relative to country's average), continent-averages suggest net output losses increasing with time for all global regions. Damages are particularly striking for Africa, South and North America, while more moderated but still significant in Europe and Australia. Finally, panel **g** Fig. 4 compares projected impacts across FE-OLS model specifications (as in panel **b**: pooled/differentiated; short/long run. See §*Methods*), where shading represents the 34% and 10% confidence intervals reflecting the 'likely' and 'very likely' ranges of the GCMs (respectively) following Hausfather et al (2022)'s recommended procedure (see §2.2. In panel **b**, we empirically showed that when projected impacts are econometrically structured with lagged temperature regressors (up to 5 years), larger cumulative damages are observed. Panel **g** extends this finding by showing that not only does the model matters (i.e., response' stratification and temporal persistence of the temperature regressor's effect); but also the spatial resolution of the global GDP models (i.e., country×year (panels **a-b**) *à la Burke et al (2015)* versus province×year (panels **c-g**) *à la Kotz et al (2024)*) used to structure the projections. Our findings therefore concur with those of Kotz et al (2024) suggesting that computing climate damages from the local-provincial level, rather than aggregating by country, yields significantly higher estimates of economic losses, thus leaving large place for patterns of spatial differences. This stems from greater accuracy in capturing localized climate and economic heterogeneity, as our approach better accounts for small-scale variations in exposure to extreme climate impacts and gross regional economic vulnerability, particularly in

densely populated regions with higher exposure of infrastructures and sectors to climate risks and lower adaptive capacity. Aggregated, country-level estimates of climate damages may understate the true economic cost of future climate shocks.

In a SSP2-4.5 future, we will have smaller changes in temperature shifts. Figs. 6 and 5 show projected damages derived from an intermediate mid-point scenario between SSP5-8.5 vigorous & SSP2-4.5 moderate warmings as well as SSP2-4.5 moderate warming GCM realizations (respectively). Compared to Fig. 4, consistent patterns of projected per capita GDP damages are found but in a lower intensity extent and showing early signs of decreasing marginal damages (rather concave shapes after 2060). In Appendix, Figs. A.13-A.27 show more holistically SSP (SSP5-8.5, SSP5-8.5-2-4.5 mid-point, SSP2-4.5) $\times$ epochs combinations of spatially- and GCM-distributed per capita GDP projected impacts which exhibit declining intensity as we move from end-century (2081-2099) towards an earlier future (2041-2060 mid-century epoch).

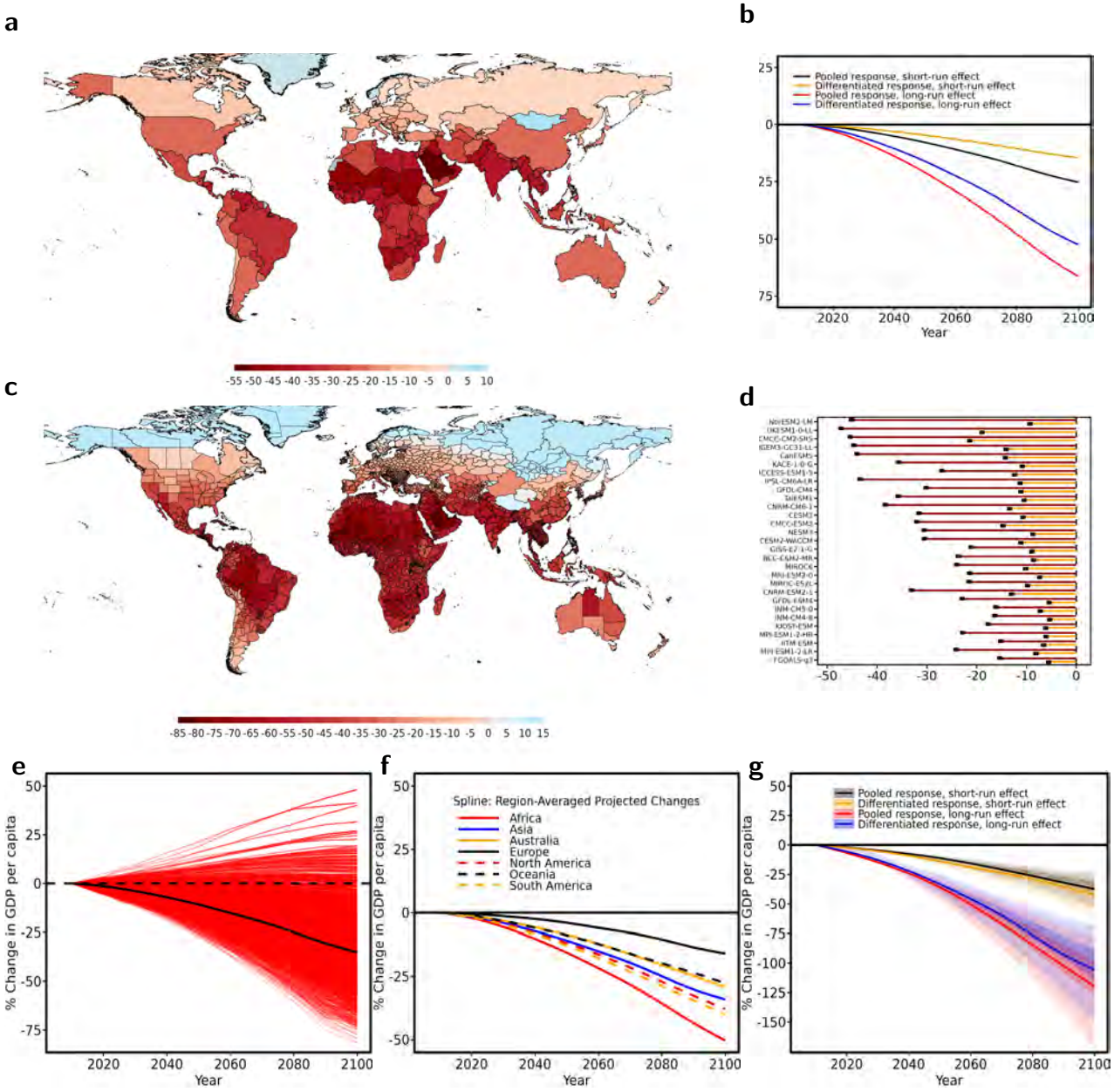

Figure 4: Projected climate-shift impacts (%) on per capita GDP, future epochs relative to constant historical 1985-2004 temperature means, SSP5-8.5 vigorous warming scenario, 15 'likely' CMIP6 global climate models (GCMs).

a Spatially distributed country-level multi-model medians of 15 'likely' CMIP6 Global Climate Models (GCMs) simulated impacts, epoch 2099, econometrically structured from country-level climatic data matched with year-to-year per capita GDP realisations (*à la Burke et al (2015)*). Chosen equation specification to calibrate the projections is pooled FE-OLS accounting for short-run temperature effects only. **b** Comparing projected damages across FE-OLS model specifications using the same econometric approach as in **a**: pooled versus differentiated (each income group is then allowed its own temperature-GDP response function); short run versus long run (the equation additionally accounts for lagged temperature regressors up to 5 years). See §*Methods*. **c** Spatially distributed province-level multi-model medians of 15 'likely' CMIP6 GCMs simulated estimates, epoch 2099, econometrically structured from sub-national administrative region-level climatic data matched with year-to-year gross regional per capita product realisations (*à la Kotz et al (2024)*, idem for **d-g**). Chosen equation specification to calibrate the projections is pooled FE-OLS accounting for short-run temperature effects only (idem for **d-f**). **d** Cross-region globally averaged projected damages (%), point-level estimates from each of the full set of 30 CMIP6 GCMs (including those falling inside and outside the 'likely' and 'very likely' ranges) at epoch 2099, SSP5-8.5 vigorous (red) versus SSP2-4.5 moderate (orange) warming scenarios. **e** Province-level mean trajectories of projected damages (%), multi-model medians of 15 'likely' CMIP6 GCMs. Black lines denote the global average. Impacts, in red, are normalised to 0 at epoch 2010. **f** Regionally averaged projected damages, multi-model medians of 15 'likely' CMIP6 GCMs. **g** Comparing projected damages across FE-OLS model specifications: pooled versus differentiated (each income group is allowed its own temperature-GDP response function); short run versus long run (the equation additionally specifies for lagged temperature regressors up to 5 years); see §*Methods*. Shading represents our exercise of intra-GCM subset stratification, where the 34% and 10% confidence intervals reflect the 'likely' and 'very likely' ranges (respectively) across the 15 GCMs that formed of the basis of our projections following Hausfather et al (2022)'s recommended procedure (see §2.2.)

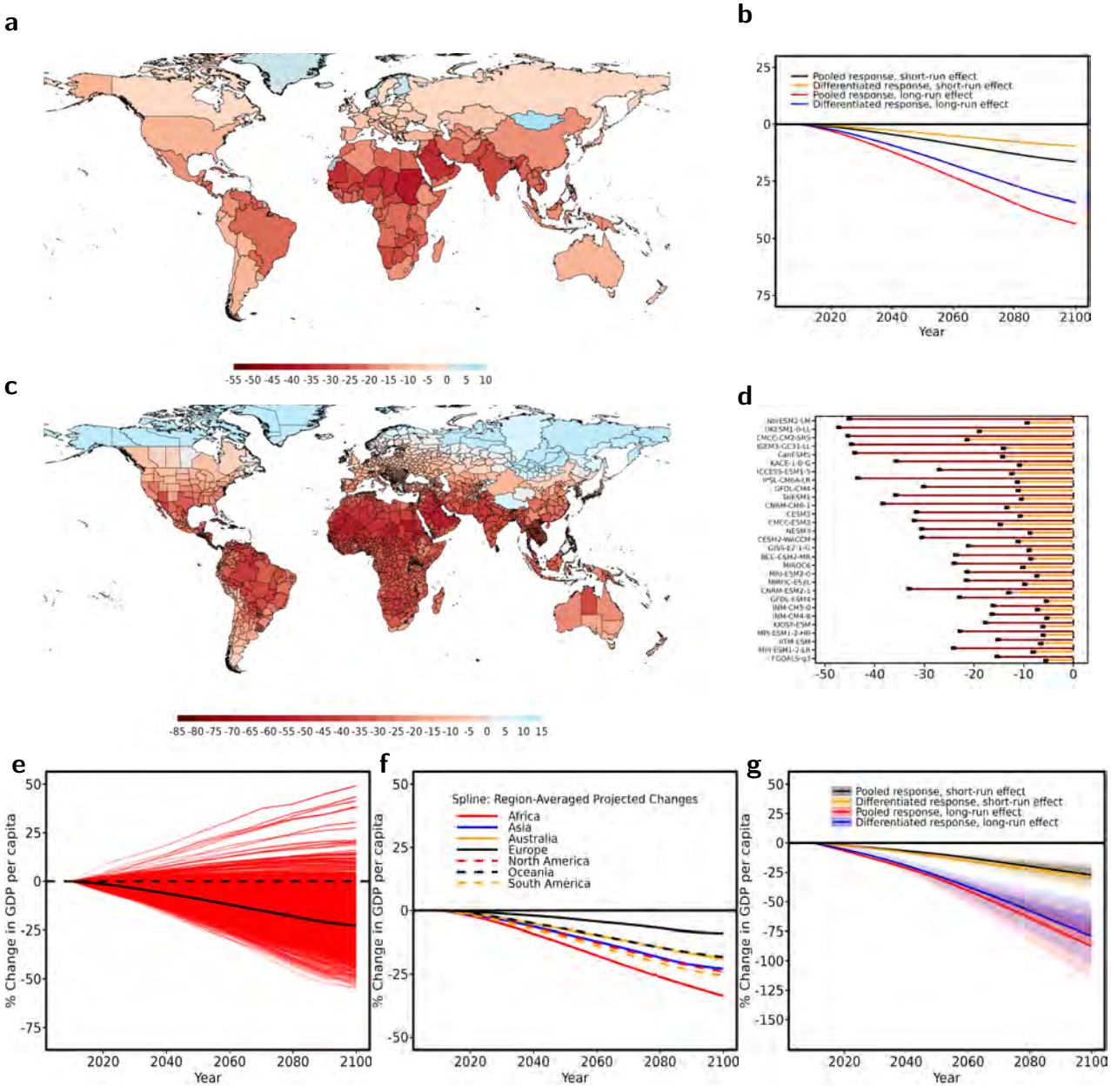

Figure 5: Projected climate-shift impacts (%) on per capita GDP, future epochs relative to constant historical 1985-2004 temperature means, intermediate mid-point scenario between SSP5-8.5 vigorous & SSP2-4.5 moderate warmings, 15 'likely' CMIP6 global climate models (GCMs).

a Spatially distributed country-level multi-model medians of 15 'likely' CMIP6 Global Climate Models (GCMs) simulated impacts, epoch 2099, econometrically structured from country-level climatic data matched with year-to-year per capita GDP realisations (*à la Burke et al (2015)*). Chosen equation specification to calibrate the projections is pooled FE-OLS accounting for short-run temperature effects only. **b** Comparing projected damages across FE-OLS model specifications using the same econometric approach as in **a**: pooled versus differentiated (each income group is then allowed its own temperature-GDP response function); short run versus long run (the equation additionally accounts for lagged temperature regressors up to 5 years). See §*Methods*. **c** Spatially distributed province-level multi-model medians of 15 'likely' CMIP6 GCMs simulated estimates, epoch 2099, econometrically structured from sub-national administrative region-level climatic data matched with year-to-year gross regional per capita product realisations (*à la Kotz et al (2024)*, idem for **d-g**). Chosen equation specification to calibrate the projections is pooled FE-OLS accounting for short-run temperature effects only (idem for **d-f**). **d** Cross-region globally averaged projected damages (%), point-level estimates from each of the full set of 30 CMIP6 GCMs (including those falling inside and outside the 'likely' and 'very likely' ranges) at epoch 2099, SSP5-8.5 vigorous (red) versus SSP2-4.5 moderate (orange) warming scenarios. **e** Province-level mean trajectories of projected damages (%), multi-model medians of 15 'likely' CMIP6 GCMs. Black lines denote the global average. Impacts, in red, are normalised to 0 at epoch 2010. **f** Regionally averaged projected damages, multi-model medians of 15 'likely' CMIP6 GCMs. **g** Comparing projected damages across FE-OLS model specifications: pooled versus differentiated (each income group is allowed its own temperature-GDP response function); short run versus long run (the equation additionally specifies for lagged temperature regressors up to 5 years); see §*Methods*. Shading represents our exercise of intra-GCM subset stratification, where the 34% and 10% confidence intervals reflect the 'likely' and 'very likely' ranges (respectively) across the 15 GCMs that formed of the basis of our projections following Hausfather et al (2022)'s recommended procedure (see §2.2.)

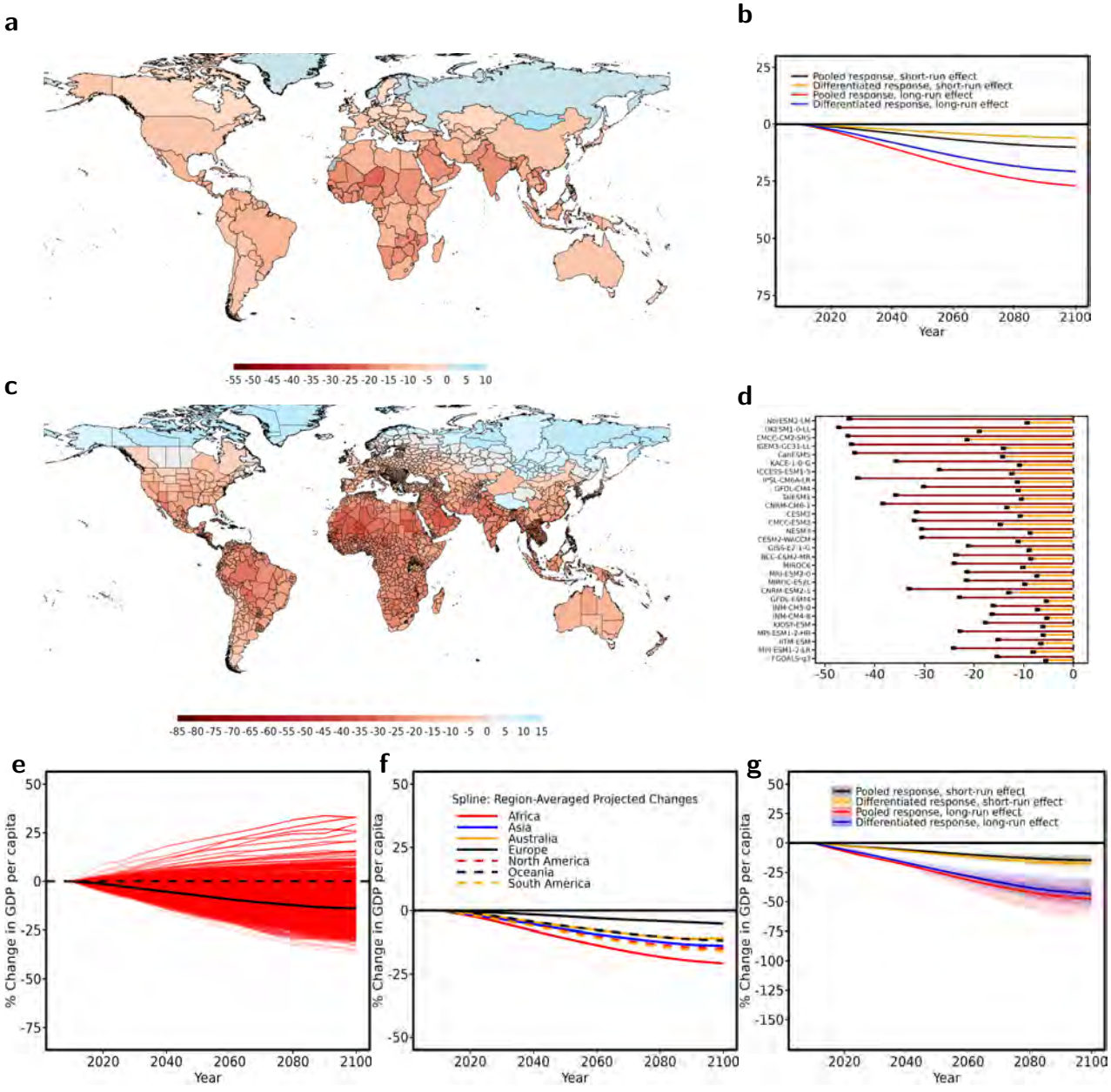

Figure 6: Projected climate-shift impacts (%) on per capita GDP, future epochs relative to constant historical 1985-2004 temperature means, SSP2-4.5 moderate warming scenario, 15 'likely' CMIP6 global climate models (GCMs).

a Spatially distributed country-level multi-model medians of 15 'likely' CMIP6 Global Climate Models (GCMs) simulated impacts, epoch 2099, econometrically structured from country-level climatic data matched with year-to-year per capita GDP realisations (*à la Burke et al (2015)*). Chosen equation specification to calibrate the projections is pooled FE-OLS accounting for short-run temperature effects only. **b** Comparing projected damages across FE-OLS model specifications using the same econometric approach as in **a**: pooled versus differentiated (each income group is then allowed its own temperature-GDP response function); short run versus long run (the equation additionally accounts for lagged temperature regressors up to 5 years). See §*Methods*. **c** Spatially distributed province-level multi-model medians of 15 'likely' CMIP6 GCMs simulated estimates, epoch 2099, econometrically structured from sub-national administrative region-level climatic data matched with year-to-year gross regional per capita product realisations (*à la Kotz et al (2024)*, idem for **d-g**). Chosen equation specification to calibrate the projections is pooled FE-OLS accounting for short-run temperature effects only (idem for **d-f**). **d** Cross-region globally averaged projected damages (%), point-level estimates from each of the full set of 30 CMIP6 GCMs (including those falling inside and outside the 'likely' and 'very likely' ranges) at epoch 2099, SSP5-8.5 vigorous (red) versus SSP2-4.5 moderate (orange) warming scenarios. **e** Province-level mean trajectories of projected damages (%), multi-model medians of 15 'likely' CMIP6 GCMs. Black lines denote the global average. Impacts, in red, are normalised to 0 at epoch 2010. **f** Regionally averaged projected damages, multi-model medians of 15 'likely' CMIP6 GCMs. **g** Comparing projected damages across FE-OLS model specifications: pooled versus differentiated (each income group is allowed its own temperature-GDP response function); short run versus long run (the equation additionally specifies for lagged temperature regressors up to 5 years); see §*Methods*. Shading represents our exercise of intra-GCM subset stratification, where the 34% and 10% confidence intervals reflect the 'likely' and 'very likely' ranges (respectively) across the 15 GCMs that formed of the basis of our projections following Hausfather et al (2022)'s recommended procedure (see §2.2.)

4 Discussion and conclusion

This paper elucidates the heterogeneity of countries' and subnational provinces' economic product responses to plausibly exogenous year-to-year fluctuations in temperature and precipitation using an unbalanced panel covering the 1970–2018 period. We draw on both the Penn World Tables version 10.01 (166 countries) and the MCC-PIK Database of Subnational Economic Output (1,661 regions), and attribute output responses to both weather fluctuations (the major propagation channels of climate change) and adaptation (which manifests itself over time in response to climate shift).

Our econometric approach is top-down and our identification strategy thus isolates most of time-series and cross-sectional variations in ambient climate measurements by exploiting the higher spatial resolution of the global administrative province-level economic dataset from Wenz et al (2023).

Both panel models approximate a global non-linear U-shaped temperature-per capita output response function, allowing us to extend Burke et al (2015)'s results - limited to countries - to sub-national administrative provinces, thus bridging with Kotz et al (2024), despite differences in the source, length and temporal/spatial resolution of the raw climatic field data prior aggregation. Again, our study uses daily 0.25 degree gridded surface weather fields from NASA's GLDAS whereas Burke et al (2015) used reconstruction data from the University of Delaware containing 0.5 degree gridded monthly average metrological fields over 1960-2010. Our results are robust to alternative (i) econometric estimators (parametric, semi-parametric, non-parametric), (ii) temperature functional forms (2^{nd}-to-8^{th} polynomial orders), (iii) specifications of the flexible trend function (i.e., includes increasing its Chebychev polynomial orders from quadratic to octic; and variation in its spatial clustering $z(i)$–from administrative areas level I to countries, and extending towards multi-country economic or geographic clusters likely to share that of a common trending effect).

We project climate change-driven damages in per capita GDP by combining our non-linear responses estimated over the period 1970-2018 with an ensemble of NEX-GDDP CMIP6 simulations from 30 distinct global climate models (GCMs).

Results draw two important conclusions. First, our study provides a basis for producing spatially disaggregated projections of climate change-induced economic damages

that consistently encompass the majority of administrative regions responsible for 95% of global economic production. Second, we show that accounting for small-scale variations in localized climatic exposure and intra-country economic heterogeneity yields aggregated losses that fundamentally alter the conclusions of previous global GDP models. We do find substantial agreement among GCMs on average end-century per capita declines of <75% from temperature shifts alone - with the largest effects in regions bordering the equator and the tropics (i.e., West Africa, Central America, South Asia), under a vigorous SSP5-8.5 warming scenario. However, while in generally good agreement with Burke et al (2015)'s country-level projections, our province-level calibrated per capita GDP changes show systematically larger mean values.

We suggest that country-level estimates of climate damages from Burke et al (2015) may have underestimated the true economic cost of future climate shocks, in line with Kotz et al (2024)'s conclusion. Moreover, the findings highlight substantial variability in projected macroeconomic damages based on econometric calibration choices. While pooled and stratified approaches yield comparable patterns, our empirical analysis shows that incorporating lagged temperature regressors—extending up to five years—results in significantly larger cumulative changes in per capita GDP. This underscores the importance of capturing long-term dynamic effects in the initial calibration of the temperature-output response function, while bridging with the recent findings of Kotz et al (2024).

Our study provides a basis for making more regionally localised projections of climate change-induced economic damages but is not without caveats. Caveats are primarily associated with the competitively higher spatial resolution of global data set of reported sub-national economic output (DOSE) (Wenz et al, 2023) that was derived by assembling values from numerous statistical agencies and yearbooks prior to apply harmonisation methods free of linear interpolations. First, the 'reported' nature of the DOSE project implies that its internal validity is inherently limited by the accuracy of national and regional administrations in displaying their economic output. Despite the increased spatial and temporal coverage of DOSE in comparison to most pre-existing datasets, data gaps in both dimensions remain, and so the use of satellite-derived data products could be a promising avenue for filling out these gaps. *Spatially*, sub-national output data for a large number of African and Middle-Eastern countries, suggesting a

sampling skewed towards relatively wealthier western regions (over-represented), and leaving an incomplete geographic coverage globally. It is an obstacle faced by Kotz et al (2024); which we addressed in the projection stage following a two-stage method described in §2.2. *Temporally*, DOSE tends to be unbalanced with the majority of observations taking place over the last three decades of coverage (1990–2020) compared to the earlier decades (1960–1990). A final limitation is that converting sub-national nominal GRP values in local currencies to real GRP data in USD is not straight-forward, partly due to the lack of auxiliary data at the sub-national level (i.e., GDP deflators are generally unavailable at the global scale).

Moreover, historical fields from NASA's Global Land Data Assimilation System (GLDAS— Rodell et al, 2004) may suffer from limitations associated with the relatively coarse spatial resolution (0.25 deg. grid) of this dataset which incompletely captures localized hydrological processes. For instance, used land surface models (Noah-LSM, VIC) rely on parametrization that oversimplify our representation of complex processes, soil properties (e.g., satellite-based soil moisture or snow cover data) and vegetation types, whereas its atmospheric forcing data (e.g., precipitation, temperature, radiation) from reanalysis may propagate measurement errors throughout the system (Viviers et al, 2024). Similar arguments limit the accuracy of NEX-GDDP CMIP6's ensemble of 29 global climate models (GCMs) simulated under the Coupled Model Intercomparison, Phase VI (CMIP6— Eyring et al, 2016) exercise. Certain feedbacks, such as those involving ice-sheet dynamics or vegetation-atmosphere interactions, are either poorly represented or absent (Zelinka et al, 2020). This explains the *'hot model problem'* discussed earlier in §2.2 of the paper. Other remaining sources of uncertainty propagation are attributable to downscaling and bias-correction which might potentially alter local climate projections in CMIP6 (Lafferty et al, 2023). A more exhaustive discussion on the limits of the methodologies used to construct the GLDAS, NEX-GDDP and DOSE datasets and their recommended usage is provided in Appendix, §A.1.

Declaration of competing interest

The author declares that he has no competing interests, and specifically, that he has no financial and personal relationships with other people or organizations that could inappropriately influence (bias) his work such as, but not limited to, employment, consultancies, stock ownership, honoraria, paid expert testimony, patent applications and registrations, and grants or other funding.

Acknowledgement

The author gratefully acknowledges support from the EDHEC Climate Institute (ECI), and particularly Riccardo Rebonato, Lionel Melin and Frederic Ducoulombier for their useful guidance and feedback.

Data and code

Climate data from GLDAS and NASA-NEX GDDP (CMIP6 GCMs) are available from their corresponding data portals linked in the paper. Macroeconomic data from DOSE, WDI and PWT are available from their corresponding data portals linked in the paper. The processed data and associated spatially distributed macroeconomic damages across CMIP6 GCMs and warming scenarios are available in the form of .csv files upon request to the author.

References

[1] Allen, M. R., Fernandez, S. J., Fu, J. S., & Olama, M. M. (2016). Impacts of climate change on sub-regional electricity demand and distribution in the southern United States. Nature Energy, 1(8), 1-9.

[2] Angrist, J. D., & Pischke, J. S. (2009). Mostly harmless econometrics: An empiricist's companion. Princeton university press.

[3] Anthoff, D., & Tol, R. S. (2013). The uncertainty about the social cost of carbon: A decomposition analysis using fund. Climatic change, 117, 515-530.

[4] Auffhammer, M., & Aroonruengsawat, A. (2011). Simulating the impacts of climate change, prices and population on California's residential electricity consumption. Climatic change, 109, 191-210.

[5] Auffhammer, M., Hsiang, S. M., Schlenker, W., & Sobel, A. (2013). Using weather data and climate model output in economic analyses of climate change. Review of Environmental Economics and Policy.

[6] Auffhammer, M., Baylis, P., & Hausman, C. H. (2017). Climate change is projected to have severe impacts on the frequency and intensity of peak electricity demand across the United States. Proceedings of the National Academy of Sciences, 114(8), 1886-1891.

[7] Auffhammer, M. (2022). Climate Adaptive Response Estimation: Short and long run impacts of climate change on residential electricity and natural gas consumption. Journal of Environmental Economics and Management, 114, 102669.

[8] Barro, R. J. (2003). Determinants of economic growth in a panel of countries. Annals of economics and finance, 4, 231-274.

[9] Blanc, E., Schlenker, W. (2017). The use of panel models in assessments of climate impacts on agriculture. Review of Environmental Economics and Policy.

[10] Bodirsky, B. L., Rolinski, S., Biewald, A., Weindl, I., Popp, A., & Lotze-Campen, H. (2015). Global food demand scenarios for the 21 st century. PloS one, 10(11), e0139201.

[11] Burke, M., Emerick, K., 2016. Adaptation to climate change: Evidence from US agriculture. American Economic Journal: Economic Policy, 8, 3, 106-40.

[12] Burke, M., & Tanutama, V. (2019). Climatic constraints on aggregate economic output (No. w25779). National Bureau of Economic Research.

[13] Burke, M., Hsiang, S. M., & Miguel, E. (2015). Global non-linear effect of temperature on economic production. Nature, 527(7577), 235-239.

[14] Callahan, C. W., & Mankin, J. S. (2022). Globally unequal effect of extreme heat on economic growth. Science Advances, 8(43), eadd3726.

[15] Cameron, A. C., Gelbach, J. B., & Miller, D. L. (2011). Robust inference with multiway clustering. Journal of Business & Economic Statistics, 29(2), 238-249.

[16] CIESIN, C. (2004). Gridded Population of the World (GPW), Version 3. Center for International Earth Science Information Network and Columbia University and Centro Internacional de Agricultura Tropical and Palisades. CIESIN, Columbia University, NY.

[17] Coffey, B., Stern, A., & Wing, I. S. (2015, January). Climate change impacts on us electricity demand: Insights from micro-consistent aggregation of a structural model. In International Energy Workshop (pp. 1-34). University of South Carolina.

[18] Dell, M., Jones, B. F., & Olken, B. A. (2009). Temperature and income: reconciling new cross-sectional and panel estimates. American Economic Review, 99(2), 198-204.

[19] Dell, M., Jones, B. F., & Olken, B. A. (2012). Temperature shocks and economic growth: Evidence from the last half century. American Economic Journal: Macroeconomics, 4(3), 66-95.

[20] Dell, M., Jones, B. F., & Olken, B. A. (2014). What do we learn from the weather? The new climate-economy literature. Journal of Economic literature, 52(3), 740-798.

[21] Deryugina, T., & Hsiang, S. M. (2014). Does the environment still matter? Daily temperature and income in the United States (No. w20750). National Bureau of Economic Research.

[22] Deschênes, O., & Greenstone, M. (2011). Climate change, mortality, and adaptation: Evidence from annual fluctuations in weather in the US. American Economic Journal: Applied Economics, 3(4), 152-185.

[23] Drupp, M. A., Freeman, M. C., Groom, B., & Nesje, F. (2018). Discounting disentangled. American Economic Journal: Economic Policy, 10(4), 109-134.

[24] Eyring, V., Bony, S., Meehl, G. A., Senior, C. A., Stevens, B., Stouffer, R. J., & Taylor, K. E. (2016). Overview of the Coupled Model Intercomparison Project Phase 6 (CMIP6) experimental design and organization. Geoscientific Model Development, 9(5), 1937-1958. Bulletin of the American Meteorological society, 85(3), 381-394.

[25] Feenstra, R. C., Inklaar, R., & Timmer, M. P. (2015). The next generation of the Penn World Table. American economic review, 105(10), 3150-3182.

[26] Foley, J. A., DeFries, R., Asner, G. P., Barford, C., Bonan, G., Carpenter, S. R., ... & Snyder, P. K. (2005). Global consequences of land use. science, 309(5734), 570-574.

[27] Franco, G., & Sanstad, A. H. (2008). Climate change and electricity demand in California. Climatic Change, 87(Suppl 1), 139-151.

[28] Gennaioli, N., & La Porta, R. (2014). Florencio Lopez De Silanes & Andrei Shleifer. J Econ Growth, 19, 259-309.

[29] Graff Zivin, J., & Neidell, M. (2014). Temperature and the allocation of time: Implications for climate change. Journal of Labor Economics, 32(1), 1-26.

[30] Graff Zivin, J., Hsiang, S. M., & Neidell, M. (2018). Temperature and human capital in the short and long run. Journal of the Association of Environmental and Resource Economists, 5(1), 77-105.

[31] Granger, C. W., & Newbold, P. (1974). Spurious regressions in econometrics. Journal of econometrics, 2(2), 111-120.

[32] Haqiqi, I., Grogan, D. S., Hertel, T. W., Schlenker, W. (2021). Quantifying the impacts of compound extremes on agriculture. Hydrology and Earth System Sciences, 25(2), 551-564.

[33] Hausfather, Z., Marvel, K., Schmidt, G. A., Nielsen-Gammon, J. W., & Zelinka, M. (2022). Climate simulations: recognize the 'hot model' problem. Nature, 605(7908), 26-29.

[34] Heal, G., & Park, J. (2013). Feeling the heat: Temperature, physiology & the wealth of nations (No. w19725). National Bureau of Economic Research.

[35] Hsiang, S. M., & Jina, A. S. (2014). The causal effect of environmental catastrophe on long-run economic growth: Evidence from 6,700 cyclones (No. w20352). National Bureau of Economic Research.

[36] Hsiang, S. M., Burke, M., & Miguel, E. (2013). Quantifying the influence of climate on human conflict. Science, 341(6151), 1235367.

[37] Hsiang, S. M. (2010). Temperatures and cyclones strongly associated with economic production in the Caribbean and Central America. Proceedings of the National Academy of sciences, 107(35), 15367-15372.

[38] Kalkuhl, M., & Wenz, L. (2020). The impact of climate conditions on economic production. Evidence from a global panel of regions. Journal of Environmental Economics and Management, 103, 102360.

[39] Kotz, M., Wenz, L., Stechemesser, A., Kalkuhl, M., & Levermann, A. (2021). Day-to-day temperature variability reduces economic growth. Nature Climate Change, 11(4), 319-325.

[40] Kotz, M., Levermann, A., & Wenz, L. (2022). The effect of rainfall changes on economic production. Nature, 601(7892), 223-227.

[41] Kotz, M., Levermann, A., & Wenz, L. (2024). The economic commitment of climate change. Nature, 628(8008), 551-557.

[42] Lafferty, D. C., & Sriver, R. L. (2023). Downscaling and bias-correction contribute considerable uncertainty to local climate projections in CMIP6. npj Climate and Atmospheric Science, 6(1), 158.

[43] Mahlstein, I., Daniel, J. S., & Solomon, S. (2013). Pace of shifts in climate regions increases with global temperature. Nature Climate Change, 3(8), 739-743.

[44] Massetti, E., Mendelsohn, R. (2020). Temperature thresholds and the effect of warming on American farmland value. Climatic Change, 161(4), 601-615.

[45] McIntosh, C. T., & Schlenker, W. (2006). Identifying non-linearities in fixed effects models. UC-San Diego Working Paper.

[46] Meinshausen, M., Nicholls, Z. R., Lewis, J., Gidden, M. J., Vogel, E., Freund, M., ... & Wang, R. H. (2020). The shared socio-economic pathway (SSP) greenhouse gas concentrations and their extensions to 2500. Geoscientific Model Development, 13(8), 3571-3605.

[47] Mendelsohn R., Massetti E. (2017). The use of cross-sectional analysis to measure climate impacts on agriculture: theory and evidence. Review of Environmental Economics and Policy.

[48] Millar, R. J., Nicholls, Z. R., Friedlingstein, P., & Allen, M. R. (2017). A modified impulse-response representation of the global near-surface air temperature and atmospheric concentration response to carbon dioxide emissions. Atmospheric Chemistry and Physics, 17(11), 7213-7228.

[49] Miller, N. L., Hayhoe, K., Jin, J., & Auffhammer, M. (2008). Climate, extreme heat, and electricity demand in California. Journal of Applied Meteorology and Climatology, 47(6), 1834-1844.

[50] Moore, F. C., & Diaz, D. B. (2015). Temperature impacts on economic growth warrant stringent mitigation policy. Nature Climate Change, 5(2), 127-131.

[51] Newell, R. G., Pizer, W. A., & Prest, B. C. (2022). A discounting rule for the social cost of carbon. Journal of the Association of Environmental and Resource Economists, 9(5), 1017-1046.

[52] Nordhaus, W. D. (2006). Geography and macroeconomics: New data and new findings. Proceedings of the National Academy of Sciences, 103(10), 3510-3517.

[53] Nordhaus, W. D. (2017). Revisiting the social cost of carbon. Proceedings of the National Academy of Sciences, 114(7), 1518-1523.

[54] Orlowsky, B., & Seneviratne, S. I. (2012). Global changes in extreme events: regional and seasonal dimension. Climatic change, 110, 669-696.

[55] Ortiz-Bobea, A., Wang, H., Carrillo, C. M., Ault, T. R. (2019). Unpacking the climatic drivers of US agricultural yields. Environmental Research Letters, 14(6), 064003.

[56] Pindyck, R. S. (2013). Climate change policy: what do the models tell us?. Journal of Economic Literature, 51(3), 860-872.

[57] Rennert, K., Errickson, F., Prest, B. C., Rennels, L., Newell, R. G., Pizer, W., ... & Anthoff, D. (2022). Comprehensive evidence implies a higher social cost of CO2. Nature, 610(7933), 687-692.

[58] Ricke, K., Drouet, L., Caldeira, K., & Tavoni, M. (2018). Country-level social cost of carbon. Nature Climate Change, 8(10), 895-900.

[59] Rodell, M., Houser, P. R., Jambor, U. E. A., Gottschalck, J., Mitchell, K., Meng, C. J., ... & Toll, D. (2004). The global land data assimilation system. Bulletin of the American Meteorological society, 85(3), 381-394.

[60] Romitti, Y., & Sue Wing, I. (2022). Heterogeneous climate change impacts on electricity demand in world cities circa mid-century. Scientific reports,12, (1), 4280.

[61] Schlenker, W., Lobell, D. B. (2010). Robust negative impacts of climate change on African agriculture. Environmental Research Letters, 5(1), 014010.

[63] Schlenker, W., & Roberts, M. J. (2009). Nonlinear temperature effects indicate severe damages to US crop yields under climate change. Proceedings of the National Academy of sciences, 106(37), 15594-15598.

[63] Schlenker, W., Roberts, M. J. (2009). Nonlinear temperature effects indicate severe damages to US crop yields under climate change. Proceedings of the National Academy of sciences, 106(37), 15594-15598.

[64] Schlenker, W., & Walker, W. R. (2016). Airports, air pollution, and contemporaneous health. The Review of economic studies, 83(2), 768-809.

[65] Seo, S. N., Mendelsohn, R., Dinar, A., Hassan, R., Kurukulasuriya, P. (2009). A Ricardian analysis of the distribution of climate change impacts on agriculture across agro-ecological zones in Africa. Environmental and Resource Economics, 43, 313-332.

[66] Sherwood, S. C., Webb, M. J., Annan, J. D., Armour, K. C., Forster, P. M., Hargreaves, J. C., ... & Zelinka, M. D. (2020). An assessment of Earth's climate sensitivity using multiple lines of evidence. Reviews of Geophysics, 58(4), e2019RG000678.

[67] Wing, I. S., De Cian, E., & Mistry, M. N. (2021). Global vulnerability of crop yields to climate change. Journal of Environmental Economics and Management, 109, 102462.

[68] Tokarska, K. B., Stolpe, M. B., Sippel, S., Fischer, E. M., Smith, C. J., Lehner, F., & Knutti, R. (2020). Past warming trend constrains future warming in CMIP6 models. Science advances, 6(12), eaaz9549.

[69] Viviers, C., van der Laan, M., Gaffoor, Z., & Dippenaar, M. (2024). Downscaling and validating GLDAS groundwater storage anomalies by integrating precipitation for recharge and actual evapotranspiration for discharge. Journal of Hydrology: Regional Studies, 54, 101879.

[70] Wenz, L., Carr, R. D., Kögel, N., Kotz, M., & Kalkuhl, M. (2023). DOSE–Global data set of reported sub-national economic output. Scientific Data, 10(1), 425.

[71] Willmott, C. J., & Matsuura, K. (2012). Terrestrial air temperature and precipitation: Monthly and annual time series (1900–2010). Data Retrieved From: http://climate.geog.udel.edu/âĹijclimate/htmlpages/Global2011/README.GlobalTsT2011.html.

[72] Wood, S. N. (2004). Stable and efficient multiple smoothing parameter estimation for generalized additive models. Journal of the American Statistical Association, 99(467), 673-686.

[73] Zelinka, M. D., Myers, T. A., McCoy, D. T., Po Chedley, S., Caldwell, P. M., Ceppi, P., ... & Taylor, K. E. (2020). Causes of higher climate sensitivity in CMIP6 models. Geophysical Research Letters, 47(1), e2019GL085782.

A Appendix - For Online Publication

'The Global Geography of Long-Term Projected Macroeconomic Damages from Chronic Physical Climate Risk: Country vs. Intra-Country Distribution'

Contents

A.1 Supplementary data discussion

This section discusses the limits of the methodologies used to construct the GLDAS, NEX-GDDP and DOSE datasets as well as their recommended usage.

A valid concern can arise from the statistical downscaling methodology employed in NASA's Earth Exchange Global Daily Downscaled Projections (NEX-GDDP CMIP6— Eyring et al, 2016) which does not adequately account for the effects of local land use changes (e.g., urban heat island effects or deforestation impacts), topography or highly localized climate dynamics (Zhang et al, 2024). This is particularly pronounced in regions with complex terrain or limited observational data such as high-altitude areas (Wu et al, 2023). Moreover, the literature has highlighted some models' tendency in underestimating precipitation in humid regions and overestimating temperature in arid zones, with for instance the multi-model ensemble (MME) simulations showing biased accuracy of resulting indices of drought and evapotranspiration in China (particularly in the Qinghai–Tibet Plateau and central Xinjiang, where observational data are sparse) (Liu et al, 2024). Climate extremes uncertainty (e.g, droughts or heavy rainfall) are incompletely solved due to limitations in the multi-model averaging process which over-homogenize (dampen) performance and sort out some of the frequency and intensity of extreme event variability crucial to impact assessments (like in the present study) (Dioha et al, 2024). Note that the downscaling itself introduces additional challenges in correctly capturing drought indices. While indices like SPI (Standardized Precipitation Index) perform better in specific regions, others like SPEI (Standardized Precipitation Evapotranspiration Index) may misrepresent conditions due to biases in the input climate variables (zhai et al, 2020). Temporal heterogeneity biases stem from a likely mismatch in seasonal and annual trends. While the models effectively reproduce long-term warming trends, they struggle to accurately represent inter-annual variability and seasonal cycles. This issue is particularly prominent in monsoon regions, where precipitation trends are seasonal specific-humidity is high (Sylvestre et al, 2024). Research directions to improve both spatial and temporal accuracy include dynamic downscaling methods that incorporate physical mechanisms (i.e., topography and land-atmosphere interactions) and advanced ensemble techniques (i.e., Bayesian model averaging).

Data from NASA's Global Land Data Assimilation System (GLDAS— Rodell et al, 2004), which relies on observation-based meteorological forcing precipitation and radiation data, suffer from similar limitations ranging from resolution constraints, forcing data quality, temporal coverage, model simplifications, validation of uncertainty and an inadequate representation of human activities (Mistry, 2019). GLDAS uses multiple land surface models (e.g., Noah, CLM, and Mosaic) which employ simplified representations of physical processes (e.g., assumptions in soil moisture dynamics or vegetation parameters might not reflect actual conditions). Also, processes like irrigation, urbanization, and land management are either oversimplified or excluded in some models; which may lead to inaccuracies in regions were the feedback effect of anthropogenic activities is significant (Gu et al, 2019). While validation of GLDAS outputs against independent regional/global datasets is ongoing, discrepancies often arise due to differences in spatial resolution, data sources, or model physics (Viviers et al, 2024). For instance, Ji et al (2015) compare the GLDAS daily surface air temperature at 0.25 deg. gridded resolution with two reference datasets: (a) Daymet data (2002 and 2010) for the conterminous U.S. at 1-km gridded resolution and (b) global meteorological observations (2000) from the Global Historical Climatology Network (GHCN). Other limitations such as larger uncertainty in the surface air temperature estimates over high mountainous areas are well documented in the literature, as well as missing data in the grid-cells close to water bodies (which can be filled using the appropriate interpolating technique: bilinear, near neighbour or inverse-distance mapping). Users of the GLDAS-derived data products in econometric analyses (De Cian et al, 2019; Sue Wing et al, 2021) have recommended to pay attention to these caveats.

The global data set of reported sub-national economic output (DOSE) (Wenz et al, 2023) exhibits several caveats, including temporal and spatial inconsistencies (i.e., only 83 countries are represented) mentioned earlier in the paper. See Fig. A.1 for a look at the spatial coverage of administrative province-level per capita GDP time-series data (fraction of countries) in the raw DOSE product. Although the dataset harmonizes data for aggregate and sectoral outputs, variations in sectoral reporting standards across countries may introduce biases in sector-specific analyses. DOSE aggregates information and presents both the advantage and the drawback of be-

ing strictly grounded in reported macroeconomic values from heterogeneous national statistical offices and yearbooks (i.e., Wenz et al (2023) voluntarily excluded interpolation methods to fill out missing data); which limits the continuous nature of time series in under-reported provinces. Finally, boundary consistency challenges remain due to historical change leading to mismatches when we integrate with geospatial climate information in §2.2. A relevant assessments of the social cost of carbon (SCC) implications of reduced-form steeper damage functions estimated from DOSE can be found in Wenz et al (2024).

A.2 Identifying non-linearities in a fixed effects model

McIntosh and Schlenker (2006) demonstrated that structuring a fixed-effects model with a higher-order polynomial temperature function allows a mix of within-country and cross-country sources of variation to play out. Contrary to the standard interpretation wherein fixed effects models are identified solely by deviations from the group mean, a quadratic explanatory variable causes group means to re-enter the identification which has implications for our global GDP econometric model. A summary of the formalization is presented below.

One can algebraically demonstrate that a quadratic term in the fixed effects estimator captures non-linearity between units.Let $x_{i,t}$ in group i in period t to be covariate drawn from a distribution with group mean μ_i. Assuming the true data-generating process can be written as:

$$y_{i,t} = \beta_1 x_{i,t} + \beta_2 x_{i,t}^2 + \beta_3 (x_{i,t} - \mu_i)^2 + c_i + \epsilon_{i,t} \tag{17}$$

This specification incorporates three distinct channels through which $y_{i,t}$ can display a non-linear association with $x_{i,t}$. The first mechanism involves the potential non-linear dependence of the fixed effects (c_i) on the covariate, or alternatively, the possibility that the conditional mean of the outcome across units exhibits convexity or concavity in the distribution of x. To evaluate this, one could perform a dummy-variable fixed effect regression and subsequently examine the relationship between the dummy coefficients and the group-specific averages of x. Nevertheless, since the primary objective of employing the within transformation is to eliminate c_i from the outcomes, we presume that such convexity lies outside the focus of researchers utilizing fixed-effects models and therefore omit it from further analysis.

The two critical types of non-linearities pertinent to fixed-effects models are the global non-linearity stemming from a quadratic relationship in $x_{i,t}$ and the within-unit non-linearity originating from a quadratic term in $(x_{i,t} - \mu_i)$. Specifically, if $\beta_3 = 0$ in Eq. 17, the model simplifies to a quadratic functional form with fixed effects, a structure extensively examined in prior studies and referred to here as the *global* model. Conversely, if $\beta_2 = 0$, the specification includes only deviations from the group mean, which we denote as the *within* model. Finally, the *hybrid* model

extends this framework by allowing both β_2 and β_3 to take non-zero values.
Consider the standard estimate of the *global* model:

$$y_{it} = \beta_1 x_{it} + \beta_2 x_{it}^2 + c_i + \varepsilon_{it} \tag{18}$$

The key insight into the difference between global and within non-linearity comes from the fact that equation Eq. (18) first squares the covariate and then demeans it. Recall that

$$\mu_i = \mathbb{E}[x_{it} \mid i], \quad \text{which can be estimated by } \bar{x}_i = \frac{1}{T}\sum_{t=1}^{T} x_{it}.$$

To fix notation, let $\tilde{x}_{it} = x_{it} - \bar{x}_i$ and $\tilde{x}_i^2 = \frac{1}{T}\sum_{t=1}^{T} x_{it}^2$. The quantity which we arrive at by squaring and then demeaning, which we denote by $\ddot{x}_{it}^2$, can be written as

$$\ddot{x}_{it}^2 = [x_{it} - \bar{x}_i + \bar{x}_i]^2 - \bar{x}_i^2 = \tilde{x}_{it}^2 + 2\tilde{x}_{it}\bar{x}_i + [\bar{x}_i]^2 - \bar{x}_i^2.$$

In other words, the canonical use of non-linear fixed effects given by Eq. (18) does not measure non-linearity within units, as the terminology used to describe the estimator might suggest, because $\ddot{x}_{it}^2$ is in general not equal to $\tilde{x}_{it}^2$. Further, we see that by squaring the covariate before demeaning it, we re-introduce a function of the mean of the covariate into the identification.
What does the standard non-linear fixed effects estimator measure? A simple way to see this is to use our DGP to write out the mean of the outcome for each fixed effect unit. Taking averages over group i one gets:

$$\bar{y}_i = \beta_1 \bar{x}_i + \beta_2 \bar{x}_i^2 + \beta_3 (x_{it} - \mu_i)^2 + c_i + \varepsilon_i \tag{19}$$

First noting that

$$(x_{it} - \mu_i)^2 - (x_{it} - \mu_i)^2 = \tilde{x}_{it}^2 - 2x_{it}\mu_i + \mu_i^2 = \frac{1}{T}\sum_{t=1}^{T}\left[x_{it}^2 - 2x_{it}\mu_i + \mu_i^2\right] =$$

$$x_{it}^2 - 2x_{it}\mu_i + \mu_i^2 - \bar{x}_i^2 + 2\bar{x}_i\mu_i - \mu_i^2 = \tilde{x}_{it}^2 - 2x_{it}\mu_i.$$

We can subtract Eq. (19) from Eq. (17) to give an explicit representation of both

the global and the within variation in the conditional mean as:

$$\mathbb{E}[y_{it} \mid x_{it}] = \beta_1 \bar{x}_i + \beta_2 \bar{x}_i^2 + \beta_3 \Big[\tilde{x}_{it}^2 - \bar{x}_i^2\Big] \tag{20}$$

$$= \Big[\beta_1 - 2\beta_3 \mu_i\Big] \tilde{x}_{it} + \Big[\beta_2 + \beta_3\Big] \tilde{x}_{it}^2 \tag{21}$$

$$= \Big[\beta_1 + 2\beta_2 \mu_i\Big] \tilde{x}_{it} + \Big[\beta_2 + \beta_3\Big] \tilde{x}_{it}^2 - \Big[\bar{x}_i^2 - \mu_i^2\Big]. \tag{22}$$

Several notable aspects emerge regarding the practical application of non-linear functional forms with fixed effects, as highlighted by these equations. Equation Eq. (20) specifies the appropriate model to simultaneously account for both global and within-unit non-linearities. When the two types of non-linearity are expressed in the additively separable form outlined in Eq. (17), it becomes necessary to incorporate two distinct squared terms: the squared demeaned variable, which captures *global* non-linearities, and the demeaned squared variable, which accounts for *within-group* non-linearities. This combined approach is referred to as the *hybrid estimator*.

Eq. (21) and Eq. (22) demonstrate the implications of using a model that is misspecified by including only one type of non-linearity as a regressor while the other is also present in the data-generating process (DGP). Eq. (21) reveals that estimating Eq. (18) in the presence of within-group non-linearities can induce bias not only in the estimation of the quadratic coefficient but also in the linear coefficient. To accurately recover global non-linearity, it is essential to square the covariate and subsequently demean it, provided that within-group non-linearity is absent from the data. In such cases, $\beta_3 = 0$, leading to the recovery of $b_1 = \beta_1$ and $b_2 = \beta_2$.

Eq. (22) addresses the opposite scenario, illustrating that a model which accounts only for within-group non-linearity will be misspecified unless $\beta_2 = 0$, indicating the absence of global non-linearity in the DGP. When $\beta_2 \neq 0$, the presence of global non-linearity introduces potential bias into both the linear and quadratic terms. For an extended review of this methodological issue, see the reference paper McIntosh and Schlenker (2006).

A.3 Tables and figures

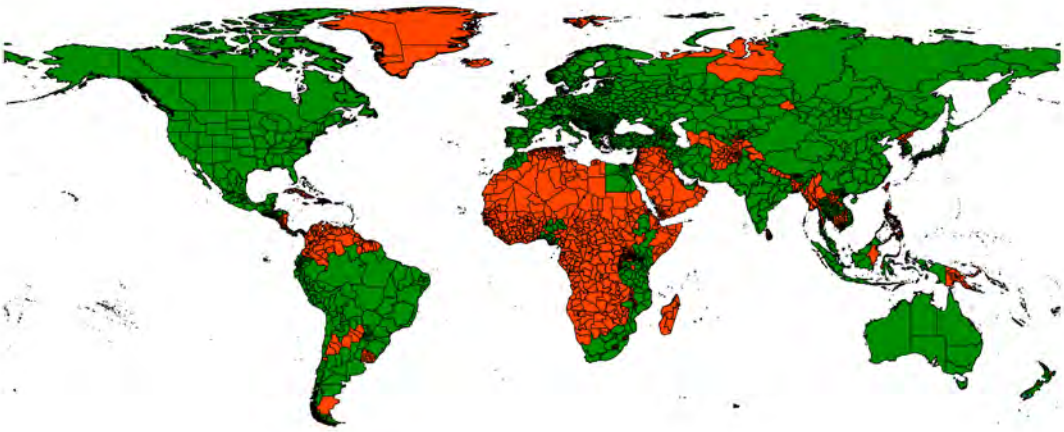

Figure A.1: Spatial coverage of the global data set of reported sub-national economic output (DOSE) (Wenz et al, 2023) across administrative provinces.
Notes: Colours green and red denote the sub-national administrative provinces (i) covered by the raw DOSE dataset (1,661 regions) over 1970-2018 years versus (ii) those where time-series per capita GDP data are insufficient for panel regressions (respectively). For (i), see §A.1 for a detailed discussion on the reporting and aggregation methods used in Wenz et al (2023). For (ii), we overcome missing administrative data in DOSE by extrapolating our gridded CMIP6 climate change simulations available globally for locations with no reported economic outputs and obtain a synthetic 'enhanced' vectorized matrix linking projected per capita GDP impacts to each administrative provinces, and offering a consistent coverage of all countries (166) and sub-national regions (3,672) globally (see §2.5).

Table A.1: Regional Descriptive Statistics

Variable	Mean	S.D.
	World	
Regional GDP per capita (local 2015 prices converted to US dollars)	13014	15670
Regional GDP per capita (US dollars, US 2015 prices)	13449	17223
Annual average Temperature (deg. C)	14.47	7.49
Annual cumulative degree days $DD \geq 0$ and $DD < 29$ (°C)	5173	2126
Annual cumulative degree days $DD \geq 29$ (°C)	18.66	74.95
Annual cumulative daily Precipitation (mm)	8000	5564
Annual average Precipitation (mm)	21.91	15.24
Num. GID(0)	75	
Num. GID(1)	1481	
	Americas	
Regional GDP per capita (local 2015 prices converted to US dollars)	19519	18874
Regional GDP per capita (US dollars, US 2015 prices)	16721	18812
Annual average Temperature (deg. C)	16.38	6.97
Annual cumulative degree days $DD \geq 0$ and $DD < 29$ (°C)	5953	2186
Annual cumulative degree days $DD \geq 29$ (°C)	8.09	37.82
Annual cumulative daily Precipitation (mm)	8489	5646
Annual average Precipitation (mm)	23.25	15.46
Num. GID(0)	13	
Num. GID(1)	270	
	Europe	
Regional GDP per capita (local 2015 prices converted to US dollars)	17901	16821
Regional GDP per capita (US dollars, US 2015 prices)	19217	18712
Annual average Temperature (deg. C)	8.9	3.9
Annual cumulative degree days $DD \geq 0$ and $DD < 29$ (°C)	3594	985
Annual cumulative degree days $DD \geq 29$ (°C)	0.32	2.4
Annual cumulative daily Precipitation (mm)	5660	2329
Annual average Precipitation (mm)	15.5	6.38
Num. GID(0)	33	
Num. GID(1)	545	
	Asia	
Regional GDP per capita (local 2015 prices converted to US dollars)	6723	8808
Regional GDP per capita (US dollars, US 2015 prices)	7921	12657
Annual average Temperature (deg. C)	16.99	7.81
Annual cumulative degree days $DD \geq 0$ and $DD < 29$ (°C)	5702	2099
Annual cumulative degree days $DD \geq 29$ (°C)	40.96	110.94
Annual cumulative daily Precipitation (mm)	9981	6875
Annual average Precipitation (mm)	27.33	18.83
Num. GID(0)	19	
Num. GID(1)	495	
	Africa	
Regional GDP per capita (local 2015 prices converted to US dollars)	1269	3031
Regional GDP per capita (US dollars, US 2015 prices)	1209	3029
Annual average Temperature (deg. C)	21.62	3.4
Annual cumulative degree days $DD \geq 0$ and $DD < 29$ (°C)	7449	1162
Annual cumulative degree days $DD \geq 29$ (°C)	22.7	78.36
Annual cumulative daily Precipitation (mm)	7013	4151
Annual average Precipitation (mm)	19.2	11.36
Num. GID(0)	8	
Num. GID(1)	151	
	Oceania	
Regional GDP per capita (local 2015 prices converted to US dollars)	36329	11745
Regional GDP per capita (US dollars, US 2015 prices)	34526	16011
Annual average Temperature (deg. C)	14.34	4.17
Annual cumulative degree days $DD \geq 0$ and $DD < 29$ (°C)	5078	1225
Annual cumulative degree days $DD \geq 29$ (°C)	5.98	22.65
Annual cumulative daily Precipitation (mm)	8153	3680
Annual average Precipitation (mm)	22.33	10.08
Num. GID(0)	2	
Num. GID(1)	20	

Notes: S.D. indicates standard deviation. GID(0) and GID(1) denote country and sub-national administrative province identifiers (respectively) and are extracted from the Database of Global Administrative Areas (GADM). Country-level descriptive statistics are available upon request to the authors. For further information on the methods used to convert regional economic outputs into U.S. dollars and U.S. 2015 prices, see Eqs. (1) and (2) in Wenz et al (2023) (respectively).

Table A.2: Classification of GCMs to correct Hausfather et al (2022)'s hot model problem

GCM	ID	Model Classification
ACCESS-ESM1-5	1	likely
BCC-CSM2-MR	2	likely
CESM2	3	not-likely
CESM2-WACCM	4	not-likely
CMCC-CM2-SR5	5	likely
CMCC-ESM2	6	likely
CNRM-CM6-1	7	not-likely
CNRM-ESM2-1	8	not-likely
CanESM5	9	not-likely
EC-Earth3	10	none
EC-Earth3-Veg-LR	11	not-likely
FGOALS-g3	12	likely
GFDL-CM4	13	likely
GFDL-ESM4	14	likely
HadGEM3-GC31-LL	15	not-likely
IITM-ESM	15	not-likely
INM-CM4-8	16	likely
INM-CM5-0	17	none
IPSL-CM6A-LR	18	likely
KACE-1-0-G	19	none
KIOST-ESM	20	none
MIROC6	21	likely
MIROC-ES2L	22	likely
MPI-ESM1-2-HR	23	likely
MPI-ESM1-2-LR	24	likely
MRI-ESM2-0	25	likely
NorESM2-LM	26	likely
NorESM2-MM	27	none
TaiESM1	28	none
UKESM1-0-LL	29	not-likely

Note: This model classification is based on Hausfather et al's (2022) recommended procedure of excluding models with TCR and ECS outside "likely" ranges (1.4-2.2°C, 66% likelihood, and 2.5-4°C, 90% likelihood, respectively). That leaves us with 15 "likely" GCMs that form the basis of our modelling of projected economic impacts and which accounts for the 'hot models' identified in the last generation of climate model simulations in CMIP6. For a more exhaustive review of this probem, see Hausfather et al (2022).

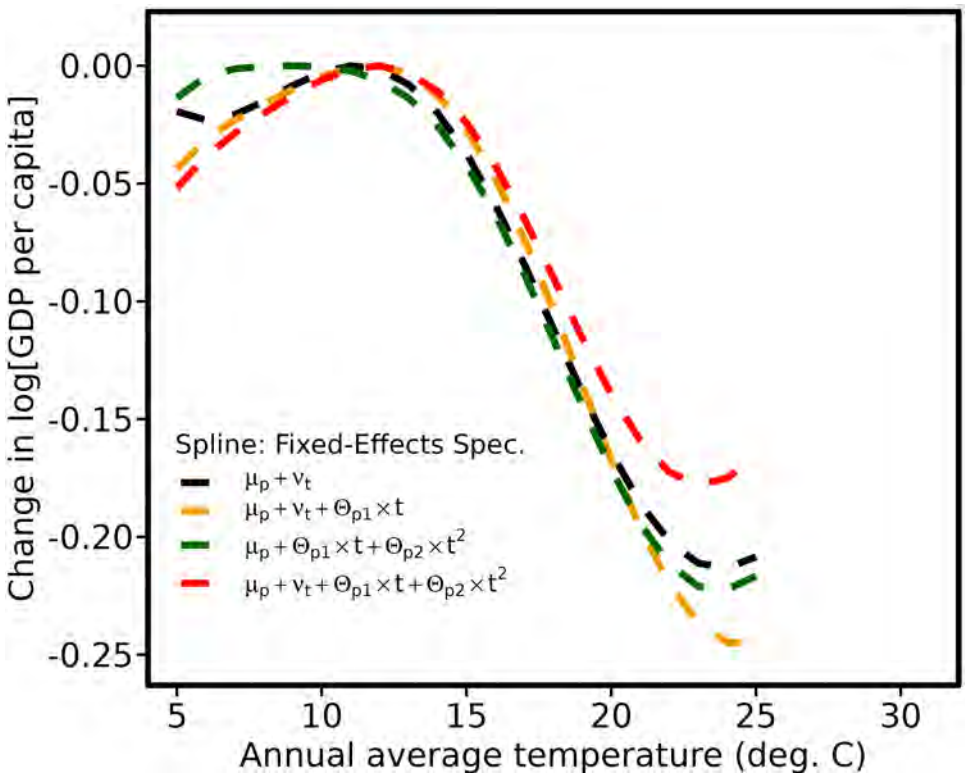

Figure A.2: Robustness test: Parametric FE-OLS global log[GDP per capita] responses to administrative province-annual average temperature exposure per year [deg.°C] against varying specifications of the Fixed-Effects (FEs).

Parametric FE-OLS splines are restricted with a 3^{rd} polynomial order function of average temperature exposure. Predicted responses are obtained by multiplying point-level estimated coefficients with the average temperature distribution reflected in the x-axis. Assuming index p denotes administrative provinces of the estimation dataset; red, green, orange, and black dashed lines indicate the following specifications of the constant terms (respectively): province-by-year fixed effects and province-specific quadratic time trends ($\mu_p + \nu_t + \Theta_{p,1}t + \Theta_{p,2}t^2$); province fixed effects and province-specific quadratic time trends ($\mu_p + \Theta_{p,1}t + \Theta_{p,2}t^2$); province-by-year fixed effects and province-specific linear time trends ($\mu_p + \nu_t + \Theta_{p,1}t$); province-by-year fixed effects excluding province-level time trends ($\mu_p + \nu_t$). For all GAM regressions, standard errors are clustered at the administrative province-level. Across all FEs specifications, parametric FE-OLS cubic functions of average temperature show highly similar non-linear shapes that empirically confirm our main parametric FE-OLS result displayed in panel **a** Fig. 3.

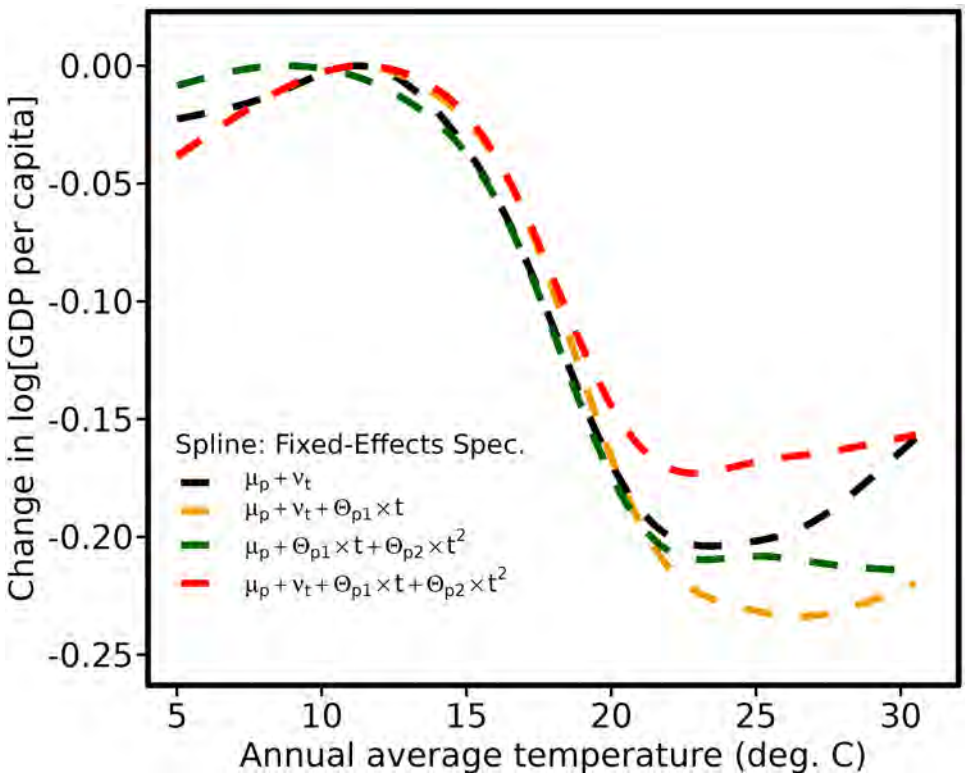

Figure A.3: Robustness test: Non-parametric Generalized Additive Model (GAM) global log[GDP per capita] responses to administrative province-annual average temperature exposure per year [deg.°C] against varying specifications of the Fixed-Effects (FEs).

Assuming index p denotes administrative provinces of the estimation dataset; red, green, orange, and black dashed lines indicate the following specifications of the constant terms (respectively): province-by-year fixed effects and province-specific quadratic time trends ($\mu_p + \nu_t + \Theta_{p,1}t + \Theta_{p,2}t^2$); province fixed effects and province-specific quadratic time trends ($\mu_p + \Theta_{p,1}t + \Theta_{p,2}t^2$); province-by-year fixed effects and province-specific linear time trends ($\mu_p + \nu_t + \Theta_{p,1}t$); province-by-year fixed effects excluding province-level time trends ($\mu_p + \nu_t$). For all GAM regressions, standard errors are clustered at the administrative province-level. Across all FEs specifications, non-parametric GAM responses yield highly similar non-linear shapes that empirically confirm our main non-parametric result displayed in panel **b** Fig. 3.

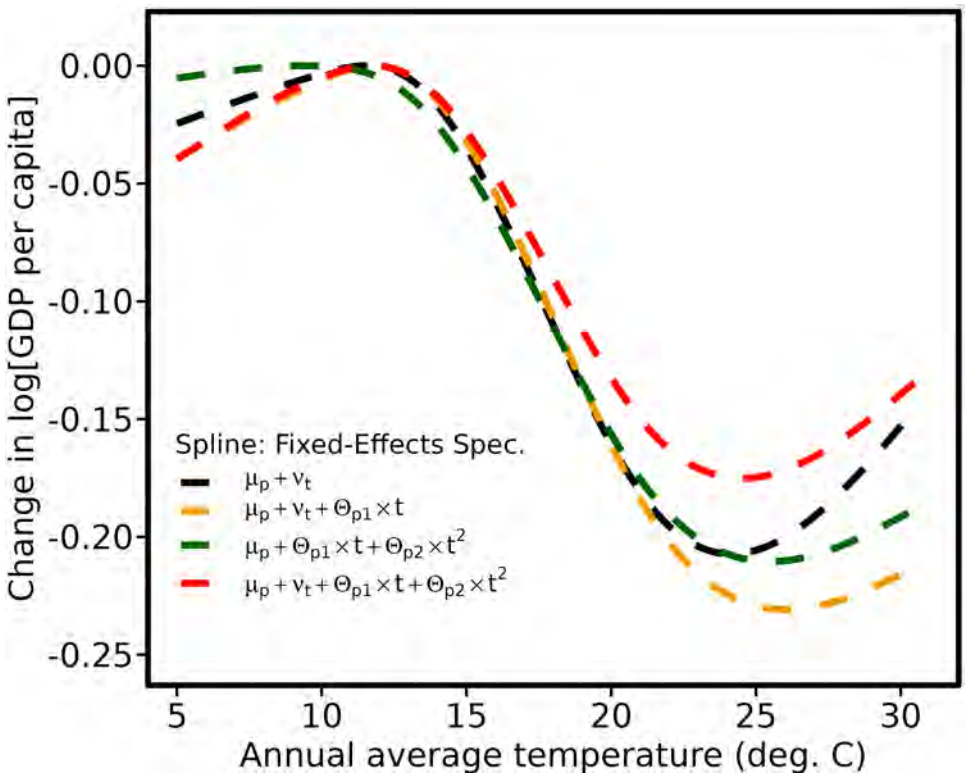

Figure A.4: Robustness test: Semi-parametric restricted cubic splines of global log[GDP per capita] responses to administrative province-annual average temperature exposure per year [deg.°C] against varying specifications of the Fixed-Effects (FEs).

Semi-parametric restricted cubic splines are calibrated with 6 Knots. Knots are locations along a predictor variable's range where pieces of the smooth function join; and thus where the shape of the smooth function can change. Splines fit the data in sections divided by these Knots, with each section's shape adjusted to minimize error. Assuming index p denotes administrative provinces of the estimation dataset; red, green, orange, and black dashed lines indicate the following specifications of the constant terms (respectively): province-by-year fixed effects and province-specific quadratic time trends ($\mu_p + \nu_t + \Theta_{p,1}t + \Theta_{p,2}t^2$); province fixed effects and province-specific quadratic time trends ($\mu_p + \Theta_{p,1}t + \Theta_{p,2}t^2$); province-by-year fixed effects and province-specific linear time trends ($\mu_p + \nu_t + \Theta_{p,1}t$); province-by-year fixed effects excluding province-level time trends ($\mu_p + \nu_t$). For all GAM regressions, standard errors are clustered at the administrative province-level. Across all FEs specifications, semi-parametric restricted cubic splines show highly similar non-linear shapes that empirically confirm our main semi-parametric result displayed in panel **c** Fig. 3.

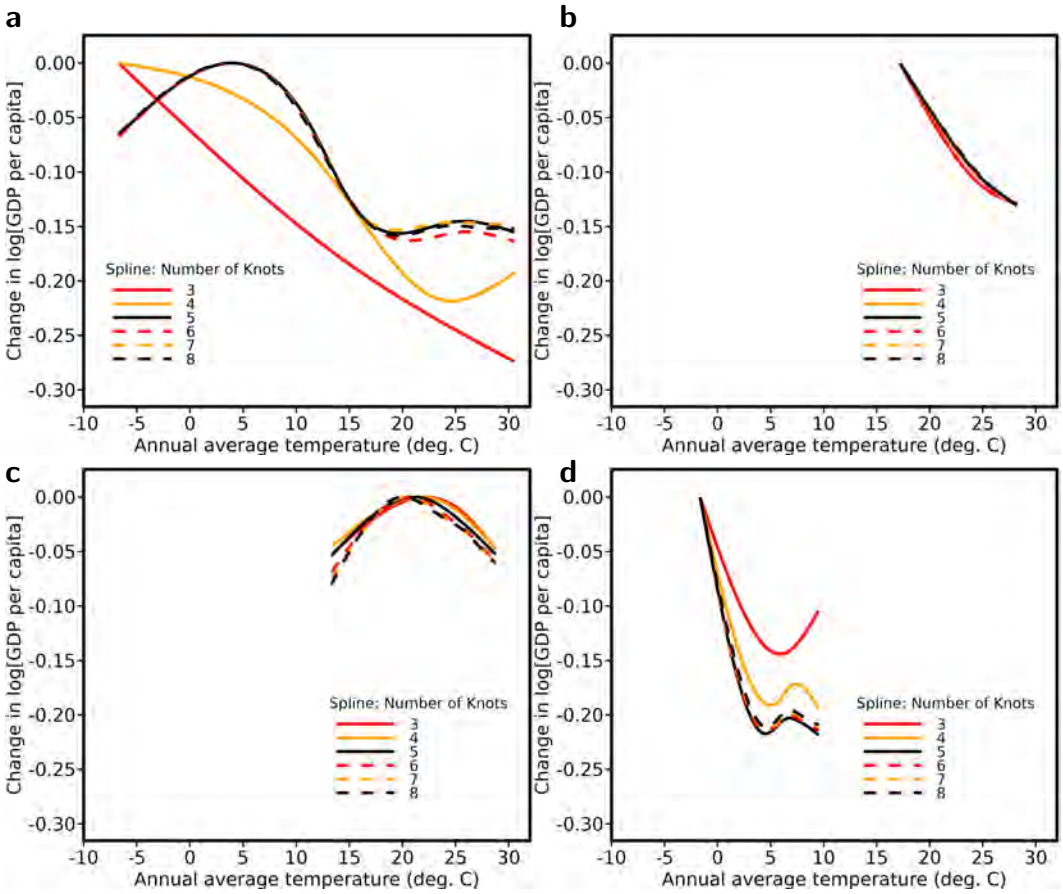

Figure A.5: Regionally-stratified non-linear log[GDP per capita] responses to administrative province-annual average temperature exposure per year [deg.°C] in typical climate zones.
Panels show semi-parametric restricted cubic splines with up to 3-8 Knots estimated regionally on typical climate zones (i.e., **a** Asia [temperate continental]; **b** Brazil [tropical savanna]; **c** India [tropical monsoon]; **d** Sweden [temperate to subarctic]). Knots are locations along a range of predictor variables where pieces of the smooth function join; and thus where the shape of the smooth function can change. Splines fit the data in sections divided by these Knots, with each section' shape adjusted to minimize error. All regionally stratified semi-parametric regressions in **a-b-c-d** include (sub-national) province-specific quadratic time trends in years of sample, province-by-year fixed effects and a quadric function of precipitation controls.

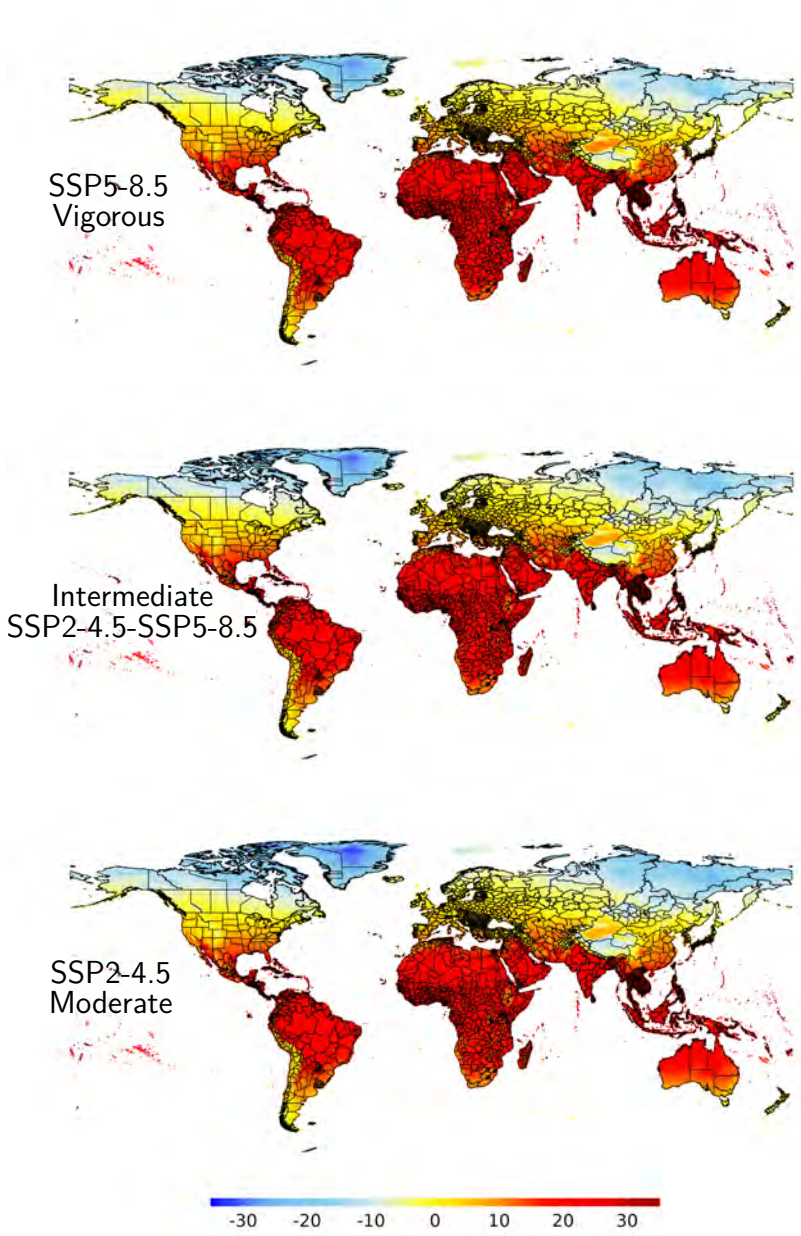

Figure A.6: Spatially distributed SSP-specific temperature 'Deltas' between multi-GCM median 2099 simulations and the global 1985-2004 historical mid-point in each of the 249,000 unique 0.25×0.25 grid-cells from NEX-GDDP CMIP6 and covering all land surfaces globally
For each cell, deltas are computed as the inter-epoch difference between the average multi-model median temperatures simulated by 30 distinct Global Climate Models (GCMs) from NASA's Earth Exchange Global Daily Downscaled Projections (NEX-GDDP CMIP6— Eyring et al, 2016) at epoch 2099 minus the 20-year mid-point 1985-2004 historical temperature referential (i.e., 1995 mid-point) averaged globally. This leaves an *ensemble* of absolute Deltas (Δ) showing the spatial distribution of future climatically-driven shifts in temperature simulated under SSP2-4.5 moderate (bottom panel), intermediate SSP2-4.5-SSP5-8.5 (centre panel) and SSP5-8.5 vigorous (top panel) warming scenarios, and with respect to the global temperature baseline ($\overline{T}$) recorded historically.

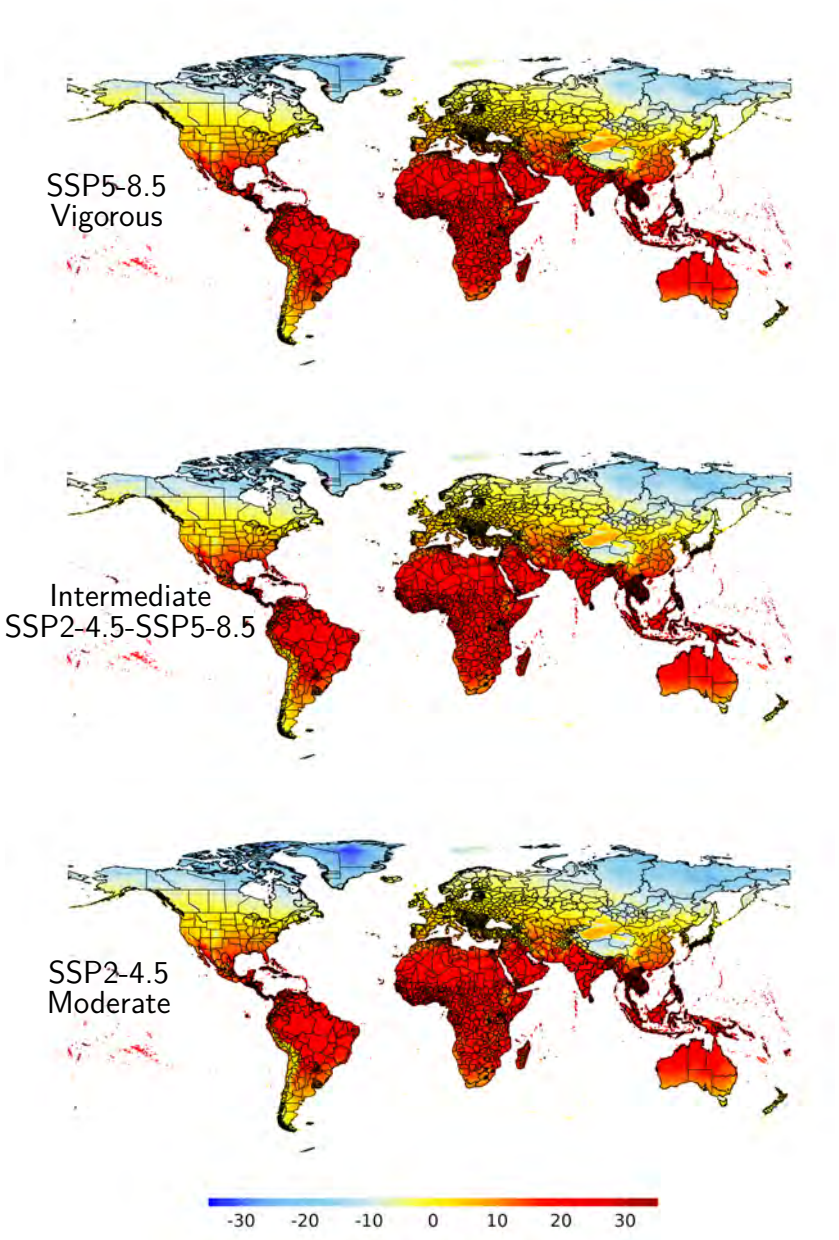

Figure A.7: Spatially distributed SSP-specific average temperature 'Deltas' between multi-GCM median 20-year average 2081-2099 simulations and the global 1985-2004 historical mid-point in each of the 249,000 unique 0.25 × 0.25 grid-cells from NEX-GDDP CMIP6 and covering all land surfaces globally

For each cell, deltas are computed as the inter-epoch difference between the average multi-model median temperatures simulated by 30 distinct Global Climate Models (GCMs) from NASA's Earth Exchange Global Daily Downscaled Projections (NEX-GDDP CMIP6— Eyring et al, 2016) at epoch 2081-2099 minus the 20-year mid-point 1985-2004 historical temperature referential (i.e., 1995 mid-point) averaged globally. This leaves an *ensemble* of absolute Deltas (Δ) showing the spatial distribution of future climatically-driven shifts in temperature simulated under SSP2-4.5 moderate (bottom panel), intermediate SSP2-4.5-SSP5-8.5 (centre panel) and SSP5-8.5 vigorous (top panel) warming scenarios, and with respect to the global temperature baseline ($\overline{T}$) recorded historically.

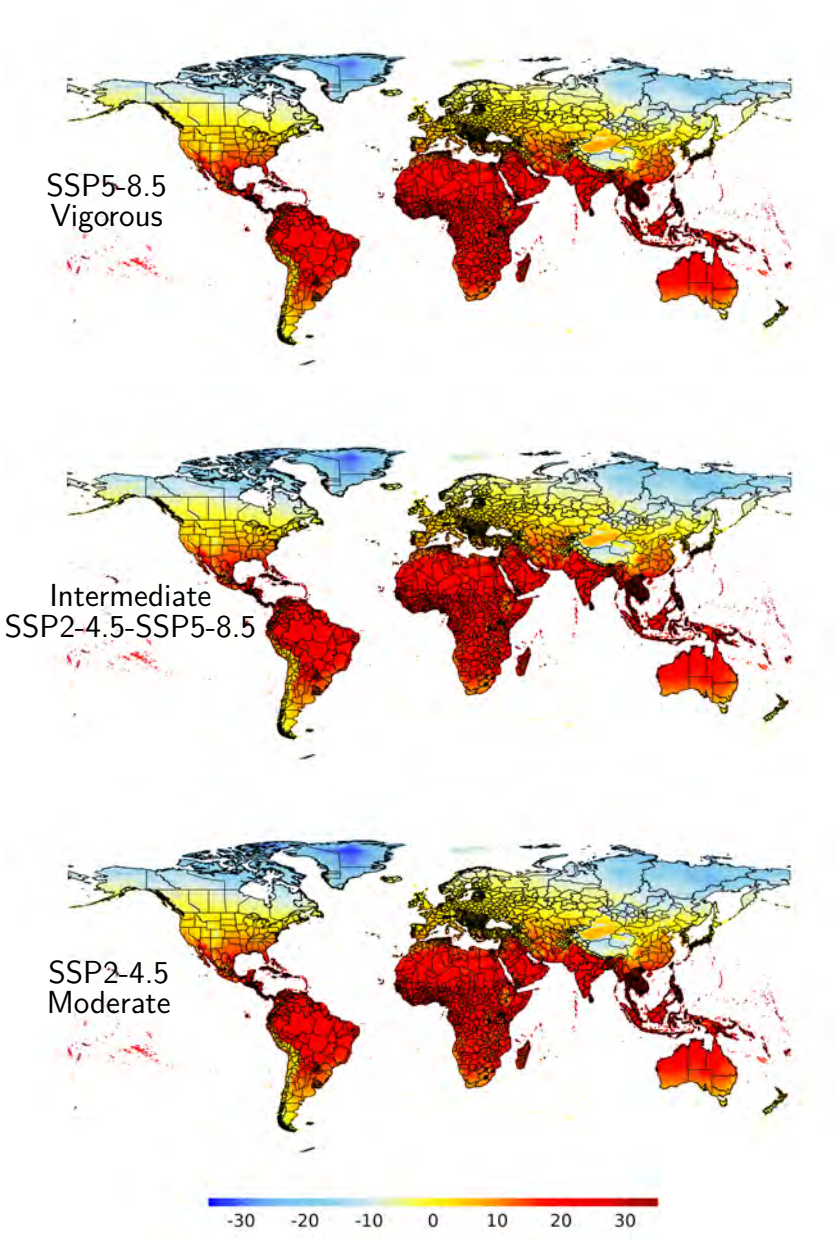

Figure A.8: Spatially distributed SSP-specific average temperature 'Deltas' between multi-GCM median 20-year average 2071-2090 simulations and the global 1985-2004 historical mid-point in each of the 249,000 unique 0.25 × 0.25 grid-cells from NEX-GDDP CMIP6 and covering all land surfaces globally

For each cell, deltas are computed as the inter-epoch difference between the average multi-model median temperatures simulated by 30 distinct Global Climate Models (GCMs) from NASA's Earth Exchange Global Daily Downscaled Projections (NEX-GDDP CMIP6— Eyring et al, 2016) at epoch 2071-2090 minus the 20-year mid-point 1985-2004 historical temperature referential (i.e., 1995 mid-point) averaged globally. This leaves an *ensemble* of absolute Deltas (Δ) showing the spatial distribution of future climatically-driven shifts in temperature simulated under SSP2-4.5 moderate (bottom panel), intermediate SSP2-4.5-SSP5-8.5 (centre panel) and SSP5-8.5 vigorous (top panel) warming scenarios, and with respect to the global temperature baseline ($\overline{T}$) recorded historically.

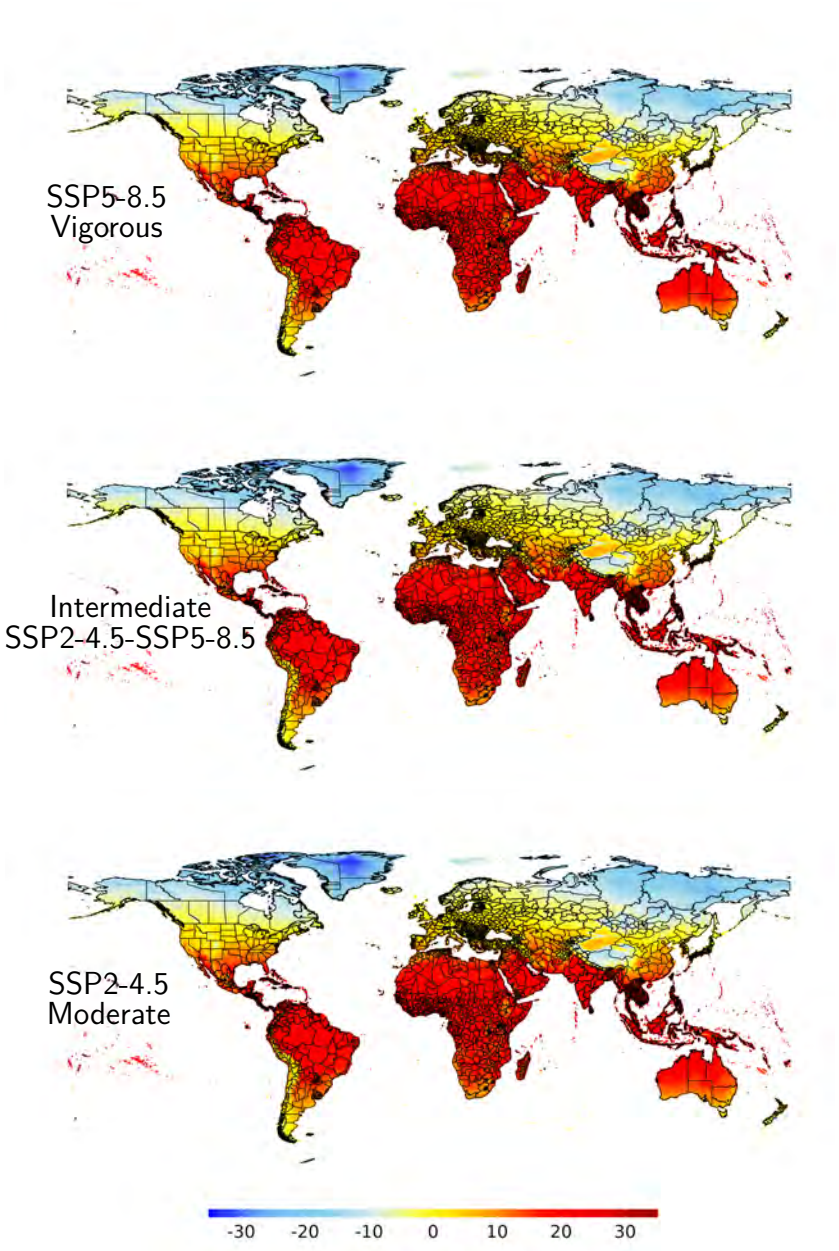

Figure A.9: Spatially distributed SSP-specific average temperature 'Deltas' between multi-GCM median 20-year average 2061-2080 simulations and the global 1985-2004 historical mid-point in each of the 249,000 unique 0.25 × 0.25 grid-cells from NEX-GDDP CMIP6 and covering all land surfaces globally

For each cell, deltas are computed as the inter-epoch difference between the average multi-model median temperatures simulated by 30 distinct Global Climate Models (GCMs) from NASA's Earth Exchange Global Daily Downscaled Projections (NEX-GDDP CMIP6— Eyring et al, 2016) at epoch 2061-2080 minus the 20-year mid-point 1985-2004 historical temperature referential (i.e., 1995 mid-point) averaged globally. This leaves an *ensemble* of absolute Deltas (Δ) showing the spatial distribution of future climatically-driven shifts in temperature simulated under SSP2-4.5 moderate (bottom panel), intermediate SSP2-4.5-SSP5-8.5 (centre panel) and SSP5-8.5 vigorous (top panel) warming scenarios, and with respect to the global temperature baseline ($\overline{T}$) recorded historically.

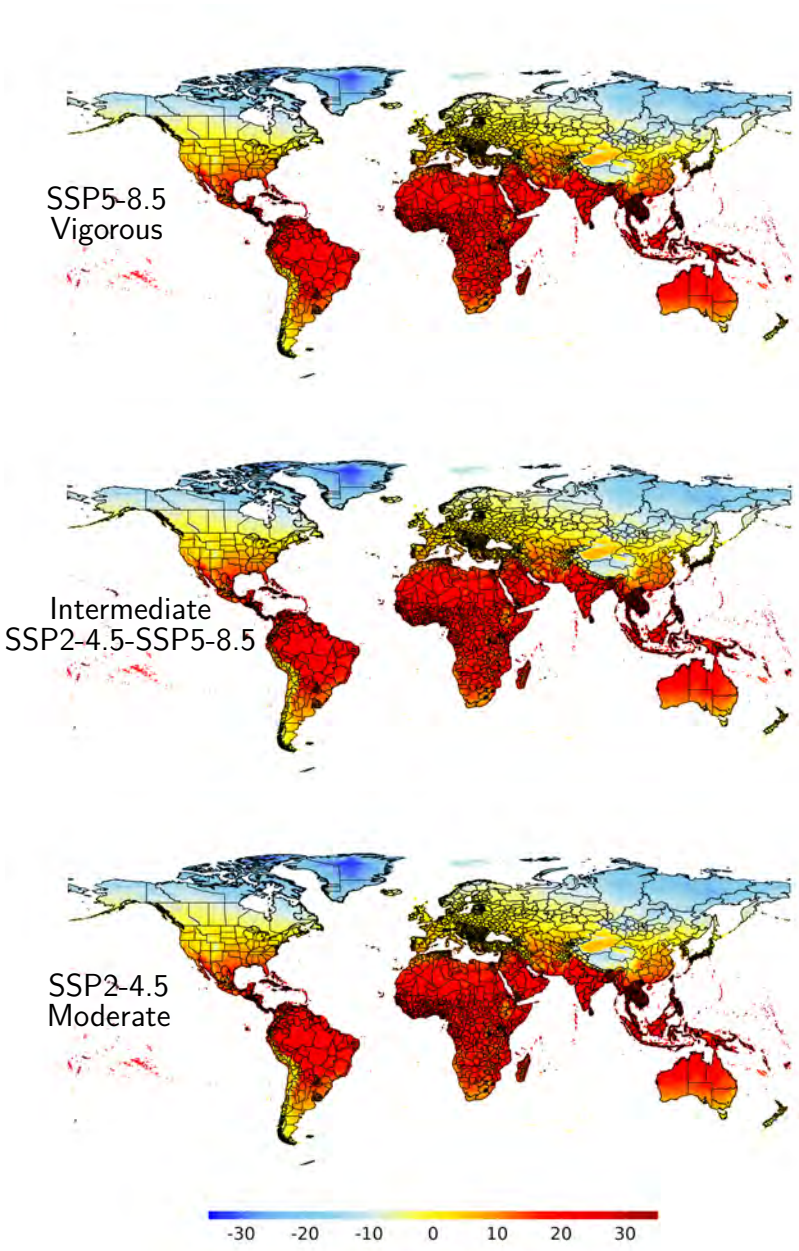

Figure A.10: Spatially distributed SSP-specific average temperature 'Deltas' between multi-GCM median 20-year average 2051-2070 simulations and the global 1985-2004 historical mid-point in each of the 249,000 unique 0.25 × 0.25 grid-cells from NEX-GDDP CMIP6 and covering all land surfaces globally

For each cell, deltas are computed as the inter-epoch difference between the average multi-model median temperatures simulated by 30 distinct Global Climate Models (GCMs) from NASA's Earth Exchange Global Daily Downscaled Projections (NEX-GDDP CMIP6— Eyring et al, 2016) at epoch 2051-2070 minus the 20-year mid-point 1985-2004 historical temperature referential (i.e., 1995 mid-point) averaged globally. This leaves an *ensemble* of absolute Deltas (Δ) showing the spatial distribution of future climatically-driven shifts in temperature simulated under SSP2-4.5 moderate (bottom panel), intermediate SSP2-4.5-SSP5-8.5 (centre panel) and SSP5-8.5 vigorous (top panel) warming scenarios, and with respect to the global temperature baseline ($\overline{T}$) recorded historically.

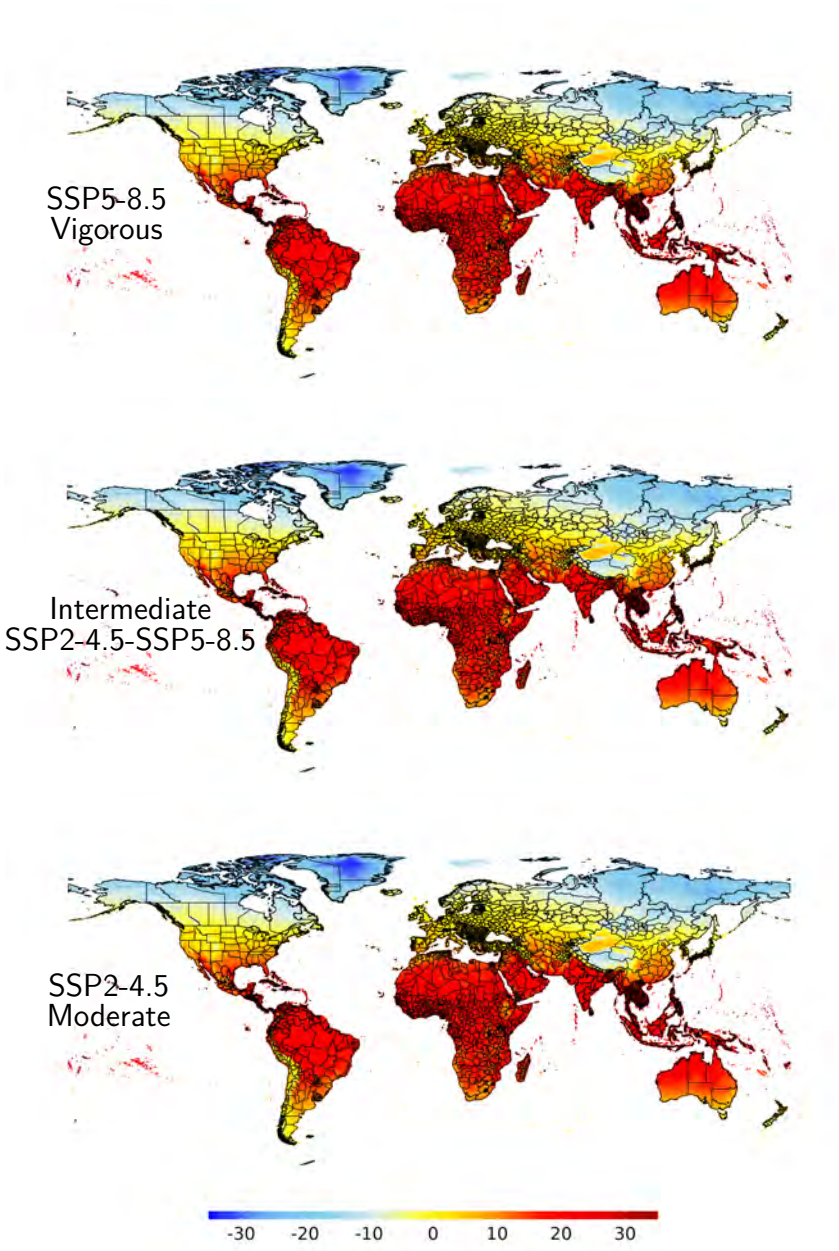

Figure A.11: Spatially distributed SSP-specific average temperature 'Deltas' between multi-GCM median 20-year average 2041-2060 simulations and the global 1985-2004 historical mid-point in each of the 249,000 unique 0.25 × 0.25 grid-cells from NEX-GDDP CMIP6 and covering all land surfaces globally

For each cell, deltas are computed as the inter-epoch difference between the average multi-model median temperatures simulated by 30 distinct Global Climate Models (GCMs) from NASA's Earth Exchange Global Daily Downscaled Projections (NEX-GDDP CMIP6— Eyring et al, 2016) at epoch 2041-2060 minus the 20-year mid-point 1985-2004 historical temperature referential (i.e., 1995 mid-point) averaged globally. This leaves an *ensemble* of absolute Deltas (Δ) showing the spatial distribution of future climatically-driven shifts in temperature simulated under SSP2-4.5 moderate (bottom panel), intermediate SSP2-4.5-SSP5-8.5 (centre panel) and SSP5-8.5 vigorous (top panel) warming scenarios, and with respect to the global temperature baseline ($\overline{T}$) recorded historically.

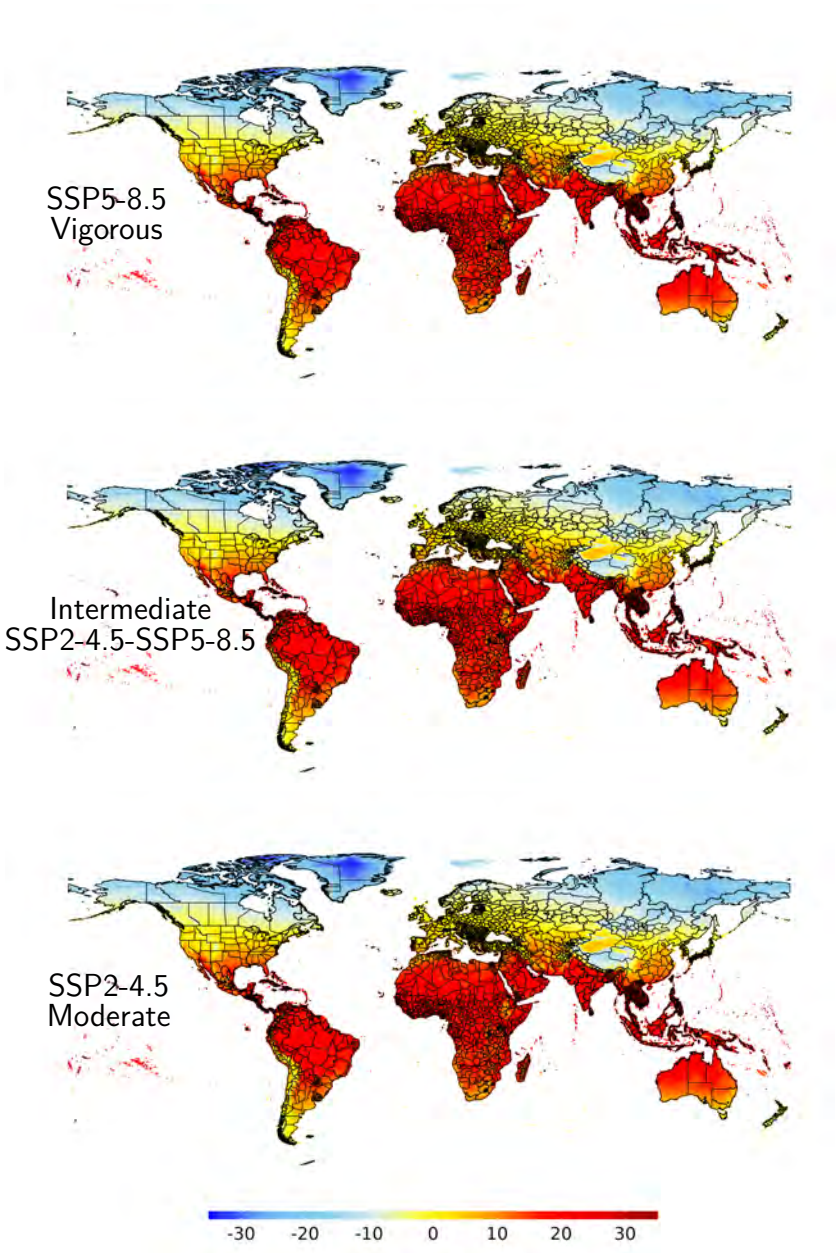

Figure A.12: Spatially distributed SSP-specific average temperature 'Deltas' between multi-GCM median 20-year average 2031-2050 simulations and the global 1985-2004 historical mid-point in each of the 249,000 unique 0.25 × 0.25 grid-cells from NEX-GDDP CMIP6 and covering all land surfaces globally

For each cell, deltas are computed as the inter-epoch difference between the average multi-model median temperatures simulated by 30 distinct Global Climate Models (GCMs) from NASA's Earth Exchange Global Daily Downscaled Projections (NEX-GDDP CMIP6— Eyring et al, 2016) at epoch 2031-2050 minus the 20-year mid-point 1985-2004 historical temperature referential (i.e., 1995 mid-point) averaged globally. This leaves an *ensemble* of absolute Deltas (Δ) showing the spatial distribution of future climatically-driven shifts in temperature simulated under SSP2-4.5 moderate (bottom panel), intermediate SSP2-4.5-SSP5-8.5 (centre panel) and SSP5-8.5 vigorous (top panel) warming scenarios, and with respect to the global temperature baseline ($\overline{T}$) recorded historically.

Table A.3: Global Δlog(GDP/Pop) responses to the quadratic FF - GDP per capita from WDI & weather from NASA's 0.25° GLDAS cells spatially collapsed to ISOs weighting by gridded population density from GPW dataset

Estimation period	1970-2018						1970-1994						1995-2018					
FEs specification	I	II	III	IV	V	VI	I	II	III	IV	V	VI	I	II	III	IV	V	VI
$Temp._{i,t}$	0.01230*	0.01230*	0.01250*	0.00954*	0.00739*	-0.00024	0.01271*	0.01271*	0.01008*	0.01160*	0.01321*	0.00004	0.00573*	0.00573*	0.00531*	0.00279	0.00250	-0.00058
	(0.002)	(0.002)	(0.001)	(0.015)	(0.044)	(0.486)	(0.012)	(0.012)	(0.023)	(0.041)	(0.032)	(0.968)	(0.031)	(0.031)	(0.036)	(0.301)	(0.279)	(0.262)
$(Temp._{i,t})^2$	-0.00042*	-0.00042*	-0.00042*	-0.00032*	-0.00027*	-0.00001	-0.00064*	-0.00064*	-0.00049*	-0.00059*	-0.00048*	-0.00001	-0.00026*	-0.00026*	-0.00027*	-0.00016+	-0.00015+	-0.00001+
	(0.000)	(0.000)	(0.000)	(0.002)	(0.003)	(0.144)	(0.000)	(0.000)	(0.001)	(0.000)	(0.004)	(0.71)	(0.004)	(0.004)	(0.001)	(0.088)	(0.06)	(0.091)
$Precip._{i,t}$	-0.000129	-0.000129	0.000157	-0.000158	-0.000115	0.000528	0.001726+	0.001726+	0.002208*	0.002228*	0.002781*	0.000796	-0.000377+	-0.000377+	-0.000274	-0.00041*	-0.000705*	0.000508
	(0.601)	(0.601)	(0.521)	(0.505)	(0.658)	(0.335)	(0.051)	(0.051)	(0.018)	(0.01)	(0.005)	(0.483)	(0.096)	(0.097)	(0.254)	(0.046)	(0.001)	(0.276)
$(Precip._{i,t})^2$	-0.000001	-0.000001	-0.000001	0.000000	0.000000	-0.000005	-0.000021*	-0.000021*	-0.000024*	-0.000025*	-0.000031*	-0.000010	0.000000	0.000000	0.000001	0.00000	0.000003*	-0.000004
	(0.591)	(0.591)	(0.357)	(0.831)	(0.848)	(0.381)	(0.014)	(0.014)	(0.009)	(0.003)	(0.001)	(0.495)	(0.92)	(0.92)	(0.65)	(0.71)	(0.001)	(0.363)
Adj-R^2	0.25	0.25	0.21	0.18	0.13	0.07	0.4	0.4	0.38	0.31	0.21	0.05	0.37	0.37	0.33	0.31	0.19	0.07
Obs.	6,697	6,697	6,697	6,697	6,697	6,697	2,849	2,849	2,849	2,849	2,849	2,849	3,848	3,848	3,848	3,848	3,848	3,848

Notes: *, and + denote statistical significance at 5% and 10% level, respectively. FF: Functional Form - herein, quadratic functions of weather components. Unless otherwise indicated, all panel fixed-effect OLS regressions include standard errors, in parentheses, clustered at the country level. Temperature is measured in °C and precipitation in metres. Constant terms are specified as follows: (I) country-by-year fixed effects and country-specific quadratic time trends; (II) continent-by-year fixed effects and country-specific quadratic time trends; (III) country fixed effects and country-specific quadratic time trends; (IV) country-by-year fixed effects and country-specific linear time trends; (V) country-by-year fixed effects excluding country-level time trends; (VI) continent-by-year fixed effects excluding country-level time trends.

Table A.4: Global Δlog(GDP/Pop) responses to the quadratic FF - GDP per capita from PWT & weather from NASA's 0.25° GLDAS cells spatially collapsed to ISOs weighting by gridded population density from GPW dataset

Estimation period	1970-2018						1970-1994						1995-2018					
FEs specification	I	II	III	IV	V	VI	I	II	III	IV	V	VI	I	II	III	IV	V	VI
$Temp._{i,t}$	0.01018*	0.01018*	0.00986*	0.01115*	0.00579	-0.00011	0.01300+	0.01300+	0.00556	0.01253+	0.00961	0.00157+	0.00716*	0.00716*	0.00634*	0.00269	0.00226	-0.00163
	(0.026)	(0.026)	(0.015)	(0.018)	(0.196)	(0.632)	(0.055)	(0.055)	(0.269)	(0.077)	(0.147)	(0.085)	(0.038)	(0.038)	(0.048)	(0.414)	(0.491)	(0.108)
$(Temp._{i,t})^2$	-0.00039*	-0.00039*	-0.00035*	-0.00039*	-0.00022+	-0.00001*	-0.00059*	-0.00059*	-0.00033*	-0.00060*	-0.00040*	-0.00005+	-0.00026*	-0.00026*	-0.00029*	-0.00013	-0.00015	0.00002
	(0.003)	(0.003)	(0.002)	(0.004)	(0.055)	(0.025)	(0.006)	(0.006)	(0.046)	(0.004)	(0.034)	(0.055)	(0.024)	(0.024)	(0.006)	(0.259)	(0.207)	(0.314)
$Precip._{i,t}$	0.00061	0.00061	0.000629	0.000632	0.001037+	0.000866	0.002546*	0.002546*	0.002809*	0.002271*	0.002752*	0.000918	-0.000504	-0.000504	-0.000679	-0.000401	-0.000471	0.000819
	(0.205)	(0.205)	(0.21)	(0.186)	(0.092)	(0.344)	(0.005)	(0.005)	(0.004)	(0.01)	(0.001)	(0.42)	(0.297)	(0.297)	(0.161)	(0.366)	(0.495)	(0.29)
$(Precip._{i,t})^2$	-0.00001*	-0.00001*	-0.000007	-0.000011*	-0.000015*	-0.000010	-0.000026*	-0.000026*	-0.000027*	-0.000023*	-0.000027*	-0.000011	0.000000	0.000000	0.000004	-0.000001	-0.000002	-0.000009
	(0.035)	(0.035)	(0.159)	(0.04)	(0.018)	(0.343)	(0.005)	(0.005)	(0.006)	(0.013)	(0.002)	(0.418)	(0.988)	(0.988)	(0.465)	(0.85)	(0.844)	(0.31)
Adj-R^2	0.25	0.25	0.21	0.19	0.12	0.07	0.38	0.38	0.37	0.31	0.23	0.05	0.39	0.39	0.35	0.31	0.2	0.07
Obs.	6,893	6,893	6,893	6,893	6,893	6,893	3,197	3,197	3,197	3,197	3,197	3,197	3,696	3,696	3,696	3,696	3,696	3,696

Notes: *, and + denote statistical significance at 5% and 10% level, respectively.FF: Functional Form - herein, quadratic functions of weather components. Unless otherwise indicated, all panel fixed-effect OLS regressions include standard errors, in parentheses, clustered at the country level. Temperature is measured in °C and precipitation in metres. Constant terms are specified as follows: (I) country-by-year fixed effects and country-specific quadratic time trends; (II) continent-by-year fixed effects and country-specific quadratic time trends; (III) country fixed effects and country-specific quadratic time trends; (IV) country-by-year fixed effects and country-specific linear time trends; (V) country-by-year fixed effects excluding country-level time trends; (VI) continent-by-year fixed effects excluding country-level time trends.

Table A.5: Global Δlog(GDP/Pop) responses to the interaction FF - GDP per capita from WDI & weather from NASA's 0.25° GLDAS cells spatially collapsed to ISOs weighting by gridded population density from GPW dataset

Estimation period	1970-2018						1970-1994						1995-2018					
FEs specification	I	II	III	IV	V	VI	I	II	III	IV	V	VI	I	II	III	IV	V	VI
Temp.$_{i,t}$	0.01245*	0.01245*	0.01254*	0.00974*	0.00728*	-0.00033	0.01309*	0.01309*	0.01046*	0.0121*	0.01372*	0.00007	0.00546*	0.00546*	0.00509*	0.00264	0.00245	-0.00073
	(0.002)	(0.002)	(0.001)	(0.012)	(0.042)	(0.399)	(0.011)	(0.011)	(0.018)	(0.033)	(0.027)	(0.928)	(0.036)	(0.036)	(0.04)	(0.321)	(0.286)	(0.33)
Temp.$_{i,t} \times \overline{T}_i$	-0.00086*	-0.00086*	-0.00085*	-0.00066*	-0.00054*	-0.00001	-0.00129*	-0.00129*	-0.00100*	-0.0012*	-0.00098*	-0.00001	-0.00052*	-0.00052*	-0.00053*	-0.00031+	-0.00031+	-0.00001
	(0.000)	(0.000)	(0.000)	(0.001)	(0.002)	(0.422)	(0.000)	(0.000)	(0.001)	(0.000)	(0.003)	(0.68)	(0.004)	(0.004)	(0.001)	(0.085)	(0.05)	(0.64)
Precip.$_{i,t}$	-0.000046	-0.000046	0.000091	-0.000078	0.000032	0.000602	0.001496+	0.001496+	0.002033*	0.001957*	0.002577*	0.000638	-0.000621	-0.000621	-0.000636	-0.000548+	-0.001078*	0.000579
	(0.907)	(0.907)	(0.828)	(0.826)	(0.937)	(0.456)	(0.096)	(0.096)	(0.031)	(0.03)	(0.012)	(0.535)	(0.116)	(0.117)	(0.129)	(0.081)	(0.001)	(0.428)
Precip.$_{i,t} \times \overline{P}_i$	-0.000004	-0.000004	-0.000002	-0.000003	-0.000004	-0.000007	-0.000036*	-0.000036*	-0.000043*	-0.000043*	-0.000056*	-0.000008	0.000005	0.000005	0.000010	0.000004	0.000017*	-0.000006
	(0.59)	(0.59)	(0.798)	(0.686)	(0.596)	(0.513)	(0.036)	(0.036)	(0.017)	(0.017)	(0.005)	(0.561)	(0.499)	(0.499)	(0.233)	(0.482)	(0.003)	(0.519)
Adj-R^2	0.25	0.25	0.21	0.18	0.13	0.07	0.4	0.4	0.38	0.31	0.21	0.05	0.37	0.37	0.33	0.31	0.2	0.07
Obs.	6,697	6,697	6,697	6,697	6,697	6,697	2,849	2,849	2,849	2,849	2,849	2,849	3,848	3,848	3,848	3,848	3,848	3,848

Notes: *, and + denote statistical significance at 5% and 10% level, respectively. FF: Functional Form - herein, interaction of weather components. Unless otherwise indicated, all panel fixed-effect OLS regressions include standard errors, in parentheses, clustered at the country level. Temperature is measured in °C and precipitation in metres. Constant terms are specified as follows: (I) country-by-year fixed effects and country-specific quadratic time trends; (II) continent-by-year fixed effects and country-specific quadratic time trends; (III) country fixed effects and country-specific quadratic time trends; (IV) country-by-year fixed effects and country-specific linear time trends; (V) country-by-year fixed effects excluding country-level time trends; (VI) continent-by-year fixed effects excluding country-level time trends.

Table A.6: Global Δlog(GDP/Pop) responses to the interaction FF - GDP per capita from PWT & weather from NASA's 0.25° GLDAS cells spatially collapsed to ISOs weighting by gridded population density from GPW dataset

Estimation period	1970-2018						1970-1994						1995-2018					
FEs specification	I	II	III	IV	V	VI	I	II	III	IV	V	VI	I	II	III	IV	V	VI
Temp.$_{i,t}$	0.01057*	0.01057*	0.00997*	0.01138*	0.00583	-0.00023	0.01373*	0.01373*	0.00597	0.01340+	0.01024	0.00154*	0.00665*	0.00665*	0.00593+	0.00245	0.00184	-0.00194
	(0.018)	(0.018)	(0.012)	(0.013)	(0.181)	(0.544)	(0.044)	(0.044)	(0.237)	(0.059)	(0.123)	(0.04)	(0.047)	(0.047)	(0.056)	(0.441)	(0.56)	(0.133)
Temp.$_{i,t} \times \overline{T}_i$	-0.00081*	-0.00081*	-0.00071*	-0.00081*	-0.00044*	-0.00001	-0.00122*	-0.00122*	-0.00067*	-0.00125*	-0.00084*	-0.00005*	-0.00050*	-0.00050*	-0.00055*	-0.00024	-0.00029	0.00003
	(0.001)	(0.001)	(0.001)	(0.002)	(0.045)	(0.303)	(0.005)	(0.005)	(0.042)	(0.002)	(0.026)	(0.019)	(0.027)	(0.028)	(0.006)	(0.259)	(0.205)	(0.288)
Precip.$_{i,t}$	0.000018	0.000018	-0.000076	0.000158	0.000397	0.000546	0.002411*	0.002411*	0.002725*	0.002089*	0.002563*	0.000872	-0.000813	-0.000813	-0.000876+	-0.000671	-0.001129+	0.000274
	(0.97)	(0.97)	(0.881)	(0.718)	(0.516)	(0.549)	(0.012)	(0.012)	(0.007)	(0.028)	(0.004)	(0.393)	(0.104)	(0.104)	(0.08)	(0.136)	(0.054)	(0.757)
Precip.$_{i,t} \times \overline{P}_i$	-0.000006	-0.000006	0.000004	-0.000010	-0.000015	-0.000005	-0.000049*	-0.000049*	-0.000052*	-0.000042*	-0.000049*	-0.000011	0.000008	0.000008	0.000013	0.000005	0.000014	-0.000001
	(0.561)	(0.561)	(0.724)	(0.27)	(0.216)	(0.65)	(0.015)	(0.015)	(0.013)	(0.042)	(0.007)	(0.382)	(0.513)	(0.513)	(0.257)	(0.602)	(0.291)	(0.943)
Adj-R^2	0.25	0.25	0.21	0.19	0.12	0.07	0.38	0.38	0.37	0.31	0.23	0.05	0.39	0.39	0.35	0.31	0.2	0.06
Obs.	6,893	6,893	6,893	6,893	6,893	6,893	3,197	3,197	3,197	3,197	3,197	3,197	3,696	3,696	3,696	3,696	3,696	3,696

Notes: *, and + denote statistical significance at 5% and 10% level, respectively. FF: Functional Form - herein, interaction of weather components. Unless otherwise indicated, all panel fixed-effect OLS regressions include standard errors, in parentheses, clustered at the country level. Temperature is measured in °C and precipitation in metres. Constant terms are specified as follows: (I) country-by-year fixed effects and country-specific quadratic time trends; (II) continent-by-year fixed effects and country-specific quadratic time trends; (III) country fixed effects and country-specific quadratic time trends; (IV) country-by-year fixed effects and country-specific linear time trends; (V) country-by-year fixed effects excluding country-level time trends; (VI) continent-by-year fixed effects excluding country-level time trends.

Table A.7: Global log(GDP/Pop) responses to the quadratic FF - GDP per capita from WDI & weather from NASA's 0.25° GLDAS cells spatially collapsed to ISOs weighting by gridded population density from GPW dataset

Estimation period	1970-2018						1970-1994						1995-2018					
FEs specification	I	II	III	IV	V	VI	I	II	III	IV	V	VI	I	II	III	IV	V	VI
Temp.$_{i,t}$	0.01360+	0.01360+	0.01149	0.02661*	0.11314*	-0.03596	0.01362+	0.01362+	0.01637*	0.02647*	0.09847*	-0.02565	0.01214+	0.01214+	0.01219+	0.01361+	0.05643*	-0.03771
	(0.083)	(0.083)	(0.131)	(0.032)	(0.003)	(0.147)	(0.054)	(0.054)	(0.018)	(0.015)	(0.002)	(0.24)	(0.059)	(0.059)	(0.061)	(0.075)	(0.022)	(0.23)
(Temp.$_{i,t}$)^2	-0.00048+	-0.00048+	-0.00068*	-0.00096*	-0.00409*	0.00073	-0.00057*	-0.00057*	-0.00059*	-0.00090*	-0.00297*	0.00017	-0.00043*	-0.00043*	-0.00059*	-0.00052+	-0.00252*	0.00094
	(0.057)	(0.057)	(0.003)	(0.02)	(0.000)	(0.454)	(0.015)	(0.015)	(0.01)	(0.004)	(0.002)	(0.594)	(0.039)	(0.039)	(0.004)	(0.052)	(0.000)	(0.478)
Precip.$_{i,t}$	-0.000843	-0.000843	-0.000812	0.000851	0.003147+	-0.030280	0.002348*	0.002348*	0.003327*	0.001906	-0.000497	-0.057065	-0.000656	-0.000656	-0.000561	-0.001838*	0.003338+	-0.024707
	(0.245)	(0.245)	(0.233)	(0.46)	(0.087)	(0.167)	(0.021)	(0.021)	(0.001)	(0.212)	(0.866)	(0.207)	(0.191)	(0.192)	(0.274)	(0.036)	(0.066)	(0.137)
(Precip.$_{i,t}$)^2	0.000007	0.000007	0.000003	-0.000002	-0.000019+	0.000223	-0.000030*	-0.000030*	-0.000039*	-0.000025	0.000012	0.000666	-0.000003	-0.000003	-0.000003	0.000015*	-0.000018+	0.000143
	(0.114)	(0.114)	(0.483)	(0.735)	(0.082)	(0.444)	(0.006)	(0.006)	(0.000)	(0.11)	(0.695)	(0.304)	(0.417)	(0.417)	(0.42)	(0.005)	(0.068)	(0.473)
Adj-R^2	1	1	0.99	0.99	0.97	0.51	1	1	1	1	0.99	0.56	1	1	1	1	0.99	0.47
Obs.	6,862	6,862	6,862	6,862	6,862	6,862	2,996	2,996	2,996	2,996	2,996	2,996	3,866	3,866	3,866	3,866	3,866	3,866

Notes: *, and + denote statistical significance at 5% and 10% level, respectively. FF: Functional Form - herein, quadratic functions of weather components. Unless otherwise indicated, all panel fixed-effect OLS regressions include standard errors, in parentheses, clustered at the country level. Temperature is measured in °C and precipitation in metres. Constant terms are specified as follows: (I) country-by-year fixed effects and country-specific quadratic time trends; (II) continent-by-year fixed effects and country-specific quadratic time trends; (III) country fixed effects and country-specific quadratic time trends; (IV) country-by-year fixed effects and country-specific linear time trends; (V) country-by-year fixed effects excluding country-level time trends; (VI) continent-by-year fixed effects excluding country-level time trends.

Table A.8: Global log(GDP/Pop) responses to the quadratic FF - GDP per capita from PWT & weather from NASA's 0.25° GLDAS cells spatially collapsed to ISOs weighting by gridded population density from GPW dataset

Estimation period	1970-2018						1970-1994						1995-2018					
FEs specification	I	II	III	IV	V	VI	I	II	III	IV	V	VI	I	II	III	IV	V	VI
Temp.$_{i,t}$	0.01914+	0.01914+	0.01900+	0.03704*	0.14466*	0.01386	0.00672	0.00672	0.00787	0.00610	0.12382*	0.02145	0.01892*	0.01892*	0.01759*	0.01776+	0.07074*	0.00573
	(0.068)	(0.068)	(0.057)	(0.025)	(0.000)	(0.8)	(0.476)	(0.476)	(0.307)	(0.581)	(0.000)	(0.728)	(0.018)	(0.018)	(0.017)	(0.071)	(0.000)	(0.913)
(Temp.$_{i,t}$)^2	-0.00052	-0.00052	-0.00084*	-0.00119+	-0.00510*	-0.00073	-0.00032	-0.00032	-0.00032	-0.00035	-0.00389*	-0.00095	-0.00056*	-0.00056*	-0.00073*	-0.00060+	-0.00280*	-0.00049
	(0.131)	(0.131)	(0.007)	(0.053)	(0.000)	(0.593)	(0.336)	(0.336)	(0.296)	(0.353)	(0.000)	(0.489)	(0.035)	(0.036)	(0.003)	(0.083)	(0.000)	(0.743)
Precip.$_{i,t}$	0.000944	0.000944	0.000920	0.002608	-0.001860	-0.072634+	0.002696*	0.002696*	0.003893*	0.000848	-0.000007	-0.086163	-0.002005*	-0.002005*	-0.002207*	-0.001700	0.001245	-0.059647*
	(0.568)	(0.568)	(0.584)	(0.322)	(0.597)	(0.068)	(0.007)	(0.007)	(0.000)	(0.562)	(0.998)	(0.125)	(0.029)	(0.029)	(0.02)	(0.541)	(0.78)	(0.032)
(Precip.$_{i,t}$)^2	-0.000020	-0.000020	-0.000024	-0.000029	0.000043	0.000956+	-0.000032*	-0.000032*	-0.000043*	-0.000014	-0.000002	0.001131	0.000013	0.000013	0.000015	0.000006	0.000000	0.000791*
	(0.413)	(0.413)	(0.33)	(0.294)	(0.269)	(0.076)	(0.003)	(0.003)	(0.000)	(0.455)	(0.959)	(0.132)	(0.21)	(0.21)	(0.147)	(0.86)	(0.994)	(0.042)
Adj-R^2	0.99	0.99	0.99	0.99	0.96	0.54	1	1	1	0.99	0.98	0.52	1	1	1	1	0.98	0.54
Obs.	7,047	7,047	7,047	7,047	7,047	7,047	3,351	3,351	3,351	3,351	3,351	3,351	3,696	3,696	3,696	3,696	3,696	3,696

Notes: *, and + denote statistical significance at 5% and 10% level, respectively.FF: Functional Form - herein, quadratic functions of weather components. Unless otherwise indicated, all panel fixed-effect OLS regressions include standard errors, in parentheses, clustered at the country level. Temperature is measured in °C and precipitation in metres. Constant terms are specified as follows: (I) country-by-year fixed effects and country-specific quadratic time trends; (II) continent-by-year fixed effects and country-specific quadratic time trends; (III) country fixed effects and country-specific quadratic time trends; (IV) country-by-year fixed effects and country-specific linear time trends; (V) country-by-year fixed effects excluding country-level time trends; (VI) continent-by-year fixed effects excluding country-level time trends.

Table A.9: Global log(GDP/Pop) responses to the interaction FF - GDP per capita from WDI & weather from NASA's 0.25° GLDAS cells spatially collapsed to ISOs weighting by gridded population density from GPW dataset

Estimation period	1970-2018						1970-1994						1995-2018					
FEs specification	I	II	III	IV	V	VI	I	II	III	IV	V	VI	I	II	III	IV	V	VI
$Temp._{i,t}$	0.01352+	0.01352+	0.01113	0.02570*	0.11220*	-0.03255	0.01435*	0.01435*	0.01700*	0.02732*	0.10214*	-0.03097	0.01274*	0.01274*	0.01278*	0.01309+	0.05246*	-0.03318
	(0.087)	(0.088)	(0.146)	(0.036)	(0.003)	(0.213)	(0.046)	(0.046)	(0.015)	(0.012)	(0.002)	(0.178)	(0.047)	(0.047)	(0.049)	(0.084)	(0.026)	(0.3)
$Temp._{i,t} \times \overline{T}_i$	-0.00096+	-0.00096+	-0.00134*	-0.00186*	-0.00822*	0.00053	-0.00116*	-0.00116*	-0.00121*	-0.00182*	-0.00608*	0.00027	-0.00091*	-0.00091*	-0.00123*	-0.00102+	-0.00491*	0.00071
	(0.058)	(0.058)	(0.004)	(0.021)	(0.000)	(0.539)	(0.013)	(0.013)	(0.009)	(0.004)	(0.002)	(0.465)	(0.029)	(0.029)	(0.002)	(0.052)	(0.000)	(0.57)
$Precip._{i,t}$	-0.000911	-0.000911	-0.001016	0.001549	0.002081	-0.043418	0.002352*	0.002352*	0.003408*	0.001934	-0.001062	-0.050951	-0.001472+	-0.001472+	-0.001650+	-0.003115*	0.003448	-0.037594
	(0.403)	(0.403)	(0.361)	(0.414)	(0.507)	(0.264)	(0.03)	(0.03)	(0.002)	(0.222)	(0.743)	(0.311)	(0.083)	(0.083)	(0.068)	(0.039)	(0.261)	(0.273)
$Precip._{i,t} \times \overline{P}_i$	0.000018	0.000018	0.000012	-0.000021	-0.000026	0.000491	-0.000060*	-0.000060*	-0.000079*	-0.000050	0.000037	0.000600	0.000011	0.000011	0.000016	0.000067*	-0.000053	0.000409
	(0.422)	(0.422)	(0.589)	(0.544)	(0.708)	(0.432)	(0.008)	(0.008)	(0.000)	(0.122)	(0.596)	(0.442)	(0.589)	(0.589)	(0.462)	(0.027)	(0.361)	(0.471)
Adj-R^2	1	1	0.99	0.99	0.97	0.51	1	1	1	1	0.99	0.55	1	1	1	1	0.99	0.47
Obs.	6,862	6,862	6,862	6,862	6,862	6,862	2,996	2,996	2,996	2,996	2,996	2,996	3,866	3,866	3,866	3,866	3,866	3,866

Notes: *, and + denote statistical significance at 5% and 10% level, respectively. FF: Functional Form - herein, interaction of weather components. Unless otherwise indicated, all panel fixed-effect OLS regressions include standard errors, in parentheses, clustered at the country level. Temperature is measured in °C and precipitation in metres. Constant terms are specified as follows: (I) country-by-year fixed effects and country-specific quadratic time trends; (II) continent-by-year fixed effects and country-specific quadratic time trends; (III) country fixed effects and country-specific quadratic time trends; (IV) country-by-year fixed effects and country-specific linear time trends; (V) country-by-year fixed effects excluding country-level time trends; (VI) continent-by-year fixed effects excluding country-level time trends.

Table A.10: Global log(GDP/Pop) responses to the interaction FF - GDP per capita from PWT & weather from NASA's 0.25° GLDAS cells spatially collapsed to ISOs weighting by gridded population density from GPW dataset

Estimation period	1970-2018						1970-1994						1995-2018					
FEs specification	I	II	III	IV	V	VI	I	II	III	IV	V	VI	I	II	III	IV	V	VI
$Temp._{i,t}$	0.01830+	0.01830+	0.01770+	0.03605*	0.14563*	0.00534	0.00695	0.00695	0.00798	0.00655	0.13042*	0.01188	0.01928*	0.01928*	0.01801*	0.01622+	0.06619*	0.00414
	(0.077)	(0.077)	(0.072)	(0.029)	(0.000)	(0.915)	(0.471)	(0.472)	(0.314)	(0.561)	(0.000)	(0.849)	(0.014)	(0.014)	(0.013)	(0.089)	(0.001)	(0.928)
$Temp._{i,t} \times \overline{T}_i$	-0.00101	-0.00101	-0.00162*	-0.00235+	-0.01040*	-0.00061	-0.00065	-0.00065	-0.00063	-0.00071	-0.00807*	-0.00077	-0.00116*	-0.00116*	-0.00151*	-0.00115+	-0.00548*	-0.00058
	(0.131)	(0.131)	(0.007)	(0.055)	(0.000)	(0.627)	(0.34)	(0.34)	(0.305)	(0.346)	(0.000)	(0.576)	(0.028)	(0.028)	(0.002)	(0.086)	(0.000)	(0.669)
$Precip._{i,t}$	0.000093	0.000093	-0.000570	0.001861	-0.004058	-0.071791+	0.002644*	0.002644*	0.003891*	0.000770	-0.000522	-0.090347	-0.002576*	-0.002576*	-0.00293*	-0.003081	-0.000926	-0.057077*
	(0.938)	(0.938)	(0.656)	(0.508)	(0.271)	(0.087)	(0.016)	(0.016)	(0.001)	(0.631)	(0.876)	(0.141)	(0.009)	(0.009)	(0.004)	(0.23)	(0.848)	(0.047)
$Precip._{i,t} \times \overline{P}_i$	-0.000019	-0.000019	-0.000013	-0.000041	0.000143+	0.001022+	-0.000063*	-0.000063*	-0.000086*	-0.000025	0.000008	0.001255	0.000041+	0.000041+	0.00005*	0.000048	0.000057	0.000841+
	(0.555)	(0.555)	(0.712)	(0.487)	(0.086)	(0.095)	(0.008)	(0.008)	(0.000)	(0.531)	(0.919)	(0.149)	(0.057)	(0.057)	(0.025)	(0.4)	(0.586)	(0.056)
Adj-R^2	0.99	0.99	0.99	0.99	0.96	0.54	1	1	1	0.99	0.98	0.52	1	1	1	1	0.98	0.54
Obs.	7,047	7,047	7,047	7,047	7,047	7,047	3,351	3,351	3,351	3,351	3,351	3,351	3,696	3,696	3,696	3,696	3,696	3,696

Notes: *, and + denote statistical significance at 5% and 10% level, respectively. FF: Functional Form - herein, interaction of weather components. Unless otherwise indicated, all panel fixed-effect OLS regressions include standard errors, in parentheses, clustered at the country level. Temperature is measured in °C and precipitation in metres. Constant terms are specified as follows: (I) country-by-year fixed effects and country-specific quadratic time trends; (II) continent-by-year fixed effects and country-specific quadratic time trends; (III) country fixed effects and country-specific quadratic time trends; (IV) country-by-year fixed effects and country-specific linear time trends; (V) country-by-year fixed effects excluding country-level time trends; (VI) continent-by-year fixed effects excluding country-level time trends.

Table A.11: Global log(GDP/Pop) responses to the quadratic FF - regional GDP per capita from DOSE & weather from NASA's 0.25° GLDAS cells spatially collapsed to GID(1)s weighting by gridded population density from the GPW dataset

Estimation period	1970-2018						1970-1994						1995-2018					
FEs specification	I	II	III	IV	V	VI	I	II	III	IV	V	VI	I	II	III	IV	V	VI
$Temp._{i,t}$	0.02455*	0.02455*	0.02552*	0.03384*	0.03433*	0.03507	-0.00823	-0.00823	-0.00782	-0.00798	0.03339*	0.0533	0.02306*	0.02306*	0.02401*	0.01637*	0.02722*	0.03192
	(0.000)	(0.000)	(0.000)	(0.000)	(0.000)	(0.348)	(0.104)	(0.104)	(0.128)	(0.407)	(0.012)	(0.372)	(0.000)	(0.000)	(0.000)	(0.000)	(0.000)	(0.367)
$(Temp._{i,t})^2$	-0.00119*	-0.00119*	-0.00140*	-0.00132*	-0.00133*	-0.00354*	0.00083*	0.00083*	0.00076*	0.00030	0.00024	-0.0048	-0.00089*	-0.00089*	-0.00096*	-0.00045*	-0.00159*	-0.00338*
	(0.000)	(0.000)	(0.000)	(0.000)	(0.001)	(0.039)	(0.001)	(0.001)	(0.002)	(0.446)	(0.688)	(0.122)	(0.000)	(0.000)	(0.000)	(0.001)	(0.000)	(0.023)
$Precip._{i,t}$	-0.001915*	-0.001915*	-0.001874*	-0.001679*	-0.001889+	0.031419	-0.001481*	-0.001481*	-0.001383*	0.000050	0.000649	0.038765	-0.000423	-0.000423	-0.000559	-0.001014+	-0.001372	0.031513
	(0.000)	(0.000)	(0.000)	(0.009)	(0.054)	(0.192)	(0.019)	(0.019)	(0.028)	(0.949)	(0.621)	(0.176)	(0.44)	(0.44)	(0.304)	(0.054)	(0.155)	(0.194)
$(Precip._{i,t})^2$	0.000016*	0.000016*	0.000014*	0.000021*	0.000030*	-0.000238	0.000013+	0.000013+	0.000015*	-0.000011	-0.000005	-0.000256	-0.000004	-0.000004	-0.000004	0.000015*	0.000030*	-0.000249
	(0.004)	(0.004)	(0.007)	(0.000)	(0.002)	(0.223)	(0.057)	(0.057)	(0.035)	(0.238)	(0.747)	(0.259)	(0.418)	(0.418)	(0.449)	(0.001)	(0.001)	(0.211)
Adj-R^2	0.99	0.99	0.99	0.99	0.96	0.5	1	1	1	0.99	0.99	0.7	0.99	0.99	0.99	0.99	0.97	0.43
Obs.	37,988	37,988	37,988	37,988	37,988	37,988	9,757	9,757	9,757	9,757	9,757	9,757	28,231	28,231	28,231	28,231	28,231	28,231

Notes: *, and + denote statistical significance at 5% and 10% level, respectively.FF: Functional Form - herein, quadratic functions of weather components. Unless otherwise indicated, all panel fixed-effect OLS regressions include standard errors, in parentheses, clustered at the country level. Temperature is measured in °C and precipitation in metres. Constant terms are specified as follows: (I) province-by-year fixed effects and province-specific quadratic time trends; (II) continent-by-year fixed effects and province-specific quadratic time trends; (III) province fixed effects and province-specific quadratic time trends; (IV) province-by-year fixed effects and province-specific linear time trends; (V) province-by-year fixed effects excluding province-level time trends; (VI) continent-by-year fixed effects excluding province-level time trends.

Table A.12: Global log(GDP/Pop) responses to the interaction FF - regional GDP per capita from DOSE & weather from NASA's 0.25° GLDAS cells spatially collapsed to GID(1)s weighting by gridded population density from the GPW dataset

Estimation period	1970-2018						1970-1994						1995-2018					
FEs specification	I	II	III	IV	V	VI	I	II	III	IV	V	VI	I	II	III	IV	V	VI
$Temp._{i,t}$	0.02361*	0.02361*	0.0247*	0.03441*	0.03521*	0.05322	-0.00918+	-0.00918+	-0.00839	-0.00914	0.03526*	0.09077	0.02292*	0.02292*	0.02400*	0.01654*	0.02816*	0.04765
	(0.000)	(0.000)	(0.000)	(0.000)	(0.000)	(0.272)	(0.086)	(0.087)	(0.122)	(0.359)	(0.011)	(0.342)	(0.000)	(0.000)	(0.000)	(0.000)	(0.000)	(0.249)
$Temp._{i,t} \times \overline{T}_i$	-0.00227*	-0.00227*	-0.0027*	-0.00269*	-0.00279*	-0.00350*	0.00172*	0.00172*	0.00154*	0.00071	0.00029	-0.00525	-0.00176*	-0.00176*	-0.00192*	-0.00091*	-0.00334*	-0.00324*
	(0.000)	(0.000)	(0.000)	(0.000)	(0.000)	(0.034)	(0.001)	(0.001)	(0.002)	(0.383)	(0.807)	(0.135)	(0.000)	(0.000)	(0.000)	(0.001)	(0.000)	(0.015)
Adj-R^2	0.99	0.99	0.99	0.99	0.96	0.48	1	1	1	0.99	0.99	0.68	0.99	0.99	0.99	0.99	0.97	0.41
Obs.	37,988	37,988	37,988	37,988	37,988	37,988	9,757	9,757	9,757	9,757	9,757	9,757	28,231	28,231	28,231	28,231	28,231	28,231

Notes: *, and + denote statistical significance at 5% and 10% level, respectively. FF: Functional Form - herein, interaction of contemporaneous temperature with its baseline average. Unless otherwise indicated, all panel fixed-effect OLS regressions include standard errors, in parentheses, clustered at the province level. Temperature is measured in °C. Constant terms are specified as follows: (I) province-by-year fixed effects and province-specific quadratic time trends; (II) continent-by-year fixed effects and province-specific quadratic time trends; (III) province fixed effects and province-specific quadratic time trends; (IV) province-by-year fixed effects and province-specific linear time trends; (V) province-by-year fixed effects excluding province-level time trends; (VI) continent-by-year fixed effects excluding province-level time trends.

Table A.13: Global Δlog(GDP/Pop) responses to the quadratic FF - regional GDP per capita from DOSE & weather from NASA's 0.25° GLDAS cells spatially collapsed to GID(1)s weighting by gridded population density from the GPW dataset

Estimation period	1970-2018						1970-1994						1995-2018					
FEs specification	I	II	III	IV	V	VI	I	II	III	IV	V	VI	I	II	III	IV	V	VI
$Temp._{i,t}$	0.01158*	0.01158*	0.00809*	0.0102*	0.00367+	-0.00051+	-0.01067	-0.01067	-0.01389*	-0.00016	0.00761	-0.00392	0.01404*	0.01404*	0.00909*	0.00961*	0.00670*	-0.00022
	(0.000)	(0.000)	(0.001)	(0.000)	(0.055)	(0.088)	(0.107)	(0.108)	(0.039)	(0.977)	(0.155)	(0.177)	(0.000)	(0.000)	(0.000)	(0.000)	(0.001)	(0.488)
$(Temp._{i,t})^2$	-0.00045*	-0.00045*	-0.00047*	-0.0005*	-0.00025*	0.00001	0.00069*	0.00069*	0.00063*	0.00035	-0.00012	0.00011	-0.00058*	-0.00058*	-0.00061*	-0.00052*	-0.00036*	0.00000
	(0.000)	(0.000)	(0.000)	(0.000)	(0.01)	(0.537)	(0.018)	(0.018)	(0.03)	(0.163)	(0.588)	(0.203)	(0.000)	(0.000)	(0.000)	(0.000)	(0.000)	(0.916)
$Precip._{i,t}$	-0.001385*	-0.001385*	-0.001578*	-0.001391*	-0.000989*	0.00016	-0.000891	-0.000891	-0.001291+	-0.001389*	-0.000486	0.002127+	-0.000205	-0.000205	-0.000574	-0.001424*	-0.001022*	-0.000167
	(0.001)	(0.001)	(0.000)	(0.000)	(0.001)	(0.295)	(0.23)	(0.231)	(0.071)	(0.046)	(0.466)	(0.062)	(0.623)	(0.623)	(0.178)	(0.004)	(0.008)	(0.347)
$(Precip._{i,t})^2$	0.000010*	0.000010*	0.000010*	0.000008*	0.000008*	0.00000	0.000002	0.000002	0.000006	0.000008	-0.000005	-0.000025+	0.000001	0.000001	0.000004	0.000007*	0.000009*	0.000003
	(0.006)	(0.006)	(0.004)	(0.004)	(0.000)	(0.787)	(0.855)	(0.855)	(0.445)	(0.279)	(0.472)	(0.06)	(0.726)	(0.726)	(0.322)	(0.042)	(0.001)	(0.166)
Adj-R^2	0.15	0.15	0.13	0.11	0.05	0.03	0.26	0.26	0.25	0.21	0.12	0.06	0.22	0.22	0.2	0.13	0.07	0.03
Obs.	36,583	36,583	36,583	36,583	36,583	36,583	9,080	9,080	9,080	9,080	9,080	9,080	27,503	27,503	27,503	27,503	27,503	27,503

Notes: *, and + denote statistical significance at 5% and 10% level, respectively.FF: Functional Form - herein, quadratic functions of weather components. Unless otherwise indicated, all panel fixed-effect OLS regressions include standard errors, in parentheses, clustered at the province level. Temperature is measured in °C and precipitation in metres. Constant terms are specified as follows: (I) province-by-year fixed effects and province-specific quadratic time trends; (II) continent-by-year fixed effects and province-specific quadratic time trends; (III) province fixed effects and province-specific quadratic time trends; (IV) province-by-year fixed effects and province-specific linear time trends; (V) province-by-year fixed effects excluding province-level time trends; (VI) continent-by-year fixed effects excluding province-level time trends.

Table A.14: Global Δlog(GDP/Pop) responses to the interaction FF - regional GDP per capita from DOSE & weather from NASA's 0.25° GLDAS cells spatially collapsed to GID(1)s weighting by gridded population density from the GPW dataset

Estimation period	1970-2018						1970-1994						1995-2018					
FEs specification	I	II	III	IV	V	VI	I	II	III	IV	V	VI	I	II	III	IV	V	VI
$Temp._{i,t}$	0.01112*	0.01112*	0.00751*	0.00985*	0.00362+	-0.00052*	-0.01201+	-0.01201+	-0.01576*	-0.00081	0.00754	-0.00198	0.01367*	0.01367*	0.00861*	0.00915*	0.00639*	-0.00043
	(0.000)	(0.000)	(0.001)	(0.000)	(0.061)	(0.025)	(0.087)	(0.087)	(0.028)	(0.893)	(0.172)	(0.533)	(0.000)	(0.000)	(0.001)	(0.000)	(0.002)	(0.305)
$Temp._{i,t} \times \overline{T}_i$	-0.00084*	-0.00084*	-0.00087*	-0.00095*	-0.00050*	0.00001+	0.00149*	0.00149*	0.00141*	0.00077	-0.00022	0.00007	-0.00113*	-0.00113*	-0.00117*	-0.00098*	-0.00071*	0.00001
	(0.000)	(0.000)	(0.000)	(0.000)	(0.011)	(0.085)	(0.013)	(0.013)	(0.019)	(0.134)	(0.624)	(0.457)	(0.000)	(0.000)	(0.000)	(0.000)	(0.000)	(0.614)
Adj-R^2	0.15	0.15	0.13	0.11	0.05	0.03	0.26	0.26	0.24	0.21	0.12	0.05	0.22	0.22	0.2	0.13	0.07	0.03
Obs.	36,583	36,583	36,583	36,583	36,583	36,583	9,080	9,080	9,080	9,080	9,080	9,080	27,503	27,503	27,503	27,503	27,503	27,503

Notes: *, and + denote statistical significance at 5% and 10% level, respectively. FF: Functional Form - herein, interaction of contemporaneous temperature with its baseline average. Unless otherwise indicated, all panel fixed-effect OLS regressions include standard errors, in parentheses, clustered at the province level. Temperature is measured in °C. Constant terms are specified as follows: (I) province-by-year fixed effects and province-specific quadratic time trends; (II) continent-by-year fixed effects and province-specific quadratic time trends; (III) province fixed effects and province-specific quadratic time trends; (IV) province-by-year fixed effects and province-specific linear time trends; (V) province-by-year fixed effects excluding province-level time trends; (VI) continent-by-year fixed effects excluding province-level time trends.

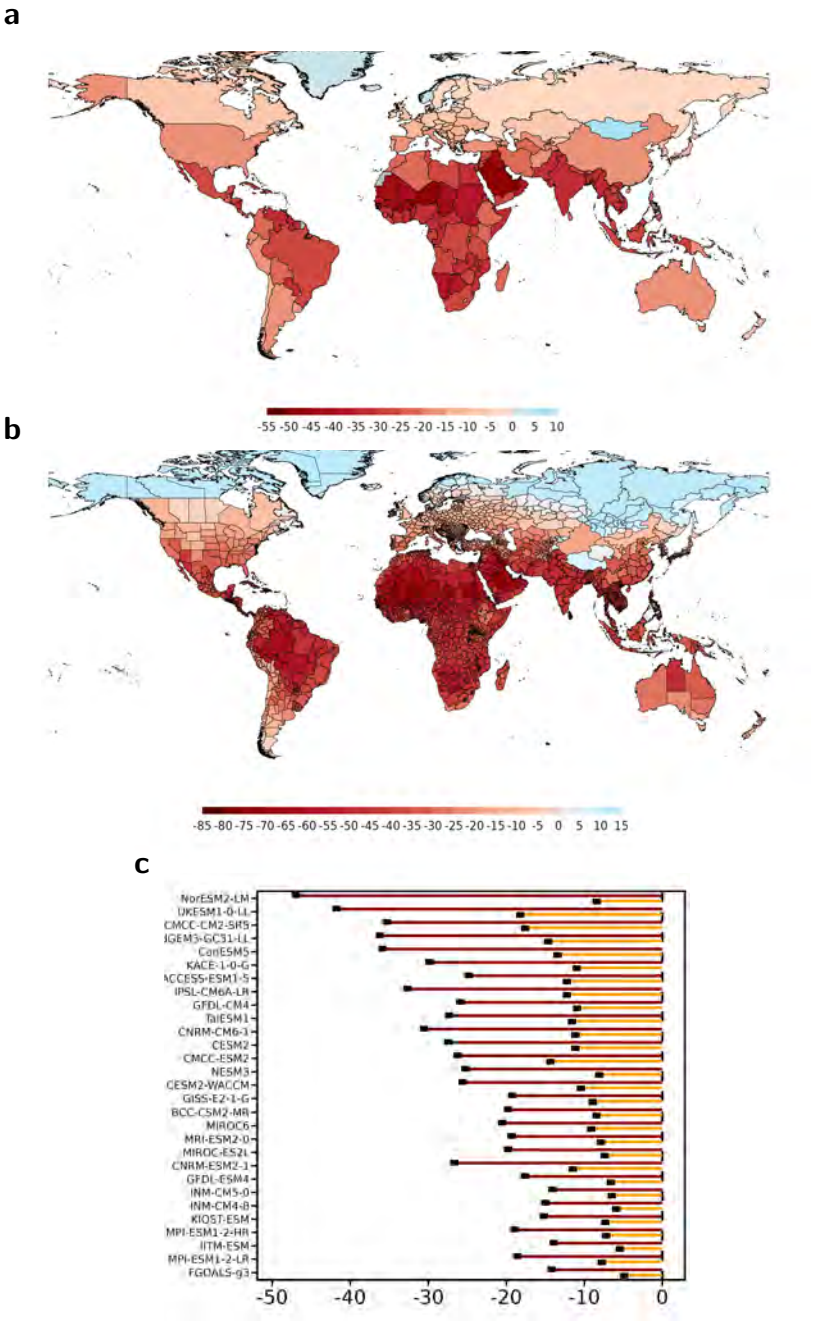

Figure A.13: Projected climate-shift impacts (%) on per capita GDP, 2081-2099 epoch relative to constant historical 1985-2004 temperature means, SSP5-8.5 vigorous warming scenario, 15 'likely' CMIP6 global climate models (GCMs).

a Spatially distributed country-level multi-model medians of 15 'likely' CMIP6 Global Climate Models (GCMs) simulated impacts, 2081-2099 epoch, econometrically structured from country-level climatic data matched with year-to-year per capita GDP realisations (*à la Burke et al (2015)*). Chosen equation specification to calibrate the projections is pooled FE-OLS accounting for short-run temperature effects only. **b** Spatially distributed province-level multi-model medians of 15 'likely' CMIP6 GCMs simulated estimates, 2081-2099 epoch, econometrically structured from sub-national administrative region-level climatic data matched with year-to-year gross regional per capita product realisations (*à la Kotz et al (2024)*). Chosen equation specification to calibrate the projections is pooled FE-OLS accounting for short-run temperature effects only. **c** Cross-region globally averaged projected damages (%), point-level estimates from each of the full set of 30 CMIP6 GCMs (including those falling inside and outside the 'likely' and 'very likely' ranges) at 2081-2099 epoch, SSP5-8.5 vigorous (red) versus SSP2-4.5 moderate (orange) warming scenarios.

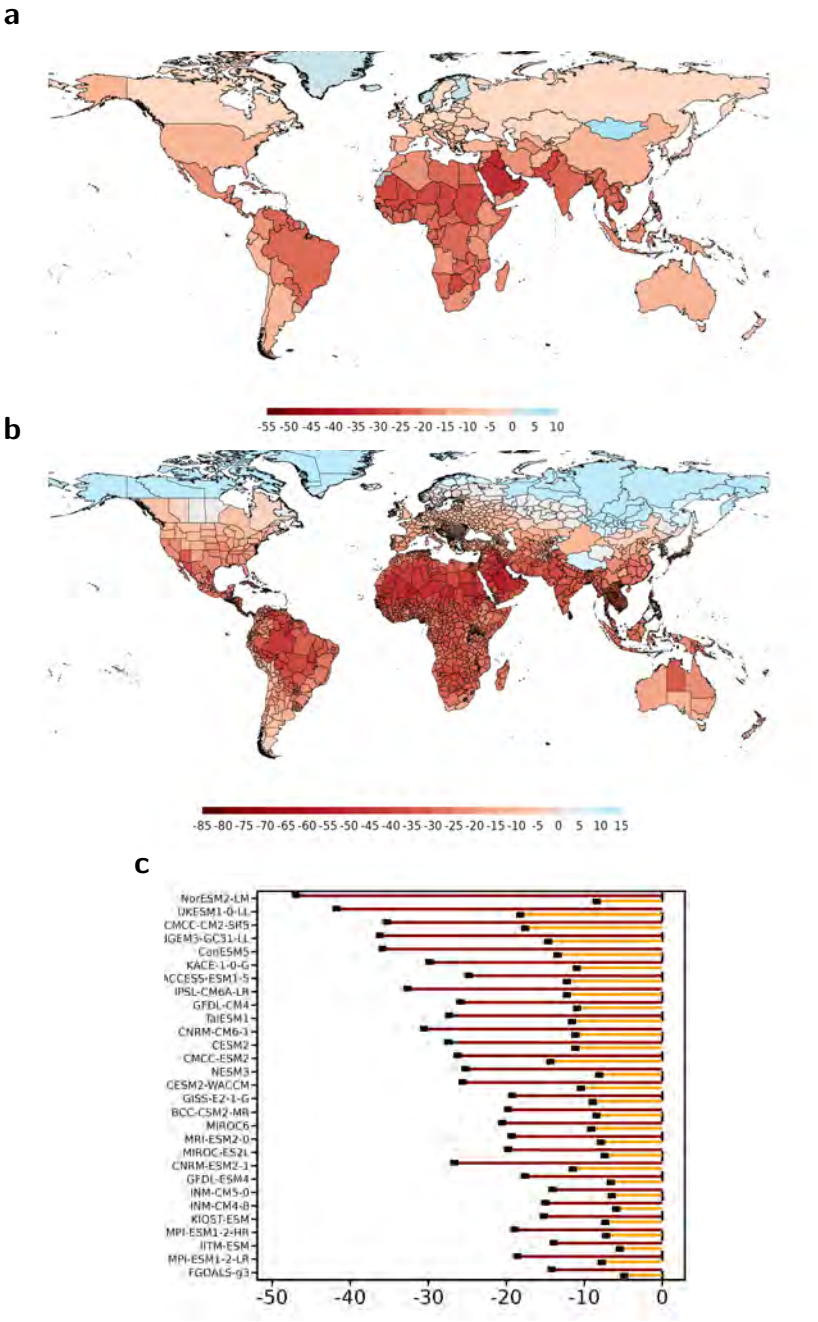

Figure A.14: Projected climate-shift impacts (%) on per capita GDP, 2081-2099 epoch relative to constant historical 1985-2004 temperature means, intermediate mid-point scenario between SSP5-8.5 vigorous & SSP2-4.5 moderate warmings, 15 'likely' CMIP6 global climate models (GCMs).

a Spatially distributed country-level multi-model medians of 15 'likely' CMIP6 Global Climate Models (GCMs) simulated impacts, 2081-2099 epoch, econometrically structured from country-level climatic data matched with year-to-year per capita GDP realisations (*à la Burke et al (2015)*). Chosen equation specification to calibrate the projections is pooled FE-OLS accounting for short-run temperature effects only. **b** Spatially distributed province-level multi-model medians of 15 'likely' CMIP6 GCMs simulated estimates, 2081-2099 epoch, econometrically structured from sub-national administrative region-level climatic data matched with year-to-year gross regional per capita product realisations (*à la Kotz et al (2024)*). Chosen equation specification to calibrate the projections is pooled FE-OLS accounting for short-run temperature effects only. **c** Cross-region globally averaged projected damages (%), point-level estimates from each of the full set of 30 CMIP6 GCMs (including those falling inside and outside the 'likely' and 'very likely' ranges) at 2081-2099 epoch, SSP5-8.5 vigorous (red) versus SSP2-4.5 moderate (orange) warming scenarios.

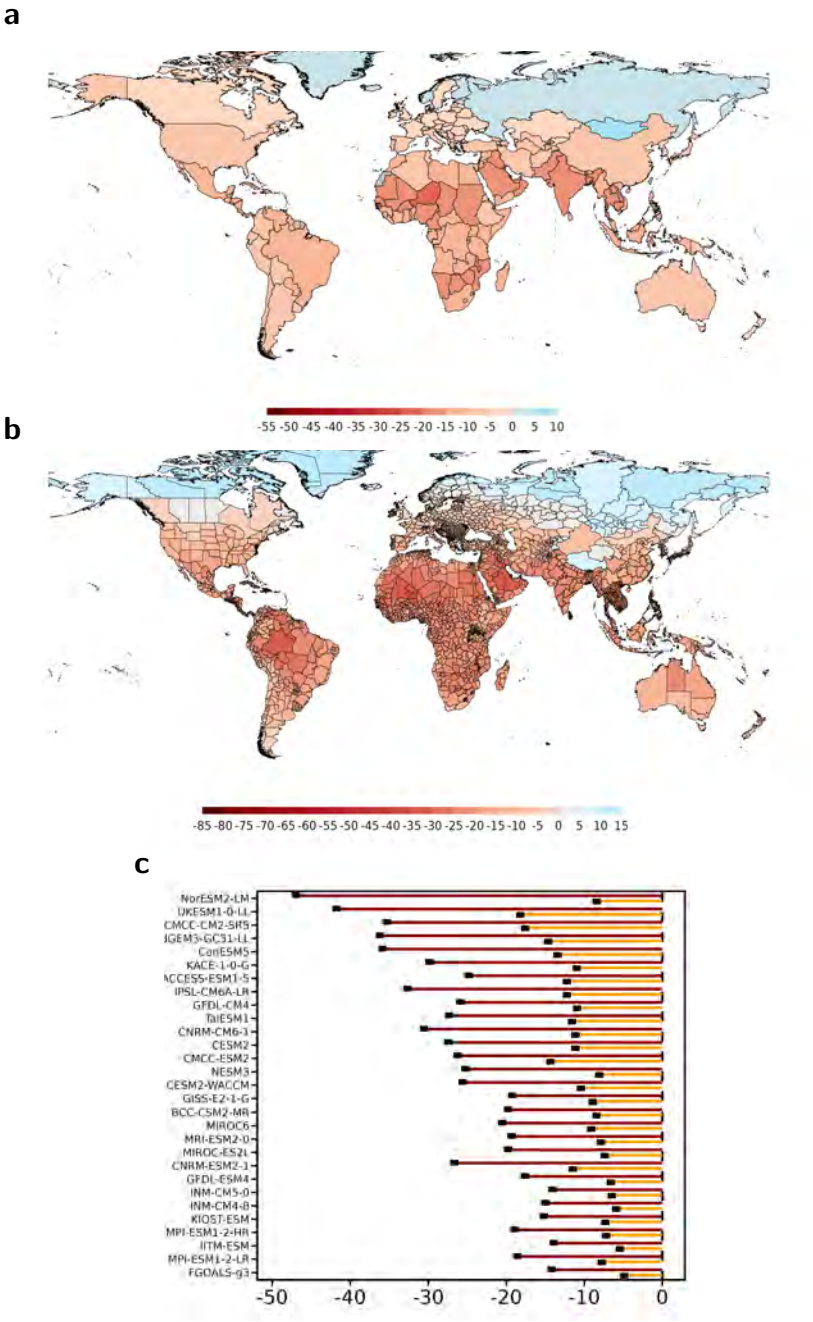

Figure A.15: Projected climate-shift impacts (%) on per capita GDP, 2081-2099 epoch relative to constant historical 1985-2004 temperature means, SSP2-4.5 moderate warming scenario, 15 'likely' CMIP6 global climate models (GCMs).

a Spatially distributed country-level multi-model medians of 15 'likely' CMIP6 Global Climate Models (GCMs) simulated impacts, 2081-2099 epoch, econometrically structured from country-level climatic data matched with year-to-year per capita GDP realisations (*à la Burke et al (2015)*). Chosen equation specification to calibrate the projections is pooled FE-OLS accounting for short-run temperature effects only. **b** Spatially distributed province-level multi-model medians of 15 'likely' CMIP6 GCMs simulated estimates, 2081-2099 epoch, econometrically structured from sub-national administrative region-level climatic data matched with year-to-year gross regional per capita product realisations (*à la Kotz et al (2024)*). Chosen equation specification to calibrate the projections is pooled FE-OLS accounting for short-run temperature effects only. **c** Cross-region globally averaged projected damages (%), point-level estimates from each of the full set of 30 CMIP6 GCMs (including those falling inside and outside the 'likely' and 'very likely' ranges) at 2081-2099 epoch, SSP5-8.5 vigorous (red) versus SSP2-4.5 moderate (orange) warming scenarios.

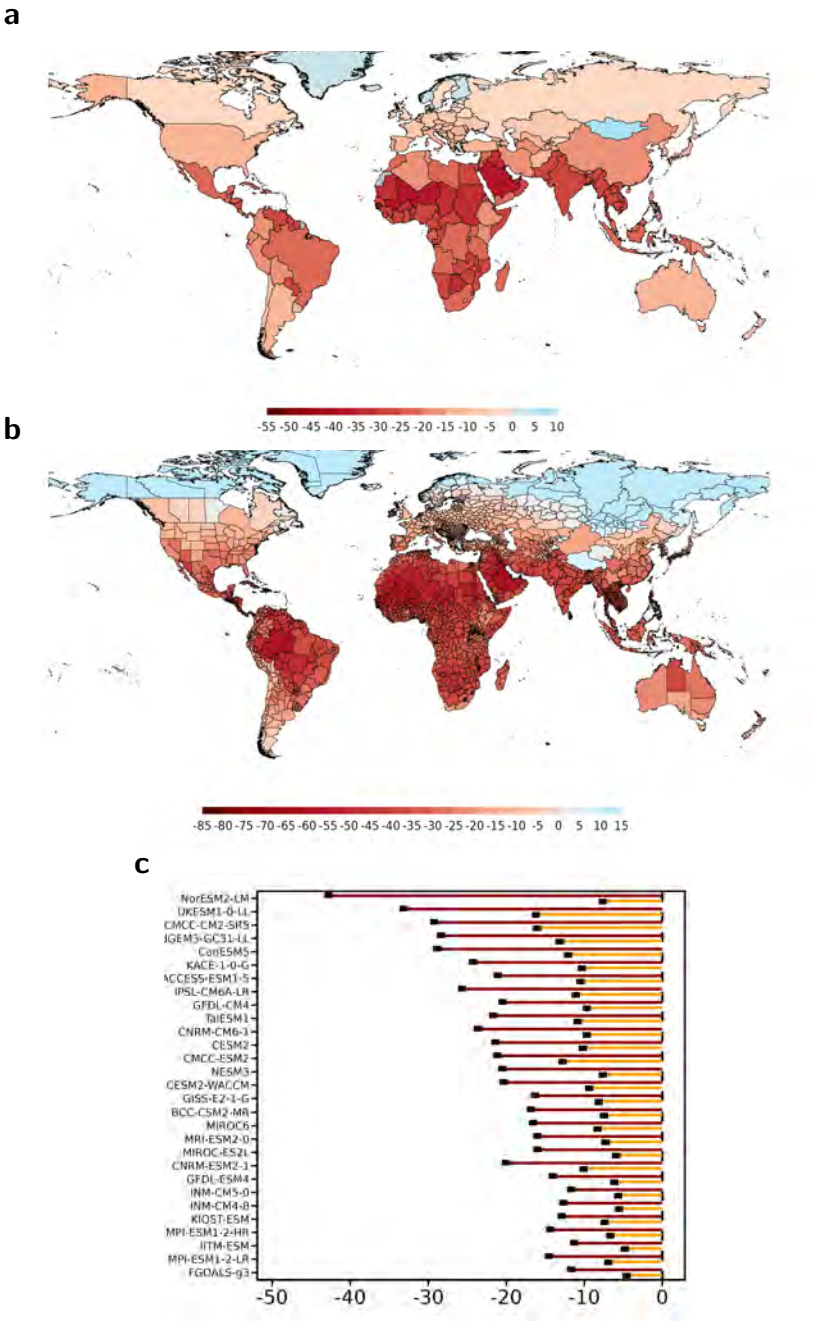

Figure A.16: Projected climate-shift impacts (%) on per capita GDP, 2071-2090 epoch relative to constant historical 1985-2004 temperature means, SSP5-8.5 vigorous warming scenario, 15 'likely' CMIP6 global climate models (GCMs).

a Spatially distributed country-level multi-model medians of 15 'likely' CMIP6 Global Climate Models (GCMs) simulated impacts, 2071-2090 epoch, econometrically structured from country-level climatic data matched with year-to-year per capita GDP realisations (*à la Burke et al (2015)*). Chosen equation specification to calibrate the projections is pooled FE-OLS accounting for short-run temperature effects only. **b** Spatially distributed province-level multi-model medians of 15 'likely' CMIP6 GCMs simulated estimates, 2071-2090 epoch, econometrically structured from sub-national administrative region-level climatic data matched with year-to-year gross regional per capita product realisations (*à la Kotz et al (2024)*). Chosen equation specification to calibrate the projections is pooled FE-OLS accounting for short-run temperature effects only. **c** Cross-region globally averaged projected damages (%), point-level estimates from each of the full set of 30 CMIP6 GCMs (including those falling inside and outside the 'likely' and 'very likely' ranges) at 2081-2099 epoch, SSP5-8.5 vigorous (red) versus SSP2-4.5 moderate (orange) warming scenarios.

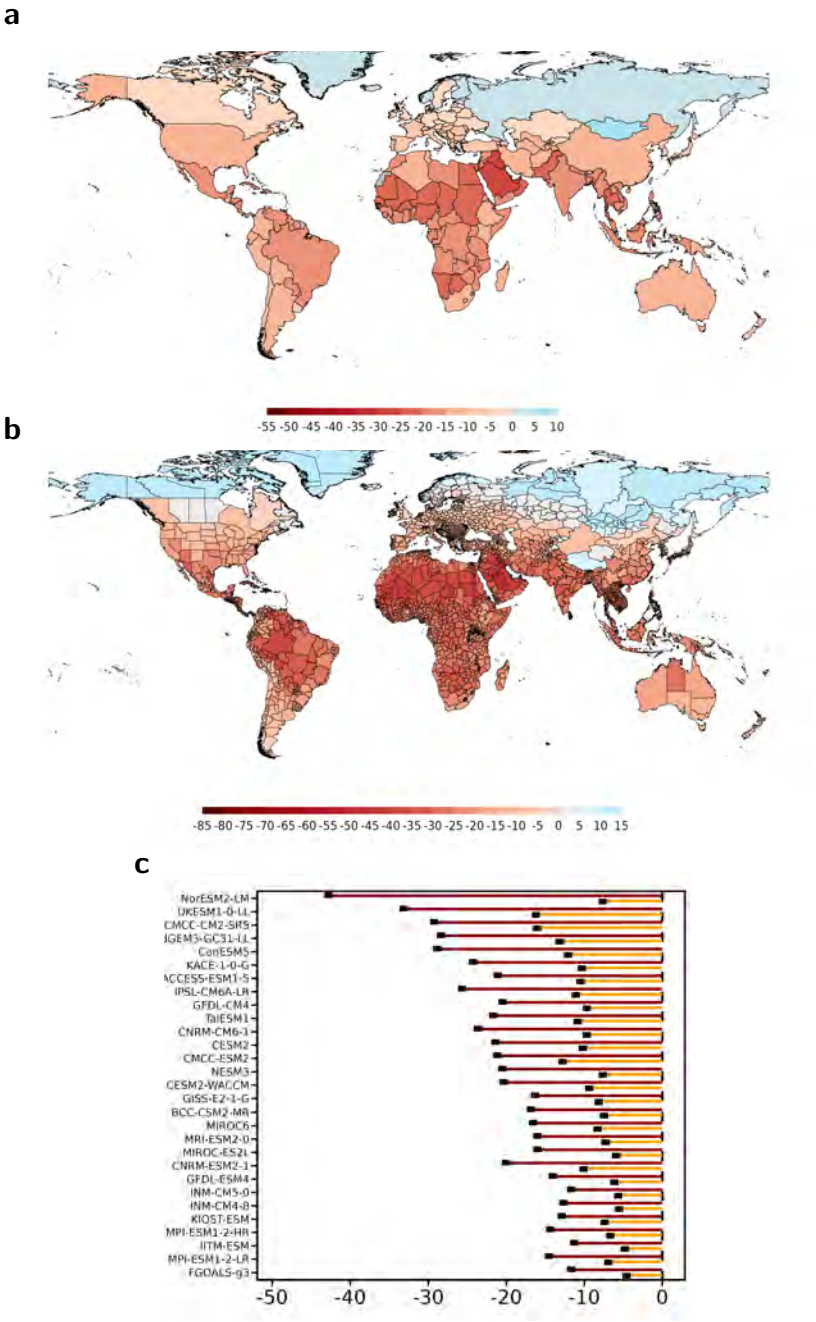

Figure A.17: Projected climate-shift impacts (%) on per capita GDP, 2071-2090 epoch relative to constant historical 1985-2004 temperature means, intermediate mid-point scenario between SSP5-8.5 vigorous & SSP2-4.5 moderate warmings, 15 'likely' CMIP6 global climate models (GCMs).

a Spatially distributed country-level multi-model medians of 15 'likely' CMIP6 Global Climate Models (GCMs) simulated impacts, 2071-2090 epoch, econometrically structured from country-level climatic data matched with year-to-year per capita GDP realisations (*à la Burke et al (2015)*). Chosen equation specification to calibrate the projections is pooled FE-OLS accounting for short-run temperature effects only. **b** Spatially distributed province-level multi-model medians of 15 'likely' CMIP6 GCMs simulated estimates, 2071-2090 epoch, econometrically structured from sub-national administrative region-level climatic data matched with year-to-year gross regional per capita product realisations (*à la Kotz et al (2024)*). Chosen equation specification to calibrate the projections is pooled FE-OLS accounting for short-run temperature effects only. **c** Cross-region globally averaged projected damages (%), point-level estimates from each of the full set of 30 CMIP6 GCMs (including those falling inside and outside the 'likely' and 'very likely' ranges) at 2081-2099 epoch, SSP5-8.5 vigorous (red) versus SSP2-4.5 moderate (orange) warming scenarios.

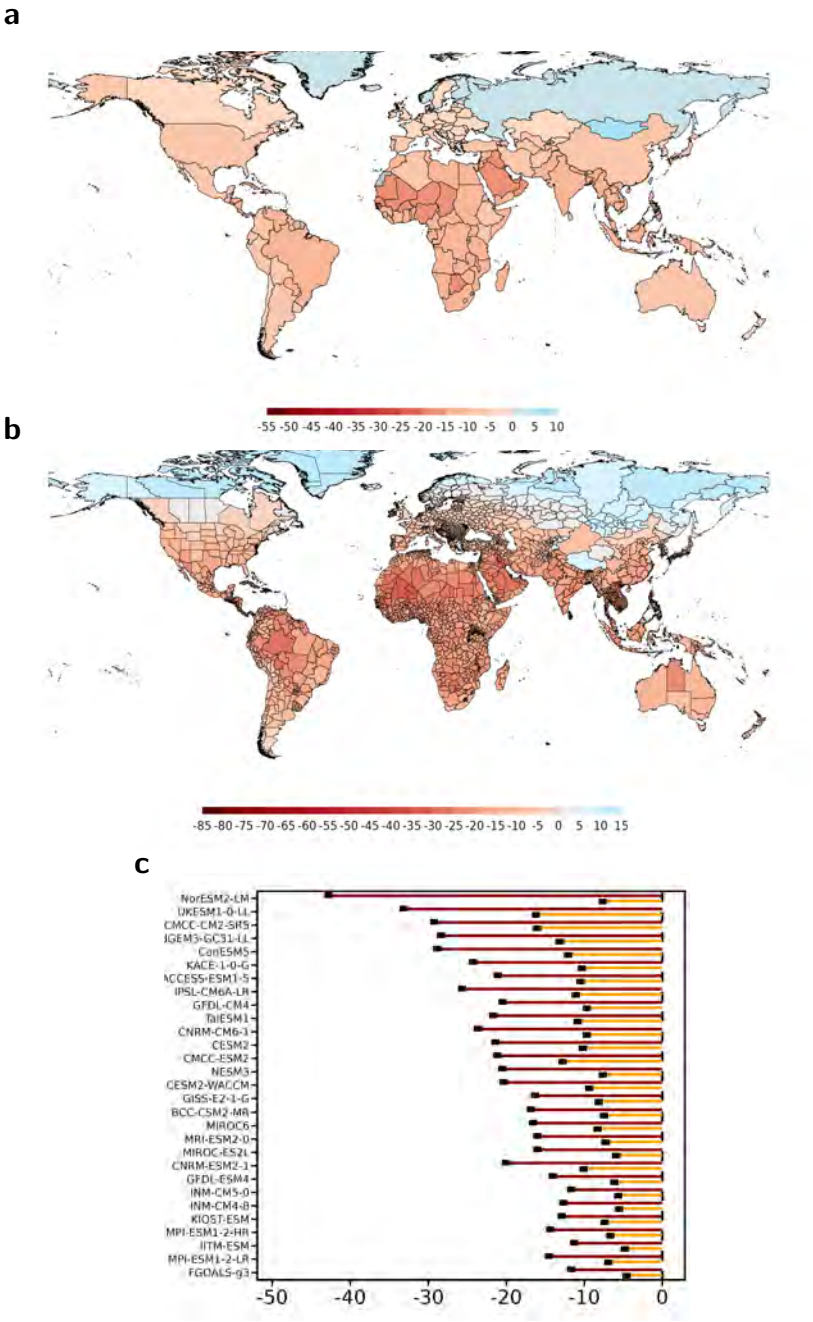

Figure A.18: Projected climate-shift impacts (%) on per capita GDP, 2071-2090 epoch relative to constant historical 1985-2004 temperature means, SSP2-4.5 moderate warming scenario, 15 'likely' CMIP6 global climate models (GCMs).

a Spatially distributed country-level multi-model medians of 15 'likely' CMIP6 Global Climate Models (GCMs) simulated impacts, 2071-2090 epoch, econometrically structured from country-level climatic data matched with year-to-year per capita GDP realisations (*à la Burke et al (2015)*). Chosen equation specification to calibrate the projections is pooled FE-OLS accounting for short-run temperature effects only. **b** Spatially distributed province-level multi-model medians of 15 'likely' CMIP6 GCMs simulated estimates, 2071-2090 epoch, econometrically structured from sub-national administrative region-level climatic data matched with year-to-year gross regional per capita product realisations (*à la Kotz et al (2024)*). Chosen equation specification to calibrate the projections is pooled FE-OLS accounting for short-run temperature effects only. **c** Cross-region globally averaged projected damages (%), point-level estimates from each of the full set of 30 CMIP6 GCMs (including those falling inside and outside the 'likely' and 'very likely' ranges) at 2071-2090 epoch, SSP5-8.5 vigorous (red) versus SSP2-4.5 moderate (orange) warming scenarios.

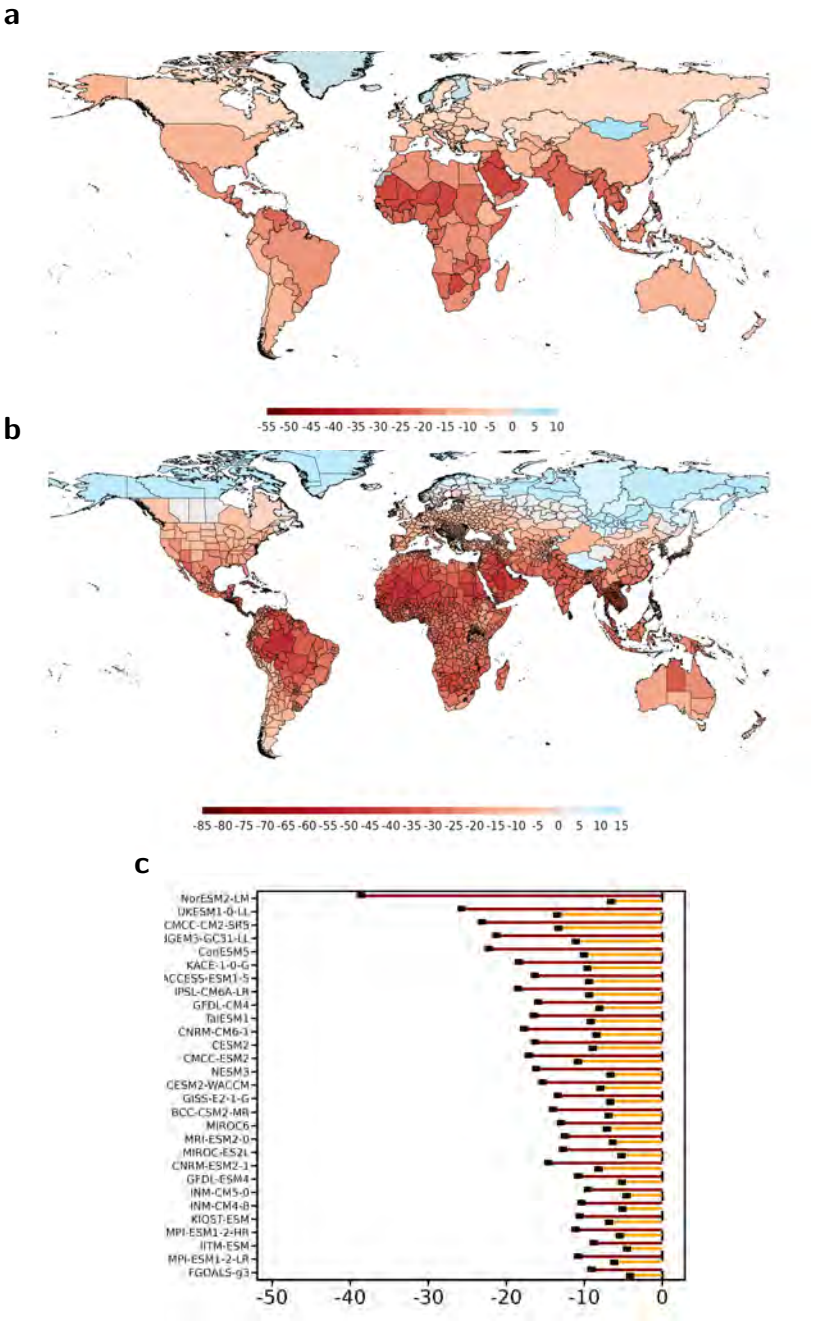

Figure A.19: Projected climate-shift impacts (%) on per capita GDP, 2061-2080 epoch relative to constant historical 1985-2004 temperature means, SSP5-8.5 vigorous warming scenario, 15 'likely' CMIP6 global climate models (GCMs).

a Spatially distributed country-level multi-model medians of 15 'likely' CMIP6 Global Climate Models (GCMs) simulated impacts, 2061-2080 epoch, econometrically structured from country-level climatic data matched with year-to-year per capita GDP realisations (*à la Burke et al (2015)*). Chosen equation specification to calibrate the projections is pooled FE-OLS accounting for short-run temperature effects only. **b** Spatially distributed province-level multi-model medians of 15 'likely' CMIP6 GCMs simulated estimates, 2061-2080 epoch, econometrically structured from sub-national administrative region-level climatic data matched with year-to-year gross regional per capita product realisations (*à la Kotz et al (2024)*). Chosen equation specification to calibrate the projections is pooled FE-OLS accounting for short-run temperature effects only. **c** Cross-region globally averaged projected damages (%), point-level estimates from each of the full set of 30 CMIP6 GCMs (including those falling inside and outside the 'likely' and 'very likely' ranges) at 2061-2080 epoch, SSP5-8.5 vigorous (red) versus SSP2-4.5 moderate (orange) warming scenarios.

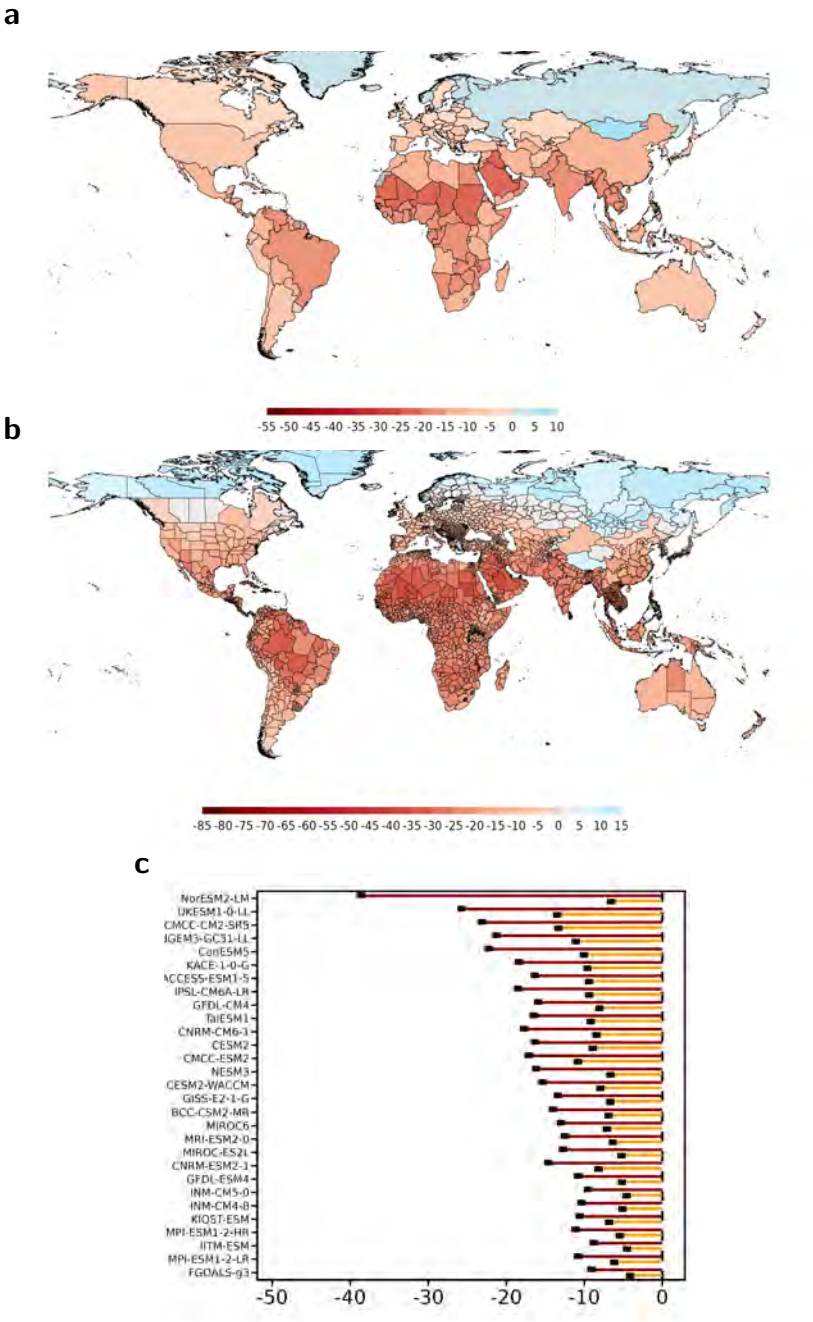

Figure A.20: Projected climate-shift impacts (%) on per capita GDP, 2061-2080 epoch relative to constant historical 1985-2004 temperature means, intermediate mid-point scenario between SSP5-8.5 vigorous & SSP2-4.5 moderate warmings, 15 'likely' CMIP6 global climate models (GCMs).

a Spatially distributed country-level multi-model medians of 15 'likely' CMIP6 Global Climate Models (GCMs) simulated impacts, 2061-2080 epoch, econometrically structured from country-level climatic data matched with year-to-year per capita GDP realisations (*à la Burke et al (2015)*). Chosen equation specification to calibrate the projections is pooled FE-OLS accounting for short-run temperature effects only. **b** Spatially distributed province-level multi-model medians of 15 'likely' CMIP6 GCMs simulated estimates, 2061-2080 epoch, econometrically structured from sub-national administrative region-level climatic data matched with year-to-year gross regional per capita product realisations (*à la Kotz et al (2024)*). Chosen equation specification to calibrate the projections is pooled FE-OLS accounting for short-run temperature effects only. **c** Cross-region globally averaged projected damages (%), point-level estimates from each of the full set of 30 CMIP6 GCMs (including those falling inside and outside the 'likely' and 'very likely' ranges) at 2061-2080 epoch, SSP5-8.5 vigorous (red) versus SSP2-4.5 moderate (orange) warming scenarios.

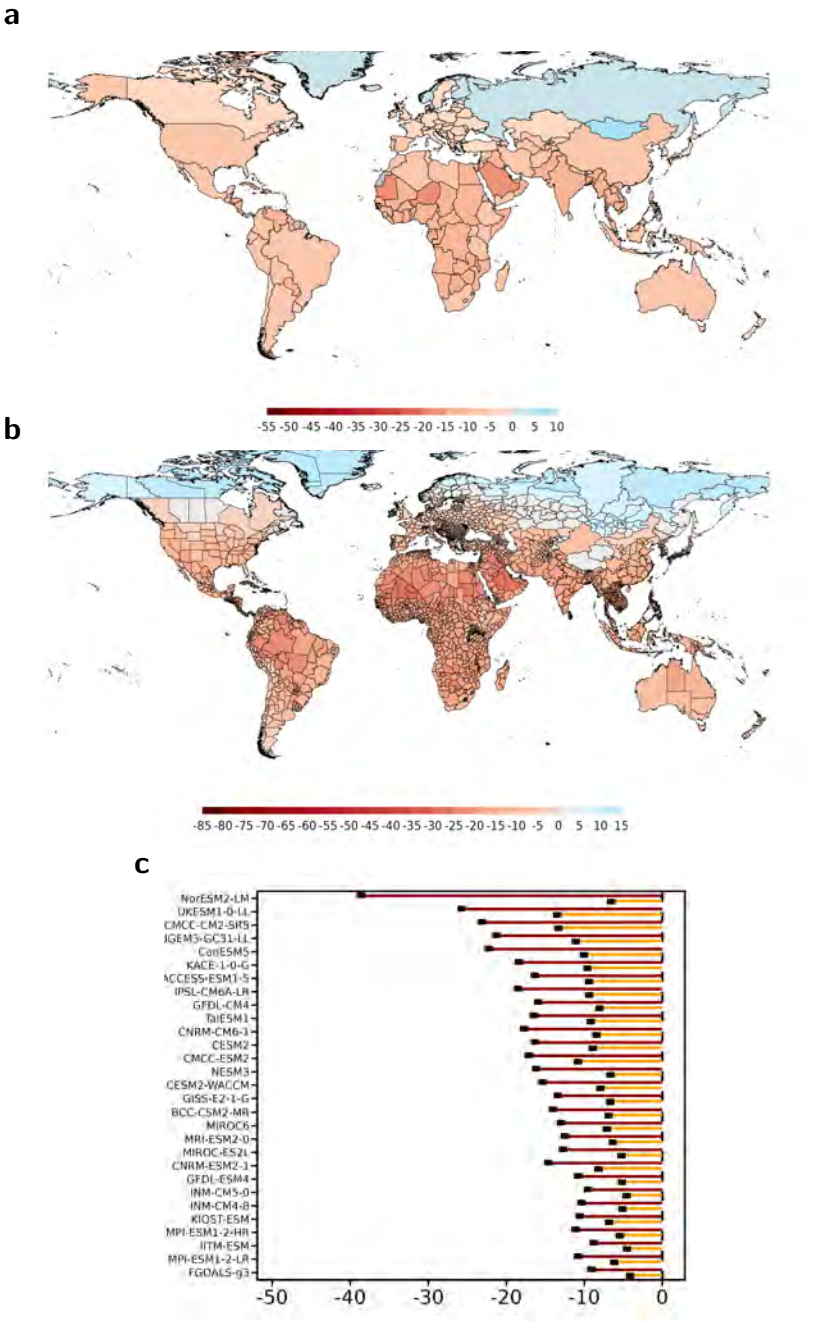

Figure A.21: Projected climate-shift impacts (%) on per capita GDP, 2061-2080 epoch relative to constant historical 1985-2004 temperature means, SSP2-4.5 moderate warming scenario, 15 'likely' CMIP6 global climate models (GCMs).

a Spatially distributed country-level multi-model medians of 15 'likely' CMIP6 Global Climate Models (GCMs) simulated impacts, 2061-2080 epoch, econometrically structured from country-level climatic data matched with year-to-year per capita GDP realisations (*à la Burke et al (2015)*). Chosen equation specification to calibrate the projections is pooled FE-OLS accounting for short-run temperature effects only. **b** Spatially distributed province-level multi-model medians of 15 'likely' CMIP6 GCMs simulated estimates, 2061-2080 epoch, econometrically structured from sub-national administrative region-level climatic data matched with year-to-year gross regional per capita product realisations (*à la Kotz et al (2024)*). Chosen equation specification to calibrate the projections is pooled FE-OLS accounting for short-run temperature effects only. **c** Cross-region globally averaged projected damages (%), point-level estimates from each of the full set of 30 CMIP6 GCMs (including those falling inside and outside the 'likely' and 'very likely' ranges) at 2061-2080 epoch, SSP5-8.5 vigorous (red) versus SSP2-4.5 moderate (orange) warming scenarios.

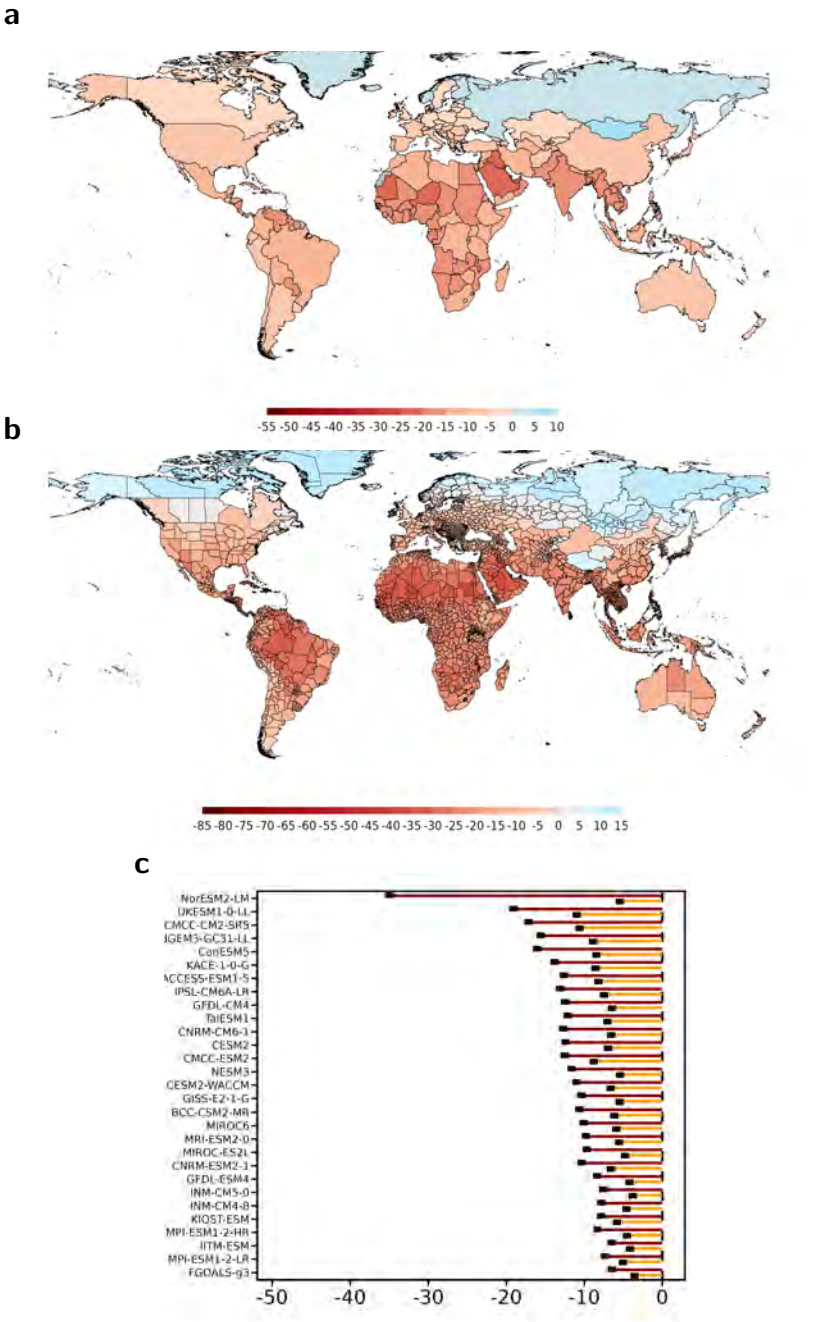

Figure A.22: Projected climate-shift impacts (%) on per capita GDP, 2051-2070 epoch relative to constant historical 1985-2004 temperature means, SSP5-8.5 vigorous warming scenario, 15 'likely' CMIP6 global climate models (GCMs).

a Spatially distributed country-level multi-model medians of 15 'likely' CMIP6 Global Climate Models (GCMs) simulated impacts, 2051-2070 epoch, econometrically structured from country-level climatic data matched with year-to-year per capita GDP realisations (*à la Burke et al (2015)*). Chosen equation specification to calibrate the projections is pooled FE-OLS accounting for short-run temperature effects only. **b** Spatially distributed province-level multi-model medians of 15 'likely' CMIP6 GCMs simulated estimates, 2051-2070 epoch, econometrically structured from sub-national administrative region-level climatic data matched with year-to-year gross regional per capita product realisations (*à la Kotz et al (2024)*). Chosen equation specification to calibrate the projections is pooled FE-OLS accounting for short-run temperature effects only. **c** Cross-region globally averaged projected damages (%), point-level estimates from each of the full set of 30 CMIP6 GCMs (including those falling inside and outside the 'likely' and 'very likely' ranges) at 2051-2070 epoch, SSP5-8.5 vigorous (red) versus SSP2-4.5 moderate (orange) warming scenarios.

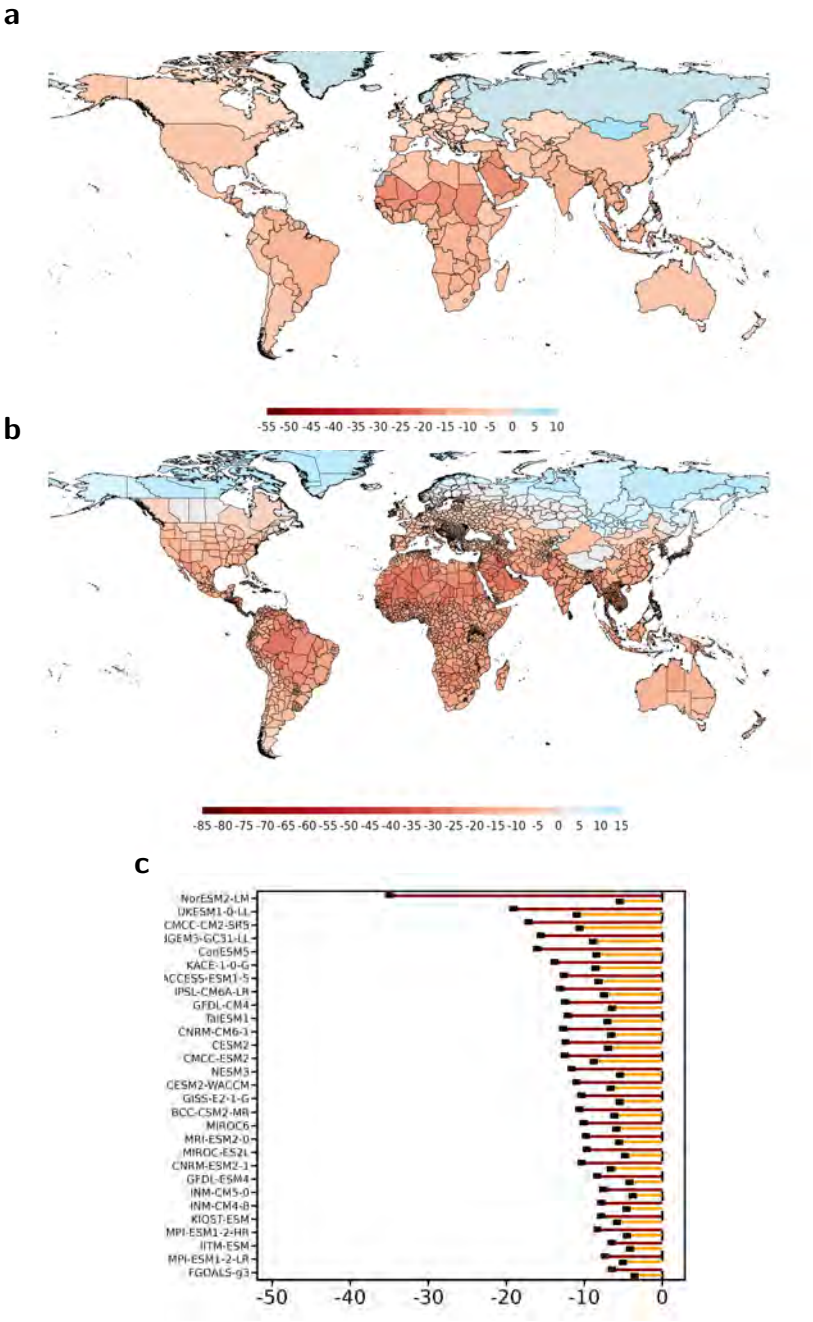

Figure A.23: Projected climate-shift impacts (%) on per capita GDP, 2051-2070 epoch relative to constant historical 1985-2004 temperature means, intermediate mid-point scenario between SSP5-8.5 vigorous & SSP2-4.5 moderate warmings, 15 'likely' CMIP6 global climate models (GCMs).

a Spatially distributed country-level multi-model medians of 15 'likely' CMIP6 Global Climate Models (GCMs) simulated impacts, 2051-2070 epoch, econometrically structured from country-level climatic data matched with year-to-year per capita GDP realisations (*à la Burke et al (2015)*). Chosen equation specification to calibrate the projections is pooled FE-OLS accounting for short-run temperature effects only. **b** Spatially distributed province-level multi-model medians of 15 'likely' CMIP6 GCMs simulated estimates, 2051-2070 epoch, econometrically structured from sub-national administrative region-level climatic data matched with year-to-year gross regional per capita product realisations (*à la Kotz et al (2024)*). Chosen equation specification to calibrate the projections is pooled FE-OLS accounting for short-run temperature effects only. **c** Cross-region globally averaged projected damages (%), point-level estimates from each of the full set of 30 CMIP6 GCMs (including those falling inside and outside the 'likely' and 'very likely' ranges) at 2051-2070 epoch, SSP5-8.5 vigorous (red) versus SSP2-4.5 moderate (orange) warming scenarios.

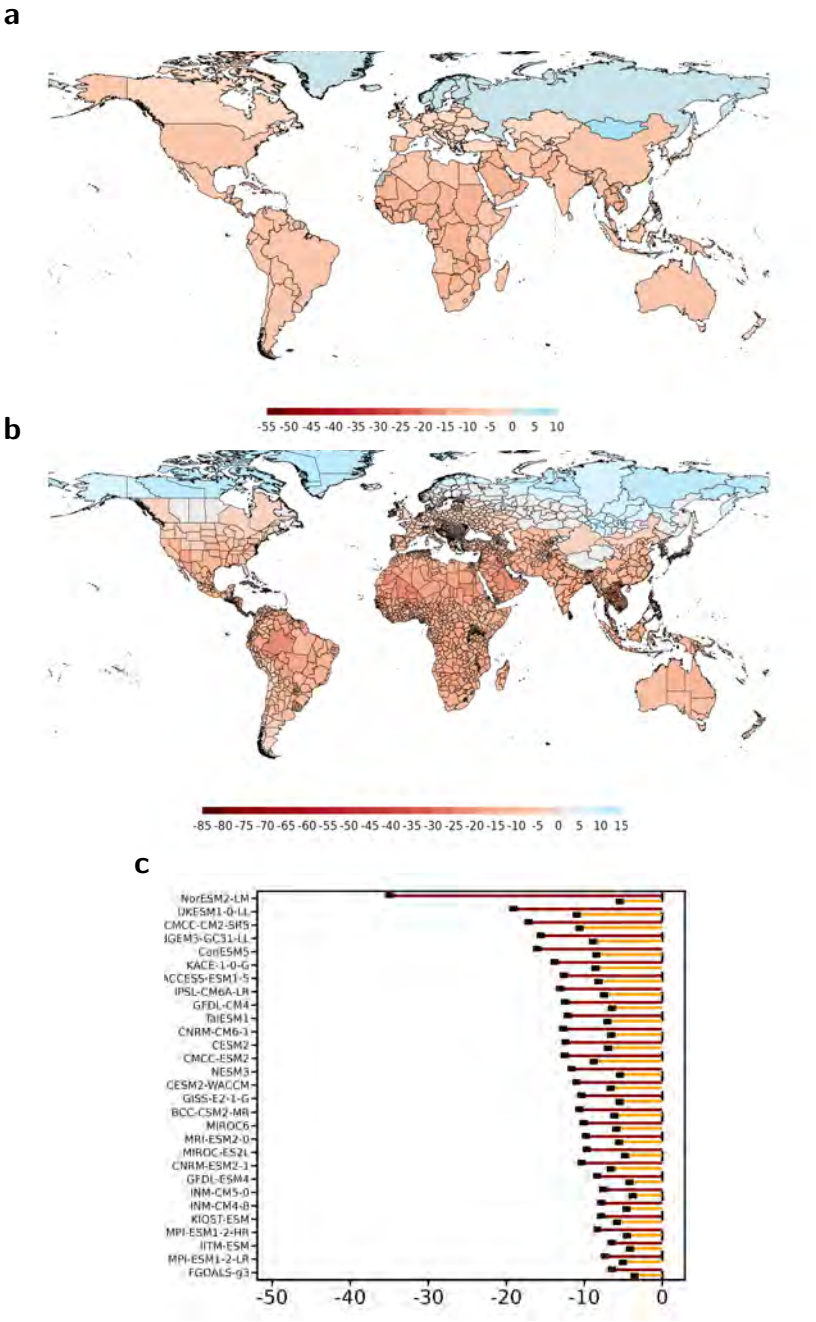

Figure A.24: Projected climate-shift impacts (%) on per capita GDP, 2051-2070 epoch relative to constant historical 1985-2004 temperature means, SSP2-4.5 moderate warming scenario, 15 'likely' CMIP6 global climate models (GCMs).

a Spatially distributed country-level multi-model medians of 15 'likely' CMIP6 Global Climate Models (GCMs) simulated impacts, 2051-2070 epoch, econometrically structured from country-level climatic data matched with year-to-year per capita GDP realisations (*à la Burke et al (2015)*). Chosen equation specification to calibrate the projections is pooled FE-OLS accounting for short-run temperature effects only. **b** Spatially distributed province-level multi-model medians of 15 'likely' CMIP6 GCMs simulated estimates, 2051-2070 epoch, econometrically structured from sub-national administrative region-level climatic data matched with year-to-year gross regional per capita product realisations (*à la Kotz et al (2024)*). Chosen equation specification to calibrate the projections is pooled FE-OLS accounting for short-run temperature effects only. **c** Cross-region globally averaged projected damages (%), point-level estimates from each of the full set of 30 CMIP6 GCMs (including those falling inside and outside the 'likely' and 'very likely' ranges) at 2051-2070 epoch, SSP5-8.5 vigorous (red) versus SSP2-4.5 moderate (orange) warming scenarios.

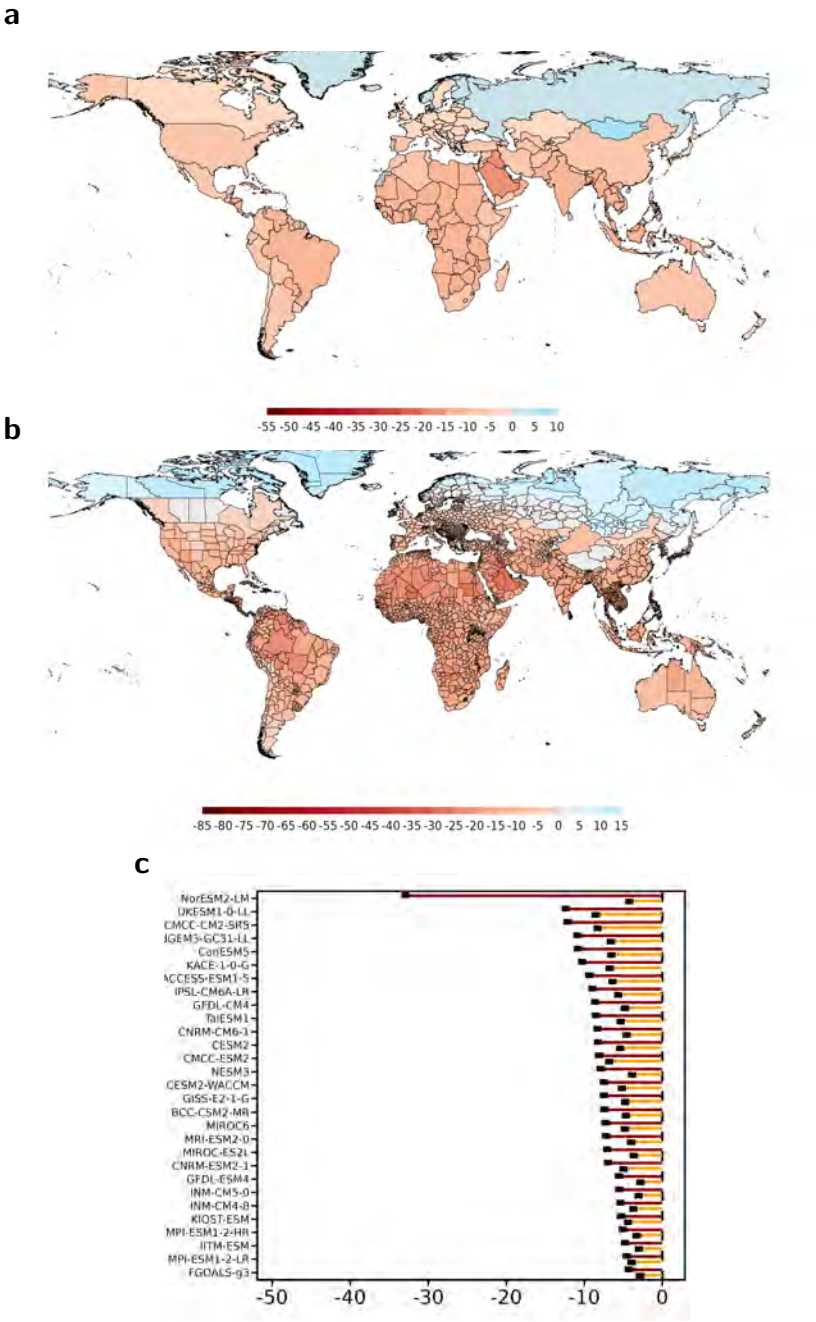

Figure A.25: Projected climate-shift impacts (%) on per capita GDP, 2041-2060 mid-century epoch relative to constant historical 1985-2004 temperature means, SSP5-8.5 vigorous warming scenario, 15 'likely' CMIP6 global climate models (GCMs).

a Spatially distributed country-level multi-model medians of 15 'likely' CMIP6 Global Climate Models (GCMs) simulated impacts, 2041-2060 mid-century epoch, econometrically structured from country-level climatic data matched with year-to-year per capita GDP realisations (*à la Burke et al (2015)*). Chosen equation specification to calibrate the projections is pooled FE-OLS accounting for short-run temperature effects only. **b** Spatially distributed province-level multi-model medians of 15 'likely' CMIP6 GCMs simulated estimates, 2041-2060 mid-century epoch, econometrically structured from sub-national administrative region-level climatic data matched with year-to-year gross regional per capita product realisations (*à la Kotz et al (2024)*). Chosen equation specification to calibrate the projections is pooled FE-OLS accounting for short-run temperature effects only. **c** Cross-region globally averaged projected damages (%), point-level estimates from each of the full set of 30 CMIP6 GCMs (including those falling inside and outside the 'likely' and 'very likely' ranges) at 2041-2060 mid-century epoch, SSP5-8.5 vigorous (red) versus SSP2-4.5 moderate (orange) warming scenarios.

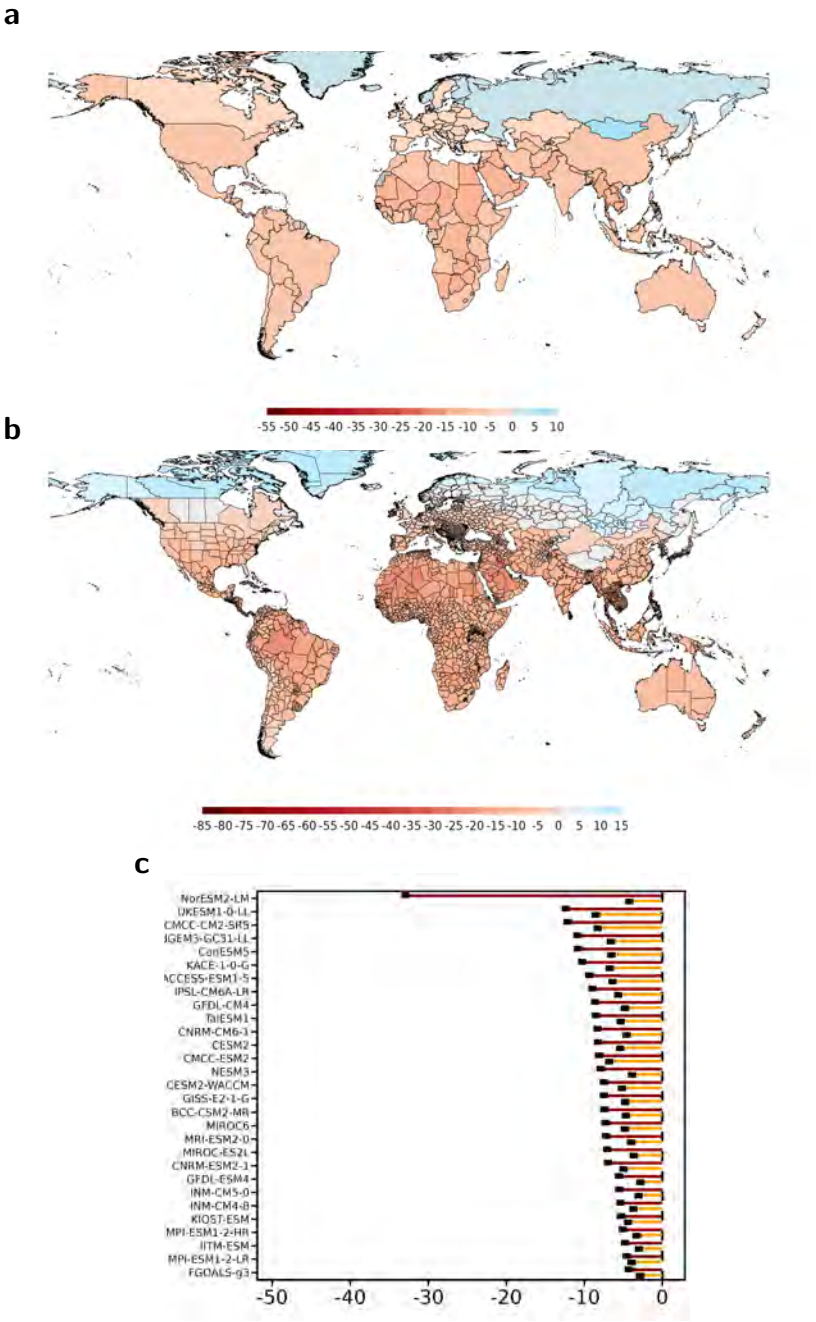

Figure A.26: Projected climate-shift impacts (%) on per capita GDP, 2041-2060 mid-century epoch relative to constant historical 1985-2004 temperature means, intermediate mid-point scenario between SSP5-8.5 vigorous & SSP2-4.5 moderate warmings, 15 'likely' CMIP6 global climate models (GCMs).

a Spatially distributed country-level multi-model medians of 15 'likely' CMIP6 Global Climate Models (GCMs) simulated impacts, 2041-2060 mid-century epoch, econometrically structured from country-level climatic data matched with year-to-year per capita GDP realisations (*à la Burke et al (2015)*). Chosen equation specification to calibrate the projections is pooled FE-OLS accounting for short-run temperature effects only. **b** Spatially distributed province-level multi-model medians of 15 'likely' CMIP6 GCMs simulated estimates, 2041-2060 mid-century epoch, econometrically structured from sub-national administrative region-level climatic data matched with year-to-year gross regional per capita product realisations (*à la Kotz et al (2024)*). Chosen equation specification to calibrate the projections is pooled FE-OLS accounting for short-run temperature effects only. **c** Cross-region globally averaged projected damages (%), point-level estimates from each of the full set of 30 CMIP6 GCMs (including those falling inside and outside the 'likely' and 'very likely' ranges) at 2041-2060 mid-century epoch, SSP5-8.5 vigorous (red) versus SSP2-4.5 moderate (orange) warming scenarios.

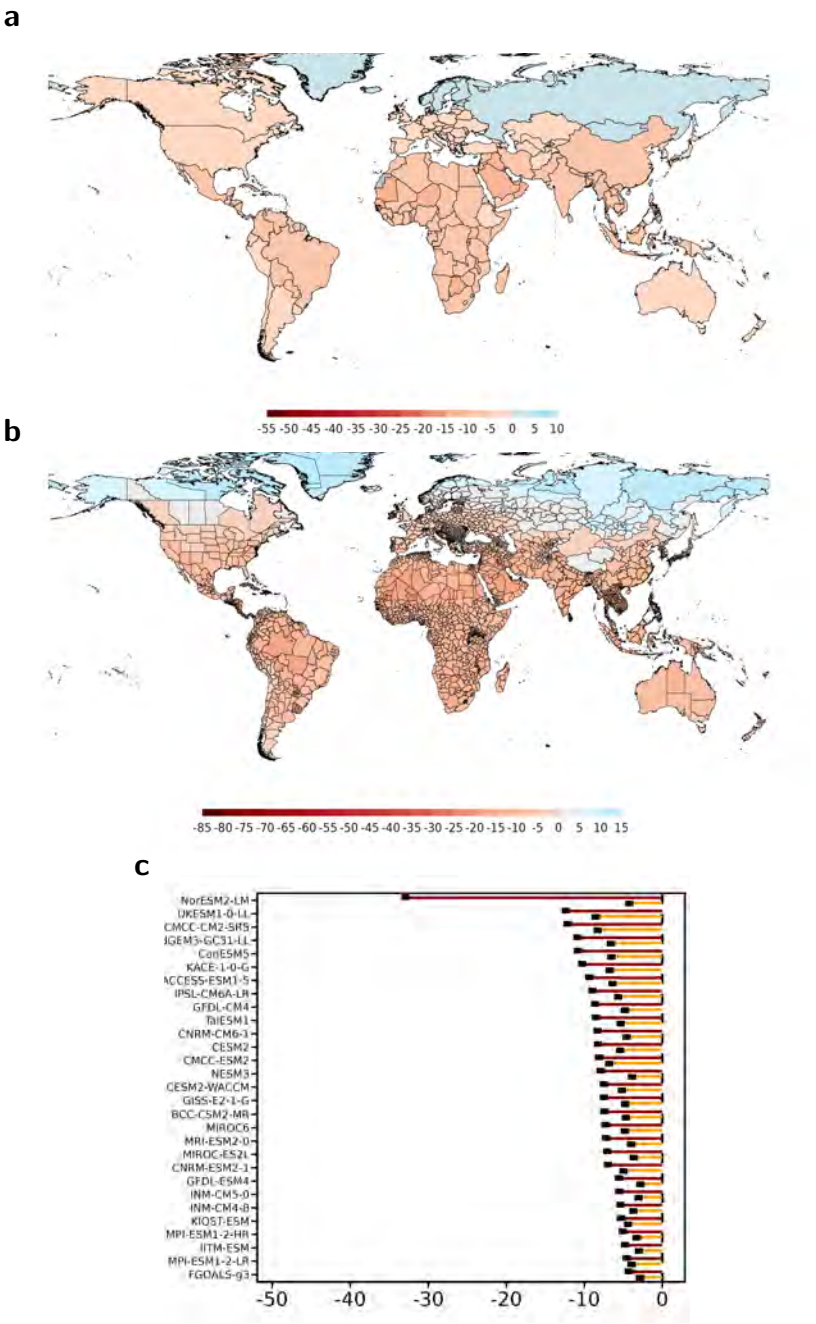

Figure A.27: Projected climate-shift impacts (%) on per capita GDP, 2041-2060 mid-century epoch relative to constant historical 1985-2004 temperature means, SSP2-4.5 moderate warming scenario, 15 'likely' CMIP6 global climate models (GCMs).

a Spatially distributed country-level multi-model medians of 15 'likely' CMIP6 Global Climate Models (GCMs) simulated impacts, 2041-2060 mid-century epoch, econometrically structured from country-level climatic data matched with year-to-year per capita GDP realisations (*à la Burke et al (2015)*). Chosen equation specification to calibrate the projections is pooled FE-OLS accounting for short-run temperature effects only. **b** Spatially distributed province-level multi-model medians of 15 'likely' CMIP6 GCMs simulated estimates, 2041-2060 mid-century epoch, econometrically structured from sub-national administrative region-level climatic data matched with year-to-year gross regional per capita product realisations (*à la Kotz et al (2024)*). Chosen equation specification to calibrate the projections is pooled FE-OLS accounting for short-run temperature effects only. **c** Cross-region globally averaged projected damages (%), point-level estimates from each of the full set of 30 CMIP6 GCMs (including those falling inside and outside the 'likely' and 'very likely' ranges) at 2041-2060 mid-century epoch, SSP5-8.5 vigorous (red) versus SSP2-4.5 moderate (orange) warming scenarios.

A.4 Nomenclature

CMIP6	Coupled Model Intercomparison, Phase VI
DOSE	MCC-PIK Database of Subnational Economic Output
ECMWF ...	European Centre for Medium-Range Weather Forecasts
ECS	Equilibrium Climate Sensitivity
ERA5	ECMWF Reanalysis V.5
GAM	Generalized Additive Model
GCMs	Global Climate Models
GLDAS	Global Land Data Assimilation System
GSFC	Goddard Space Flight Center
IAMs	Integrated Assessment Models
MPC	Microsoft Planetary Computer
NEX-GDDP	NASA Earth Exchange Global Daily Downscaled Projections
NOAH-LSM	NOAH-Land Surface Model
PWT	Penn World Table
RCPs	Representative Concentration Pathways
SCC	Social Cost of Carbon
SSPs	Shared Socioeconomic Pathways
TCR	Transient Climate Response
VIC	Variable Infiltration Capacity

References

[S1.] De Cian, E., Pavanello, F., Randazzo, T., Mistry, M. N., & Davide, M. (2019). Households' adaptation in a warming climate. Air conditioning and thermal insulation choices. Environmental Science & Policy, 100, 136-157.

[S2.] Dioha, E. C., Chung, E. S., Ayugi, B. O., Babaousmail, H., & Sian, K. T. C. L. K. (2024). Quantifying the Added Value in the NEX-GDDP-CMIP6 Models as Compared to Native CMIP6 in Simulating Africa's Diverse Precipitation Climatology. Earth Systems and Environment, 8(2), 417-436.

[S3.] Gu, X., Li, J., Chen, Y. D., Kong, D., & Liu, J. (2019). Consistency and discrepancy of global surface soil moisture changes from multiple model-based data sets against satellite observations. Journal of Geophysical Research: Atmospheres, 124(3), 1474-1495.

[S4.] Ji, L., Senay, G. B., & Verdin, J. P. (2015). Evaluation of the Global Land Data Assimilation System (GLDAS) air temperature data products. Journal of Hydrometeorology, 16(6), 2463-2480.

[S5.] Liu, T., Zhu, X., Tang, M., Guo, C., & Lu, D. (2024). Multi-model ensemble bias-corrected precipitation dataset and its application in identification of drought-flood abrupt alternation in China. Atmospheric Research, 307, 107481.

[S6.] Mistry, M. N. (2019). Historical global gridded degree-days: A high-spatial resolution database of CDD and HDD. Geoscience Data Journal, 6(2), 214-221.

[S7.] Sylvestre, F., Mahamat-Nour, A., Naradoum, T., Alcoba, M., Gal, L., Paris, A., ... & Gaya, D. (2024). Strengthening of the hydrological cycle in the Lake Chad Basin under current climate change. Scientific Reports, 14(1), 24639.

[S8.] Wenz, L., Kotz, M., Callahan, C., & Stechemesser, A. (2024). Persistent macroeconomic damages raise social cost of carbon.

[S9.] Wu, F., Jiao, D., Yang, X., Cui, Z., Zhang, H., & Wang, Y. (2023). Evaluation of NEX-GDDP-

CMIP6 in simulation performance and drought capture utility over China–based on DISO. Hydrology Research, 54(5), 703-721.

[S10.] Zhai, J., Mondal, S. K., Fischer, T., Wang, Y., Su, B., Huang, J., ... & Uddin, M. J. (2020). Future drought characteristics through a multi-model ensemble from CMIP6 over South Asia. Atmospheric Research, 246, 105111.

[S11.] Zhang, J., Li, C., Zhang, X., & Zhao, T. (2024). Improving simulations of extreme precipitation events in China by the CMIP6 global climate models through statistical downscaling. Atmospheric Research, 303, 107344.

About EDHEC Climate Institute

EDHEC Business School has been recognised for over 20 years for its expertise in finance. Its approach to climate finance is founded on a commitment to equipping finance professionals and decision-makers with the insights, tools, and solutions necessary to navigate the challenges and opportunities presented by climate change. EDHEC has developed a significant research capacity on the financial measurement of climate risk, which relies on the best researchers in climate finance, and brings together experts in climate risks as well as in quantitative analysis.

The EDHEC Climate Institute (ECI) focuses on helping private and public decision-makers manage climate-related financial risks and make the most of financial tools to support the transition to a low-emission economy that is more resilient to climate change. It has a long track record as an independent and critical reference centre in helping long-term investors to understand and manage the financial implications of climate change on asset prices and the management of investments and climate action policies. The institute has also developed an expertise in physical risks, developing proprietary research frameworks and innovative approaches. ECI is also conducting advanced research on climate transition risks, with a focus on supply chain emissions (Scope 3), consumer choices, and emerging technologies.

As part of its mission, ECI collaborates with academic partners, businesses, and financial players to establish targeted research partnerships. This includes making research outputs, publications, and data available in open source to maximise impact and accessibility.

For more information, please contact:

EDHEC Climate Institute

Maud Gauchon
maud.gauchon@climateimpactedhec.com

London
10 Fleet Place
London EC4M 7RB
United Kingdom
Tel +44 (0)20 7332 5600

Nice
393 Promenade des Anglais
06200 Nice
France
Tel +33 (0)4 93 18 78 87

Paris
16 - 18 rue du 4 Septembre
75002 Paris
France
Tel +33 (0)1 53 32 76 30

Singapore
One George Street
#15-02
Singapore 049145
Tel +65 (0)6438 0030

climateinstitute.edhec.edu